Parallel Coupled Micro-Macro Actuators

by

John Bryant Morrell

B.S., Yale University (1986)
M.S., University of Washington (1990)

Submitted to the Department of Mechanical Engineering
in partial fulfillment of the requirements for the degree of

Doctor of Philosophy

at the

MASSACHUSETTS INSTITUTE OF TECHNOLOGY

February 1996

Author .....
Department of Mechanical Engineering
December 18, 1995

Certified by .....
J. Kenneth Salisbury
Principal Research Scientist
Thesis Supervisor

Accepted by .....
Professor Ain A. Sonin
Chairman, Departmental Graduate Committee

Parallel Coupled Micro-Macro Actuators
by
John Bryant Morrell

Submitted to the Department of Mechanical Engineering
on December 18, 1995, in partial fulfillment of the
requirements for the degree of
Doctor of Philosophy

Abstract

This thesis presents a new actuator system consisting of a micro-actuator and a macro-actuator coupled in parallel via a compliant transmission. The system is called the Parallel Coupled Micro-Macro Actuator, or PaCMMA.

In this system, the micro-actuator is capable of high bandwidth force control due to its low mass and direct-drive connection to the output shaft. The compliant transmission of the macro-actuator reduces the impedance (stiffness) at the output shaft and increases the dynamic range of force. Performance improvement over single actuator systems was expected in force control, impedance control, force distortion and reduction of transient impact forces.

A set of quantitative measures is proposed and the actuator system is evaluated against them: Force Control Bandwidth, Position Bandwidth, Dynamic Range, Impact Force, Impedance ("Backdriveability"), Force Distortion and Force Performance Space.

Several theoretical performance limits are derived from the saturation limits of the system. A control law is proposed and control system performance is compared to the theoretical limits. A prototype testbed was built using permanenent magnet motors and an experimental comparison was performed between this actuator concept and two single actuator systems.

The following performance was observed: Force bandwidth of 56Hz, Torque Dynamic Range of 800:1, Peak Torque of 1040mNm, Minimum Torque of 1.3mNm. Peak Impact Force was reduced by an order of magnitude. Distortion at small amplitudes was reduced substantially. Backdriven impedance was reduced by 2-3 orders of magnitude.

This actuator system shows promise for manipulator design as well as psychophysical tests of human performance.

Thesis Supervisor: J. Kenneth Salisbury
Title: Principal Research Scientist

Acknowledgments

My committee members Ken Salisbury, Gill Pratt and Warren Seering provided direction, support and technical insight. Thanks to Ken who invited me into the Artificial Intelligence Laboratory when I first arrived at MIT. Over the years, Ken provided a comfortable environment with outstanding resources both in hardware and personnel. Gill Pratt made a huge contribution to this thesis in both his technical expertise when I got stuck and his enthusiasm for my topic. Warren Seering (and Woodie Flowers) provided me with an outstanding experience as a teaching assistant in 2.73. This experience reaffirmed my desire to both a creator of things mechanical and a teacher of engineering.

The "JKS-FOLKS" research group (Brian Eberman, Gunter Niemeyer, Tom Moyer, Cathy Anderson, Akhil Madhani, Matt Williamson, Suzanna Leveroni, Brian Anthony, Craig Latimer, and Vinay Shah) and officemate Tom Stahovich provided a great group of peers for both research and social occasions. Whether mountain biking, skiing, doing car work, or just retiring a pint at Happy Hour, the quality of the people I interacted with made my experience here a good one.

The AI laboratory is filled with people who make graduate research possible. In addition to the faculty, Jacqui Taylor, Ron Wiken and Laurel Simmons provided countless hours of help in various capacities. Leslie Regan in the Mechanical Engineering Graduate office serves as the patron saint of overdue Ph.D. students. I thank her for her constant cheer and support.

The MIT Cycling Team will always be a special group for me. So many outstanding friends emerged from this group: Tom Moyer, Jim Preisig, Paul Stek, Paul Nealey, Liz Bradley, Karon Maclean, Abe Stroock, and my wife, Kjirste. I thank them for their enthusiasm, their own victories and defeats, and for their constant encouragement and support of my athletic and intellectual pursuits.

I thank my parents, Ann and Linwood, and my siblings, Kristin, Annie, and Will for their encouragement in this long endeavor.

Finally, I would like to thank my wife, Kjirste, for her constant support (and most recently her careful proofreading). Her faith in me renewed my energy to finish and I consider our meeting to be the most wonderful event of my 6 years at MIT.

This work was supported in part by the Office of Naval Research, University Initiative Program Grant N00014-92-J-1814.

Contents

List of Figures

Nomenclature

B_t = transmission damping
B_t = environment damping

F_1 = force command to micro-actuator
F_{1sat} = Saturation force of micro-actuator
F_2 = force command to macro-actuator
F_{2sat} = Saturation force of macro-actuator
F_{des} = Desired force
F_e = Force applied to environment
F_{error} = Force error, $F_{des} - F_e$
F_{macro} = Force applied to M_1 by macro-actuator via transmission
F_{micro} = Force applied to M_1 by micro-actuator

G_{d1} = Velocity gain - transmission
G_{d2} = Velocity gain - macro-actuator
G_{ff} = feedforward gain
G_I = Integral gain
G_p = Gain of Micro-actuator effort
G_v = Force rate gain

$H_{1CL}(s)$ = Closed loop transfer function from $u_1(s)$ to $F_{micro}(s)$
$H_{1OL}(s)$ = Open loop transfer function from $u_1(s)$ to $F_{micro}(s)$
$H_{2CL}(s)$ = Closed loop transfer function from $u_2(s)$ to $F_{macro}(s)$
$H_{2OL}(s)$ = Open loop transfer function from $u_2(s)$ to $F_{macro}(s)$
$H_{fc}(\omega)$ = Closed loop transfer function from F_{des} to F_e.
K_e = Environment stiffness
K_t = transmission stiffness

M_1 = Mass of micro-actuator
M_2 = Mass of macro-actuator

x_1 = position of M_1
x_2 = position of M_2
X_{in} = Position input

u_1 = command input to micro-actuator
u_2 = command input to macro-actuator

ω = driving frequency
ω_{1co} = roll-off frequency of $H_{1CL}(s)$
ω_{2co} = roll-off frequency of $H_{2CL}(s)$

$Z(s)$ = Impedance response

Chapter 1

Introduction

Robot manipulation has been a topic of research for at least thirty years. During that period robot performance has improved and robots have surpassed human performance in a variety of tasks, especially those that require position accuracy and accurate repeatability. Despite these successes there are a large number of manipulation tasks which humans still perform faster and more accurately than robots such as picking up an unknown object or re-orienting an object in the hand.

Study of robot tasks typically breaks down into two distinct research problems. The first is using sensory information to determine an appropriate action and the second is using some manipulation system to execute the desired action. This thesis focuses on work in the latter of these areas. In examining the hardware and control algorithms available to higher order planners, it becomes clear that much of the existing robot hardware has performance characteristics which are quite different from those of humans.

In position controlled robots the ratio of the maximum to the minimum controllable displacement (position precision) can exceed 10,000:1 with standard actuators and sensors. For force controlled robots, the ratio of the maximum to the minimum controllable force remains quite small (50:1 or 0.02% for electric motors) and force accuracy remains relatively poor despite the existence of high accuracy force sensors.

Human resolution is fundamentally different from that of machines because it is logarithmic (Weber's Law (Gescheider, 1985)). For force control and sensing, the resolution of the measurement depends on the magnitude of the force and is usually about 7-10% JND (Just Noticeable Difference). That means that humans can detect a 7 lb change in a 100 lb load or a 7 gm change in a 100 gm load, but not a 7 gm change on a 700 Kg load. As a result, a human finger can control forces on the order of 1-2 grams with the same finger used for tasks requiring forces of one kilogram. The dynamic range of force allows the finger to perform very delicate sensing tasks as well as high force manipulation tasks. The principle of logarithmic resolution is also born out in position control. Humans can detect differences in position with resolution that is a fraction of the total displacement. A quick comparison of the performance of machines and humans suggests that humans have a larger force range than machines, while machines have a larger position range.

Another relevant aspect of human performance is the way human limbs accommodate position errors. As mentioned above, human position resolution from kinesthetic sensing (the location and forces of the limbs) is not nearly as accurate as most machines. Most

humans improve position resolution using vision and touch and we perform many position tasks with great precision. In the absence of vision, position sensing performance is much lower and yet many tasks can be accomplished successfully. The characteristics of human actuators are clearly quite different from machine actuators. Since humans are quite adept at manipulation it is worth examining these characteristics.

A fundamental requirement for manipulation is the ability to make and break contact with the environment in a stable, non-destructive way. In a controlled environment this is typically accomplished by knowing the exact location of various objects and moving slowly and precisely when contact is imminent. When contact does occur the forces of interaction are dependent on the mass and stiffness of the object and the manipulator and the impact velocity. The manipulator's mass and stiffness properties can be described more compactly as impedance. Large impedances (very stiff or massive) will generate large contact forces for small position disturbances, which is not desirable. A system with low impedance will generate smaller forces for the same conditions.

I believe human actuators rely on two important qualities for manipulation. The first is low impedance. Humans routinely move in both free-space and in constrained motion trajectories with stability in all regions, despite using low frequency actuators. For example, a human can absorb impacts energy by keeping the arms and legs bent. The success of these operations relies on low impedance. While human position performance is slow and inaccurate compared to machines, human impedance characteristics are superior for tasks where position errors are likely.

The second quality is dynamic range. Humans are able to sense features and acquire information during manipulation through use of a wide range of forces. Locating a feature may require a small force, use of a tool may require a large force. The versatility of many machines is limited by their force range. A surface profilometer can measure extremely small displacements but can not be used as a manipulator. Conversely, a PUMA robot can be used to lift a brick but could not detect its surface features.

This thesis will present a new concept for a Parallel Coupled, Micro-Macro Actuator (PaCMMA) which is motivated by the difficulties encountered in robot manipulation. The remainder of this chapter is devoted to background material on actuator and manipulator design and control. The actuator concept is presented in Chapter 2. Chapter 3 presents a number of performance metrics that are useful for actuator systems. Chapter 4 presents a model of the actuator system and a number of performance bounds. The model provides insight into ways to use the PaCMMA concept to its fullest capacity. Chapter 5 presents a control law and evaluates the control law's effectiveness. Chapter 6 presents some design guidelines which help a designer translate performance specifications into specifications for the individual system elements. Chapter 7 presents the results of a large number of experiments using the prototype system. The data here provide a good visual understanding of the system performance as well as some insight into the kinds of unmodelled effects that will affect performance.

In the process of designing and evaluating this actuator, it became clear that actuator technologies have various strengths and weaknesses and that the most common performance metrics fail to capture the important characteristics of actuators used in manipulation. The following section addresses some of these concerns. The remainder of this chapter provides background material for the reader. A substantial amount of research has been done in

the area of manipulation and the resulting paradigms for control and design influenced this thesis heavily.

1.1 Understanding Actuator Performance

Actuator performance may be quantified in a number of ways. Inspection of data sheets from various manufacturers identifies several important specifications: saturation force, maximum speed, inertia, power dissipation, etc. Sensor specifications such as resolution, range, and linearity affect the performance of a given actuator as well. Finally, the choice of control system affects the performance. Both the dynamic behavior of the control law and the implementation of the control architecture (servo rate, a/d resolution, etc.) will have a significant effect on system performance. Selection of an actuator system and its components should incorporate all of these specifications in a manner which allows the designer to achieve the desired performance.

In most cases the designer thinks in terms of the task to be performed by the robot and wants to translate the task requirements into component specifications. When considering actuators and sensors for robotic tasks, it is useful to consider the performance metrics in Table 1.1.

Quasi-Static Properties of the Actuator and Sensors	
	Peak Force (Transient - 10msecs)
	Peak Force (Continuous - Smoke test)
	Force Resolution
	Position Resolution
Dynamic Properties of the Actuator and Sensors	
	Inertia
	Maximum Acceleration (peak force/inertia)
Quasi-Static Properties of the Controlled System	
	Force Precision (controllable force)
	Position Precision (controllable Position)
	Force Dynamic Range
Dynamic Properties of the Controlled System	
	Position Bandwidth
	Force Bandwidth
	Impedance (backdrivability)
	Range of controllable impedances
	Distortion (RMS)

Table 1.1: Actuator Performance Specifications

At the component level most of these specifications are easy to understand. Once the system is assembled and a controller is chosen the Dynamic Properties of the Controlled System become important metrics. Unfortunately, the mapping from performance metrics above into component specifications is poorly defined. The performance of the system is highly dependent on implementation and non-ideal effects. Friction and backlash can introduce force and position errors; quantization noise and time delays can destabilize a control system. Fortunately, it is generally possible to predict, simulate, or measure the performance of a given set of components and the fourth set of metrics provides a basis for performing experiments to assess the performance of the actuator system. This thesis will define some of these metrics and present experimental techniques for measuring them.

1.2 Background

Robot manipulation tasks have typically been specified as a collection of force and position trajectories and/or impedances at the robot endpoint. The ability to control position accurately in the presence of force disturbances has been studied extensively and is well understood. Controlling forces in the presence of position disturbances has been significantly harder than achieving accurate position control. Often, analysis of manipulation and impedance control assumes that the robot will accurately produce the desired force. Experimental success has been limited and force control in the real world has become a significant research area in robot control.

The following sections provide a brief overview of past control approaches, design paradigms and technologies.

1.2.1 Robot Design Issues

Robot Impedance

Early work in force control identified two significant robot characteristics which make controlling force difficult. The first is robot impedance (Salisbury, 1980; Salisbury and Craig, 1982; Hogan, 1983; Hogan, 1985; Khatib, 1990; Sharon et al., 1988), and the second is non-collocation of the force sensor and the actuator (An, 1986; Cannon and Rosenthal, 1984; Eppinger and Seering, 1987). Robot impedance is of obvious importance. When a robot with high impedance (large mass or stiffness) is in contact with an object, a small displacement of either the robot or the object will result in large contact forces. The large forces can result in damage to both the robot and the object. Thus, successful force control relies on the ability of the robot to control the contact impedance. This may be accomplished with active control or through passive characteristics.

Robots with active control have the benefit that the impedance may be changed as the task changes. Unfortunately, active control is limited by the bandwidth of the controlled system and by the intrinsic mechanical properties of the system, e.g. stiffness, mass, natural frequency etc. Digital control systems are inherently discontinuous due to sensor resolution and quantization noise and can introduce errors or destabilizing noise. The servo period adds delay which can also destabilize the system. In a stiff environment position disturbances create force transients that can rise significantly in one or two servo cycles, leading to limit

cycles or instability. Nonlinearities such as saturation and friction turn well-behaved linear systems into ill-behaved non-linear systems and all of these nonlinearities inevitably become performance limiting factors in robot force control.

Chosen properly, passive characteristics can have the benefit of requiring little control effort and exhibiting real-time continuous response, but they can not usually be modified dynamically. For force control, good passive characteristics include low robot inertia, well-damped dynamics and frictionless, zero-backlash transmissions. Studies on remote center of compliance are an example of this approach (Whitney, 1982) while the work in (Laurin-Kovitz et al., 1991) suggests some approaches to utilizing programmable passive elements. Morita also suggests the use of passive mechanical elements which may be altered using computer control to change the robot impedance (Morita and Sugano, 1995).

The Whole-Arm-Manipulator at MIT is an excellent example of a robot with naturally low impedance (Salisbury et al., 1989). In this case the motors are located near the base of the robot and connected to the links via efficient, low reduction ratio cable transmissions. Force control is achieved through open loop torque commands to the motors. Disturbance rejection relies on low mass links and the low friction transmission. This works well but the disturbance rejection in force is limited since the force control is open loop.

Non-collocated Sensors

Non-collocation of the sensor and actuator is another dominant problem in force control (Cannon and Rosenthal, 1984; Eppinger and Seering, 1987; Colgate and Hogan, 1989). If the sensor and actuator are separated by several dynamic elements, then the obtainable control bandwidth is limited by the resonant frequencies of the system usually a transmission between the sensor and actuator . The stiffer the transmission, the higher the potential control bandwidth. This fact has led many designers to conclude that "stiffer is better". Further, friction and backlash combine to lower the control bandwidth in these situations as well. Electric motors and many other actuators require some kind of transmission to both maximize torque and to move actuator mass away from the endpoint. As a result robot design has moved in two directions: 1) direct drive actuators and 2) stiffer, low friction, low backlash transmissions.

Direct Drive Actuators

Direct drive actuators solve the non-collocation problem by providing a stiff connection between the force source and the sensor (H. Asada and Takeyama, 1983). This approach exhibits relatively high bandwidth force control (20-60Hz). The absence of a transmission reduction keeps the link inertia at a low value. (Recall that a reduction has the effect of multiplying the motor inertia by N^2, where N is the reduction ratio (Townsend, 1988)). The negative aspect of this approach is that the motor is not being used at its maximum power. Consequently, a much larger actuator must be used to get the same torque from a direct-drive system. A further consideration is the increased mass of the preceding joints due to the motor housing mass. Nonetheless, the low rotor inertia and stiff transmission of direct-drive actuators has been shown to provide superior force control performance for quasi-static environments and unforeseen impacts (Youcef-Toumi and Li, 1987: An and Hollerbach, 1987).

Macro-micro robots

Macro-micro robots in the past have been implemented in a serial configuration. In these cases, a micro-robot is mounted on a macro-robot so that their positions are summed. Since they are connected in a serial manner, the forces in the macro and micro-robots must be equal in steady state. A number of researchers have studied the control issues in these types of manipulators.

Some of the first work in macro-micro systems is reported in (Sharon and Hardt, 1984; Sharon et al., 1988; Sharon et al., 1989; Sharon et al., 1993). Sharon shows that force control bandwidth and position control bandwidth may be improved using a serial configuration and reports on the control issues associated with the serial configuration.

Khatib showed that a macro-micro system may be used to reduce endpoint inertia to the inertia of the micro-actuator alone (Khatib, 1990).

Cannon reports on a micro-manipulator attached to a flexible arm. Position control bandwidth was achieved at a frequency 8 times higher than the first structural mode of the flexible arm (Chiang et al., 1991).

A compliant, serial macro-manipulator with a fast, stiff micro-manipulator is studied in (Yoshikawa et al., 1994a; Yoshikawa et al., 1994b; Nagai and Yoshikawa, 1994). Position control of several other serial macro-micro mechanisms are explored in (Narikiyo et al., 1994; Slacudean and An, 1989).

Compliant Manipulators

The intentional use of compliance for manipulation has been identified as early as 1975 (remote center of compliance) (Drake, 1975).

Trevelyan describes a sheep shearing robot in (Trevelyan, 1993). The robot relies on effective open loop dynamics rather than using an extensive control system. The author reminds us that machines should be designed to work correctly in an open loop capacity and that closed loop control should be introduced only if open loop performance is inadequate.

Many robot arms are flexible because weight constraints prohibit additional material (space manipulators for example). A large body of research on the control of flexible structures exists though these structures have not always been used for manipulation. Some of the relevant research issues are addressed in (Cannon and Rosenthal, 1984; Chiang et al., 1991) and an interesting design for an elastic arm and controller is provided in (Park, 1992).

Morita reports on the use of a device which adjusts the mechanical impedance of a one degree-of-freedom robot (Morita and Sugano, 1995).

More recently, several researchers who study the interaction of walking and hopping robots have pointed to the benefits of compliance which include greater shock tolerance (impact tolerance) and better force control (Raibert et al., 1989; Pratt and Williamson, 1995; Williamson, 1995).

Actuator Research

Robot designers have also sought improvement from developments in component technologies. Integration of an actuator and force sensor is described in (Boulet and Hayward, 1993; Henri and Hollerbach, 1994; Grant and Hayward, 1995; Williamson, 1995) and a useful sur-

vey of a wide range of technologies is reported in (John M. Hollerbach and Ballantyne, 1991).

A consistent problem in actuator technology is the definition of useful performance metrics which allow a designer to evaluate candidate technologies. Jacobsen proposes several criteria in (Jacobsen et al., 1989) including positional accuracy, positional quickness, force generation quickness, saturation avoidance, and stability margin. Hayward proposes several criteria specifically for haptic interface devices, but these criteria may be easily applied to actuators as well (Hayward and Astley, 1995). These include some of the ideas mentioned in table 1.1.

The field of haptics a recently begun to quantify the important performance metrics in robot performance. Several papers identify the importance of impedance, backdrivability, damping, dynamic range and sensor resolution (Colgate and Brown, 1994; Hayward and Astley, 1995; Rosenberg and Adelstein, 1993).

1.2.2 Control Algorithms

Control algorithm research has yielded several important results for control of robots in manipulation. Force control was first studied as a means for performing peg-in-hole insertions. Other tasks of interest include surface following (such as sanding or window washing) and manipulation in less structured environments. Tasks like these typically have a number of phases including: moving in free space, making contact with the environment, and maintaining some kind of impedance or force control relationship with the environment. Good performance in these tasks is typically quantified by fast approach velocity, low impact force, and low bounce. It is not clear whether a single controller may be used for all phases of these tasks, but progress has been made identifying good controllers for each of these phases. The research in these areas may be broadly classified as Force Control, Impedance Control and Impact or Transition Control.

Force Control

Force Control is a broad topic and many algorithms have been proposed. This section provides a list of appropriate papers for further study.

A history of early force control methods is presented in (Whitney, 1982). Goldenberg provides additional insight in (Goldenberg, 1992) and points out than many algorithms reduce to full state feedback when linear models are used. Countless researchers have reported that stiff environments and full-state feedback result in instability. Several researchers propose integral feedback of force errors with very good results (Colgate and Hogan, 1989; Levin, 1990; Volpe and Khosla, 1992; Richter and Pfeiffer, 1991; Paljug et al., 1992).

In many cases the improvements in force control algorithm performance can be attributed to implementation and hardware issues, more than to control architecture. A commonly overlooked issue is inaccuracy in the actuator model (Paljug et al., 1992). Several papers address the use of control strategies to deal with nonlinear or non-ideal characteristics of actuators (Xu et al., 1993; Qian and DeSchutter, 1992b; Qian and DeSchutter, 1992a; Wilfinger et al., 1993). Friction, backlash, saturation, and quantization noise, to name a few, will reduce system performance. For high performance, these kinds of nonlinearities must be addressed in the design of both the hardware and control system.

Impedance Control

Impedance control is a more general case of Force Control. Nearly all systems may be characterized by some kind of mechanical impedance or admittance. The robot is programmed to exhibit an impedance based on the task. Hogan suggests the use of impedance as a general way of thinking about contact interactions (Hogan, 1985). For instance, if the task is based on position control, the robot might be programmed to be very stiff. If the task involves contact with an object, a specific stiffness and damping may be required. Control of the impedance may be achieved a number of ways.

The interface between the manipulator and the environment should be viewed as a dynamic one, regardless of the actual control law. Given measurements of position, velocity and acceleration, and given an accurate force source, impedances may be generated actively by computing the appropriate force based on the position and its derivatives. In principle, it does not matter whether the force is generated using closed loop control or by open loop commands. Salisbury proposed a control law which created a programmable stiffness for a multi-degree of freedom hand (Salisbury and Craig, 1982) using open loop torque commands. The Whole Arm Manipulator also utilizes this approach (Salisbury et al., 1989).

A large number of researchers have studied the impedance control problem and as pointed out in (Goldenberg, 1992), (Wada et al., 1994), many control laws reduce to full-state feedback. As a result, many of the results that are reported are highly dependent on implementation issues of hardware and software (Glosser and Newman, 1994; Zhen and Goldenberg, 1994; Liu and Goldenberg, 1991; Colgate and Brown, 1994; Johansson and Spong, 1994; Kazerooni, 1985; Liu and Goldenberg, 1994; Seraji, 1994).

Impact or Transition Control

Control of a manipulator in free space is well understood. When contact is made with an environment of unknown dynamics the dynamic equations change. Several researchers have been studying the control of the transition from free-space to contact (and the impact that defines this transition). The use of integral feedback is proposed in (Youcef-Toumi and Gutz, 1989; Volpe and Khosla, 1993).

Xu reports some of the difficulties in controlling unexpected contact transitions (Xu et al., 1994). These include the change in dynamics associated with contact, the large force transients that occur during impact, the limits of position sensing in stiff environments and the usefulness of pre-filtering commands to the actuator. Interestingly, humans do not suffer from the same kinds of problems.

Research presented in (Hyde and Cutkosky, 1993) uses knowledge of the impact dynamics to shape the input. The control input can be "shaped" to avoid frequencies which excite the system dynamics.

1.3 Discussion

The work done in control algorithms and robot design has produced many useful results. Control research has made significant progress on the theoretical issues facing manipulator control and has identified many of the physical characteristics which make manipulation

difficult. Algorithms for controlling position, force and impedance under various conditions have been developed and proven to be effective on real systems. However, the non-ideal properties of robot hardware can have a large influence on control law efficacy. Often times the differences in the performance of various systems can be traced to their hardware characteristics.

Research on robot design has produced a number of designs which circumvent some of the non-ideal characteristics which were identified in the control literature. Reduction of endpoint impedance and transmission friction along with increased power density have produced a number of interesting designs which have shown improvement in various kinds of tasks.

Chapter 2

The Parallel Coupled Micro-Macro Actuator

The actuator design constraints mentioned in the section 1.2.1 have limited performance of robot hardware to date. In this section a new design which overcomes some of these problems is presented.

Figure 2-1 shows a schematic of this actuator concept. A large actuator is coupled via a compliant transmission to the joint axis. A micro-actuator is directly coupled to the joint axis. We refer to this concept as a *Parallel Coupled Micro-Macro Actuator* (PaCMMA- pronounced "Pack-ma").

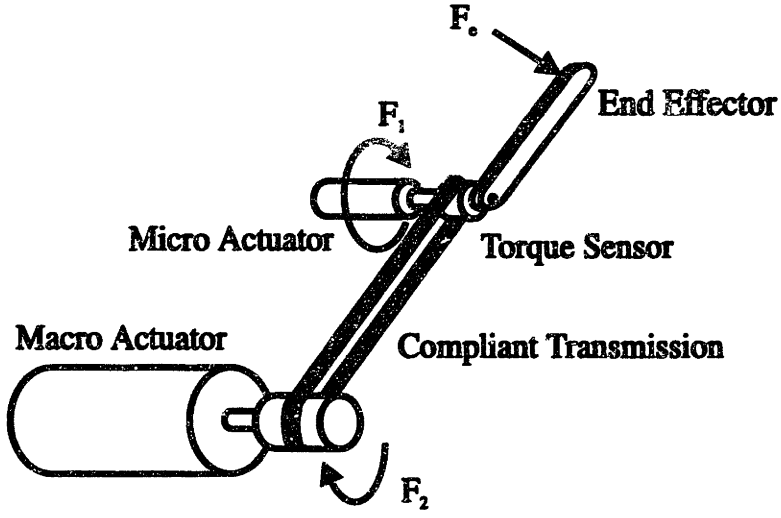

Figure 2-1: The Parallel Micro-Macro Actuator Concept

Consider the case where the stiffness of the transmission is zero, i.e., the micro-actuator is the only force acting on the output link. In this case force control may be achieved at high bandwidth due to the proximity of the sensor and the actuator. The lower limit on

controllable force is on the order of the brush friction, which results in a limit cycle or constant error. The upper limit on controllable force is limited by the saturation force of the micro-actuator.

Now allow the stiffness of the transmission between the actuators to increase. If the transmission stiffness is considerably lower than the environment stiffness then the micro-actuator closed loop performance (and stability and bandwidth) will be dominated by the stiffness of the environment. Consequently, the transmission can exert a force on the endpoint which is summed with the force of the micro-actuator without affecting the dynamics of the micro-actuator. The macro-actuator can be used to impose a low frequency force bias on the endpoint, which will have little effect on the control performance (stability) of the micro-actuator. The result is that we can now exert forces near the maximum of the macro-actuator while controlling variations at the level of the micro-actuator. A hi-fi loudspeaker provides a metaphor for this concept; the two actuators are a woofer and a tweeter, coupled in parallel by a compliant transmission, air (Pratt, 1994).

Several aspects of the design should be noted. First, the concept uses the "stiffer is better" paradigm to design the direct drive part of the system (the micro-actuator), but diverges from this principle for the macro-actuator. In fact the transmission between the two actuators must *not* be stiff for the concept to work. If the transmission were very stiff, the micro-actuator would "feel" the impedance presented by the macro-actuator and there would be no improvement in performance over the macro-actuator acting alone. Second, the concept allows the use of a lower performance actuator for the macro-actuator since its inertia and friction are "filtered" out by the transmission. Third, the concept allows a resolution bounded by the minimum controllable force of the micro-actuator and the maximum force of the macro-actuator. Micro-macro designs which are coupled in series can not achieve this kind of resolution; a series-coupled design is limited to the force range of the micro-actuator (until the actuator is at its position limit).

The PaCMMA concept may be implemented in a variety of ways. Figure 2-1 suggests that the micro-actuator should be placed proximal to the end effector. However, another instantiation of the design could place the actuators together with the end effector at a remote location as shown in figure 2-2. As long as the end effector is coupled to the micro-actuator with the stiffest transmission possible and the macro-actuator is coupled with a compliant transmission, the concept is the same. In fact, the two actuators could be inside one housing, provided the transmissions meet our design constraints.

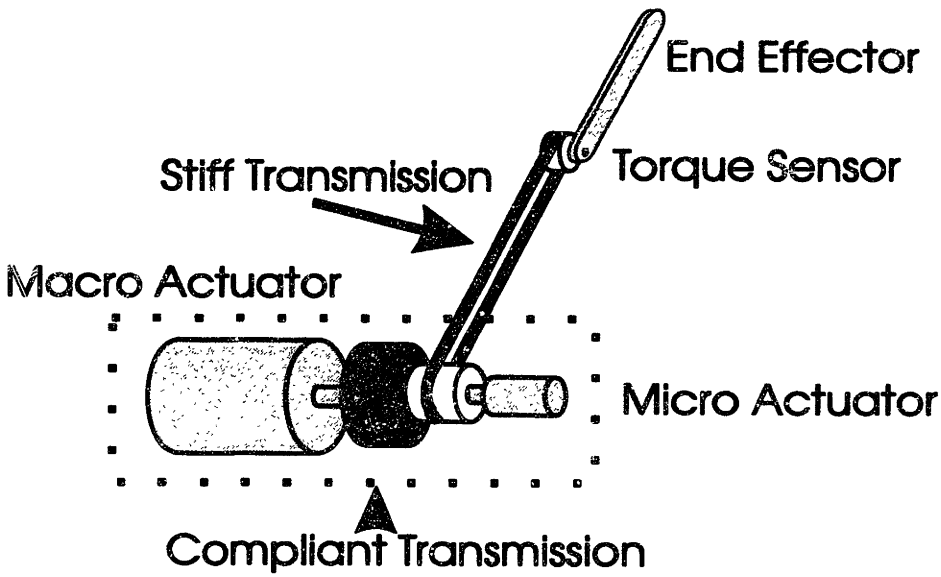

Figure 2-2: Alternative PaCMMA Configuration

Chapter 3

Actuator Systems And Performance Metrics

Evaluation of actuator technologies requires a careful look at the performance metrics available to the designer. Typically, the designer has some idea what kind of position and force control bandwidth the system should achieve. While these metrics quantify performance in some tasks quite well, most applications have additional constraints that are imposed on the design. Sometimes the device must tolerate accidental impacts with the environment or fail gracefully if the control system fails. Other times accuracy and resolution drive the design. As task complexity increases so does the number of important performance criteria. For a general purpose manipulator, there are a multitude of criteria which must be traded against one another.

This chapter defines the performance properties described in table 1.1. A quantitative method of measuring the properties is suggested whenever possible.

3.1 Properties of the Actuators and Sensors

Actuators and sensors are typically evaluated by the manufacturer across a large number of physical properties and performance specifications. In actuator systems the saturation force, inertia, and power ratings are commonly quoted while sensor systems are evaluated for resolution, linearity and accuracy. No attempt will be made to list all the component specifications which may be relevant. The most common specifications for actuator systems repeated below.

3.1.1 Quasi-static Properties

Quasi-static properties are those which can be measured while the system is in steady-state.

Peak Force

The peak force of an actuator is of obvious importance. Hayward proposes several peak force measures which are based on time intervals varying from 1 msec to continuous (a

smoke test) (Hayward and Astley, 1995). This is a useful distinction and measurement is straightforward.

Static Friction Force

Static friction force is the amount of force required to move the actuator when it is unpowered. This quantity should be specified at the output shaft if there is a reduction. Measurement may be accomplished by determining the force necessary to move the actuator from a resting position.

Force Resolution

The smallest measurable change in force is the force resolution. Most often, this is the resolution of a force sensing system where resolution is affected by sensor accuracy and noise as well as quantization noise if analog to digital conversion occurs.

Position Resolution

The smallest measurable change in position is the position resolution. In most cases, this is the resolution of a digital encoder, or the A/D resolution on an analog position sensor such as a linear potentiometer or resolver.

3.1.2 Dynamic Properties

Dynamic properties are those quantities which are measured when the system is moving. In mechanical components the inertia, damping, friction and backlash of the device are important. In electrical components slew rate, hysteresis and bias values are important. In actuator systems, the mechanical characteristics of inertia and acceleration dominate the system dynamics since they are typically slower than the electrical system.

Inertia

Inertia can be measured by applying known forces to the actuator and measuring the resulting acceleration. If friction is large, then the several trials must be run to determine the dynamic friction.

Peak Acceleration

Peak acceleration is the acceleration obtained when peak force is applied. Like peak force, a time interval should be specified. Measurement is straightforward.

Dynamic Friction Force

Dynamic friction force is the friction force applied to the actuator while moving. Measurement is most easily accomplished by applying a number of force transients to the device, recording the device acceleration and determining the net force applied to the actuator's moving element. Subtracting the net force from the total applied force yields the value of dynamic friction.

3.2 Properties of the Controlled System

Examination of inertia, backlash, and peak force will provide some idea of the system performance. Yet these measures fail to capture many of the characteristics which designers know are important. Force bandwidth, position bandwidth, position resolution, force resolution and backdrivability are just a few of the performance specifications which need to be considered. These specifications are not purely a function of hardware selection; the control system has a large influence on the performance as well. For example, certain control strategies may handle friction well but handle backlash poorly. Other control systems may not utilize the actuator's full power. For this reason it is imperative that actuator systems be evaluated with specific control laws.

3.2.1 Quasi-static Properties

As mentioned above, quasi-static properties are those properties which can measured while the system is in steady-state.

Force Precision

Force precision is the error in force when a steady state force is commanded. For example, a force error may exist and it may be measurable, but the chosen control law may not be able to eliminate it. This measurement should be expressed both as a percentage of full saturation and in units of force.

Position Precision

Position precision is the steady state position error. As with force precision, this quantity should be measured both as a percentage of the actuator system workspace and in units of position.

Force Dynamic Range

The ratio of the maximum controllable force to the minimum controllable force. Research on haptic displays suggests that the dynamic range of force plays an important role in creating a high fidelity display (Rosenberg and Adelstein, 1993).

3.2.2 Dynamic Properties

As mentioned above, dynamic properties of the controlled system are those quantities which are measured when the system is moving. These metrics are probably the most important in terms of overall system performance. Most of these metrics are frequency response measurements and can be performed using swept sinusoidal inputs. Additionally, most systems have saturation limits and the performance varies for small and large signal performance. Experiments should be specified for both small and large signals.

Position Response

Position response is the frequency response of the system to a sinusoidal position command while in free space. More specifically,

$$H_{pos}(\omega) = \frac{X(\omega)}{X_{des}(\omega)} \Bigg|_{F_e=0} \tag{3.1}$$

where

X_{des} = the desired position

X = the actual position

F_e = environmental force applied to the endpoint

This is a relatively common performance specification. The bandwidth is easily defined as the frequency at which the response function, H_{pos}, is attenuated by 3 decibels

Force Control Response

Force control bandwidth is the response of the system to sinusoidal force command with the endpoint stationary. Figure 3-1

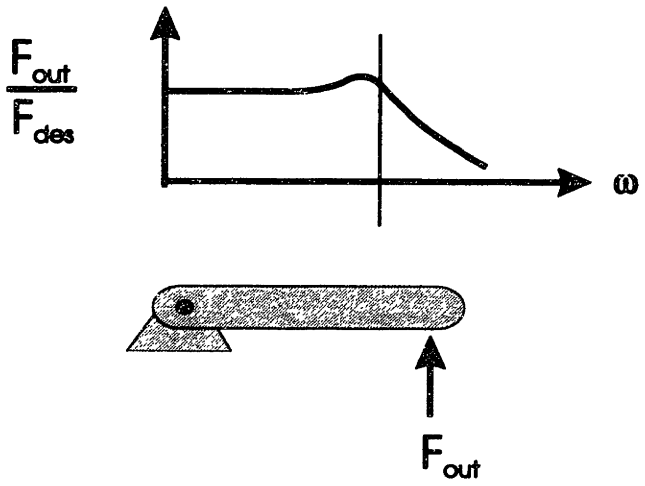

Figure 3-1: **Force Control Response.** Force control response is a frequency response measurement which is obtained with a fixed endpoint. The 3db point may be used to define force bandwidth.

Mathematically, this test is described as follows:

$$H_{fc}(\omega) = \frac{F_e(\omega)}{F_{des}(\omega)} \Bigg|_{X_e=0} \tag{3.2}$$

where

F_{des} = the desired force

F_e = the force exerted on the environment
X_e = the position of the end effector

This specification comes from the desire to quantify a robot's performance in quasi-static applications like slow manipulation or the control of a slipping object. In this case, the ability to modulate forces applied to a relatively motionless environment is of premium importance. Force control bandwidth, ω_{fc}, may be defined as the 3db point of the magnitude response of $H_{fc}(\omega)$.

Impedance

Actuator impedance is extremely important when the robot and the environment it contacts are in motion. Designers refer to "backdrivability" and "compliance" to describe the relationship between force and displacement of the actuator. In tasks such as surface following or dynamic contact sensing the actuator may be required to maintain constant force in the presence of small disturbances, whether the disturbances are due to small changes in position or unmodelled contact forces. In pure force control an ideal actuator would present zero impedance across all frequencies; in real systems this quantity should be as small as possible.

Impedance Response: The frequency response (transfer function) of the system to a position disturbance at the endpoint, i.e. the endpoint is connected to a position source while the desired force is commanded to be constant:

$$Z(\omega) = \left. \frac{F_{error}(\omega)}{X_{in}(\omega)} \right|_{F_{des}=\text{constant}}$$

where

$F_{error} = F_{des} - F_e$
X_{in} = the position disturbance

Impedance is best thought of as the forces that result from a position disturbance. An performed an experiment in which a robot link was placed on a moving cam, and given constant force command (An, 1986). Figure 3-2 depicts this experiment.

Distortion & Signal Fidelity

Distortion is an important, but often overlooked specification in robot actuator design. As interest in haptic interfaces has grown, it has become clear that human perception of distortion is quite good and that distortion of force signals in haptic display systems is undesirable. Figure 3-3 shows several force signals with varying degrees of distortion. The variation from a true sinusoidal signal may be measured in the least squares sense by computing the RMS error from a best fit sinusoid at the excitation frequency, ω:

Given a sequence of samples, T, a sinusoidal curve of frequency ω may be fit to the data using the equation:

$$RA = T$$

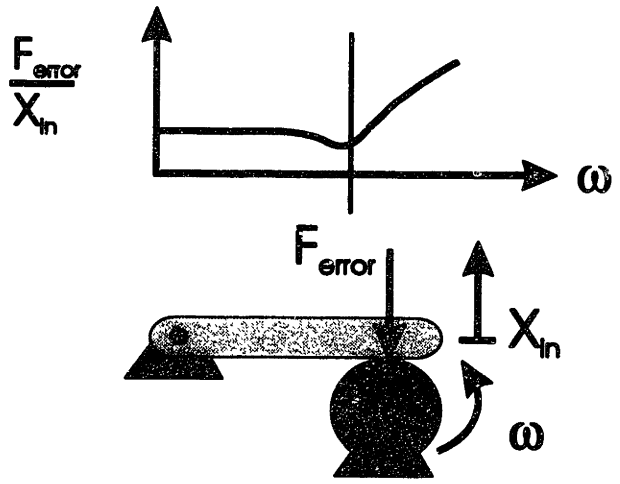

Figure 3-2: **Impedance Response.** Impedance response is a frequency response measurement which is obtained by commanding constant force and measuring the force error which results as the endpoint is moved. Impedance bandwidth may defined as the frequency where the force error begins to increase with frequency.

where

$$\begin{aligned} T &= \text{sampled signal} \\ R &= [\sin(\omega t)\ \cos(\omega t)] \\ A &= [c_1\ c_2]^T \end{aligned}$$

Solving the equation for the least squares minimum error,

$$A = (R^T R)^{-1} R^T T$$

Using the best fit signal, RA, a normalized measure of signal fidelity is:

$$\text{Signal Fidelity} = \frac{T^T RA}{T^T T}$$

or

$$\text{Signal Fidelity} = \frac{T^T R(R^T R)^{-1} R^T T}{T^T T}$$

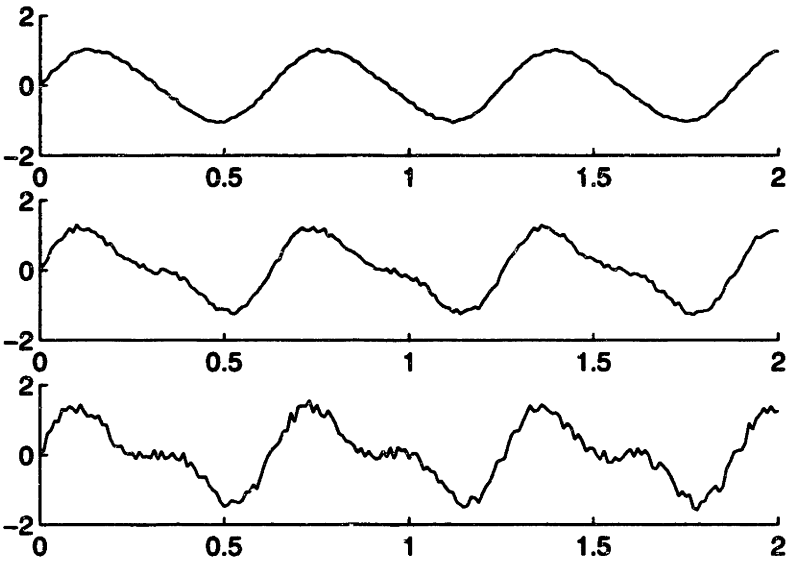

Figure 3-3: **Distortion Example.** These three graphs show examples of distorted signals. The values of Signal Fidelity for these graphs are 0.99, 0.86, and 0.74. Distortion is 1%, 14%, and 26% respectively.

The value of this matrix expression is 1.0 for a perfect sinusoid. A value of 0.99 represents 1.0% distortion.

Force Control Performance Space

All actuator systems have amplitude and frequency limitations. The performance of actuators can be visualized in a region I will call "Performance Space". The performance space is two dimensional with axes of frequency and amplitude much like a frequency response plot. Within this space there are regions where an actuator may operate with acceptable performance and there are regions where the performance is unacceptable. Figure 3-4 (left figure) shows an example of a typical force control performance space for an actuator. In this case, the shaded region represents values of amplitude and frequency where the actuator error is less than 10%.

Some actuators have the ability to exert large forces at lower frequencies, while other actuators have the ability to exert smaller forces at higher frequencies. Figure 3-4 (right figure) shows the theoretical operating regions of a micro and macro-actuator independently. The macro-actuator can attain a large force amplitude but is limited to relatively low frequencies while the micro-actuator can produce a smaller amplitude but at higher frequencies.

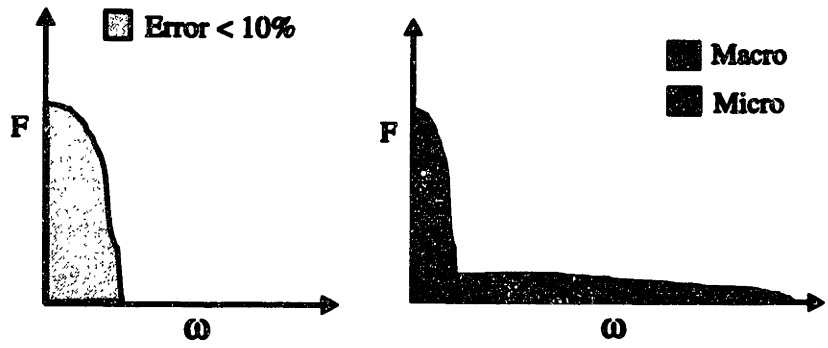

Figure 3-4: **Force Control Performance Space.** The regions are bounded by curves of constant error.

Controllable Impedances & Impedance Performance Space

The main reason to use force controlled actuators is to exploit the programmability of the device. Each actuator will have a range of impedances which it can accurately emulate. Pratt and Williamson have presented a useful method of displaying the impedances an actuator can emulate (Williamson, 1995; Pratt and Williamson, 1995). Much like the force performance space, this is an impedance performance space. Figure 3-5 illustrates this idea. The bounded region can be increased by increasing saturation torques, increasing sensor resolution and modifying the passive properties of the system (mass, stiffness, damping). For example, increasing saturation torque will allow the device to emulate a stiffer impedance whereas reducing the position resolution (less accurate) will reduce the stiffness that may be emulated.

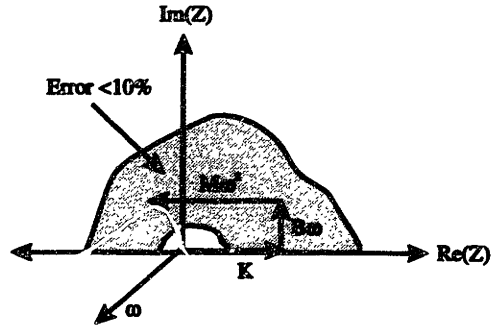

Figure 3-5: **Impedance Performance Space.** The actuator is programmed to create a desired impedance, $Z(\omega) = Ms^2 + Bs + K$ and the impedance response at each frequency is plotted in the complex plane using $s = j\omega$. If the actuator can produce the desired impedance with less than 10% error, then the impedance is contained in the shaded region; the region is bounded by a curve of constant error.

The manipulator impedance may be represented by a point in complex space. The users would like to be able to change the operating point and obtain a predictable impedance. However, non-ideal effects limit the operating region. Many parameters affect the location of the region in the complex plane: Saturation, inertia, sensor resolution, friction, backlash to name a few. To further complicate matters, the operating region for small displacement disturbances is not the same as the operating space for large displacements. To fully quantify performance, the operating region should be a three-dimensional solid, with disturbance amplitude as the third dimension.

Chapter 4

System Model and Performance Limits

All actuator systems have performance limitations that are based on saturation forces. The purpose of this chapter is to determine the maximum possible performance of the parallel coupled micro-macro actuator system operating at saturation. These results will be useful to the designer for determining best case system performance as well as providing a useful benchmark for evaluating control law performance. Much of the analysis presented here may be applied to any actuator design and would be useful in the comparison of various actuator systems.

4.1 Actuator Model

The actuator model will rely on several linear and nonlinear parameters and will be used to estimate some limits on performance. The actuator concept can be modeled using lumped elements as shown in figure 4.1. The dynamics are described by two equations:

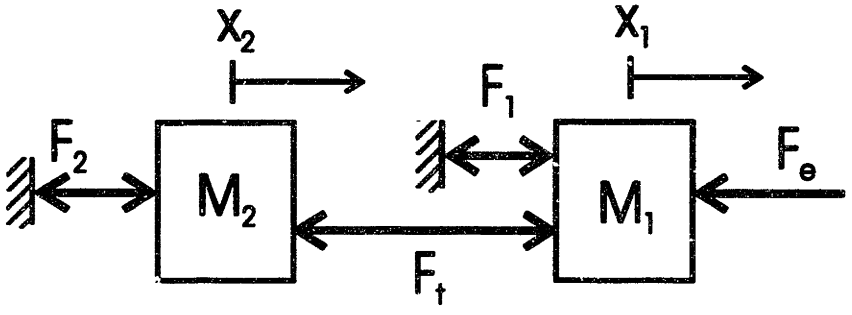

Figure 4-1: Parallel Coupled Micro-Macro Actuator Model

$$M_1\ddot{x_1} = F_1 + F_t(x_1 - x_2, \dot{x_1} - \dot{x_2}) - F_e \tag{4.1}$$

$$M_2\ddot{x}_2 = F_2 - F_t(x_1 - x_2, \dot{x}_1 - \dot{x}_2) \tag{4.2}$$

In general the input forces, F_1 and F_2, are bounded at the upper limits by some finite response time and some finite magnitude. For electric motors these limits are imposed by the electrical time constant and the motor's maximum power dissipation. In a hydraulic system these limits are imposed by the speed of the servo valve and the maximum fluid pressure and piston area of the actuator. In addition to these actuator limits, there is a bandwidth limit on force measurement. It is assumed that the force measurement bandwidth is much higher than the response bandwidth of the actuators and does not need to be included in the dynamic model.

In order to keep the model concise, the dynamics of the force sensor and the micro-actuator (F_1, M_1) will be lumped into a single function, $H_{1OL}(s)$. The function, $H_{1OL}(s)$, can be viewed as the combined open-loop force response of the force transducer and micro-actuator. Any micro-actuator can be controlled to have a well damped open loop response, $H_{1OL}(s)$, with bandwidth, ω_{1OL} without any loss of generality. This can be implemented in most systems by pre-filtering the input signal at a frequency below the first natural resonance of the system. As was pointed out by (Eppinger, 1988), control systems will have great difficulty trying to operate above the first natural resonance. To incorporate these facts in the model, I will introduce a low-pass function to limit the speed of response of the micro-actuator and two saturation parameters:

$H_{1OL}(s)$, the open loop micro actuator response
F_{1sat}, the saturation force of the micro-actuator
F_{2sat}, the saturation force of the macro-actuator

The macro-actuator also has limited bandwidth, $H_{2OL}(s)$. However, the bandwidth of F_2 will be effectively filtered by M_2 and the transmission, so $H_{2OL}(s)$ will be left out of the model.

The transmission dynamics are represented by the general function $F_t(x, \dot{x})$ which can be modeled more specifically as a spring and damper for most transmissions:

$$F_t(x, \dot{x}) = -K_t x - B_t \dot{x} \tag{4.3}$$

In this case, the equations become:

$$M_1\ddot{x}_1 = F_1 H_{1OL}(\omega) - K_t(x_1 - x_2) - B_t(\dot{x}_1 - \dot{x}_2) - F_e \tag{4.4}$$

$$M_2\ddot{x}_2 = F_2 + K_t(x_1 - x_2) + B_t(\dot{x}_1 - \dot{x}_2) \tag{4.5}$$

The environment force, F_e, can take on a number of values. In the case of an actuator in free space this may be an external force such as gravity or transmission friction acting on the load. In the case of manipulation this force may represent an environmental impedance (stiffness). Since the primary application for this actuator is manipulation, I will use a simple representation for the environmental force:

$$F_e = K_e X_1 \tag{4.6}$$

The value of the environmental stiffness, K_e, may be varied to model a wide variety of manipulation conditions. When the actuator is in contact with a very stiff environment, the contact dynamics are well modeled using this representation. In the case of free space motion the stiffness may be set to zero. This representation is also undamped. This has the benefit of being a "worst-case" environment. Undamped, stiff environments are among the most challenging of operating conditions because the slightest misuse of actuator energy will excite the environmental resonance. Further, the stiff environment makes active damping (through velocity measurement) difficult since the displacements are small.

Equations 4.4 and 4.5 represent the dynamics of the system with the two inputs. The transfer function formulation yields the following equation:

$$X_1(s) = \frac{(M_2 s^2 + B_t s + K) F_1 H_{1OL}(s)}{\Delta(s)} + \frac{(K_t + B_t s) F_2}{\Delta(s)} \tag{4.7}$$

where

$\Delta(s) = (M_1 s^2 + B_t s + K_t + K_e)(M_2 s^2 + B_t s + K_t) - (K_t + B_t s)^2$

and when $K_e = 0$,

$\Delta(s) = s^2(M_1 M_2 s^2 + B_t(M_1 + M_2)s + K_t(M_1 + M_2))$

This is a linear, fourth order system and we can examine the effect of each input independently. Insight may be gained from frequency response analysis of the system.

4.2 Frequency Response

The frequency response of the PaCMMA system is presented for both inputs and several operating cases to illustrate how the dynamics change with various environmental conditions (figures 4-2, 4-3, 4-4). The simulation values are listed in Appendix B. The output is taken to be the position of the endpoint, x_1, and consequently, the output magnitude will vary with the stiffness. A designer typically increases the transmission stiffness and decreases the mass of the endpoint so as to shift the first natural resonance to the largest possible value.

Examination of these figures will make several things clear. First, the dynamics of the system in free space are very different from the dynamics of the system in contact with the environment. In free space, the system is an integrator and the gain increases as the frequency decreases whereas the system in contact with the environment has constant gain at low frequencies. For this reason, control laws which work well in free space may not work well when the system is in contact with an environment; force feedback literature has shown that instability is a problem for stiff environments (section 1.2.2).

Consider only the first input, F_1. When the system is in free space, the phase portion of the plot reveals that the system lags the input by 180 degrees. To create a stable closed loop system, the bode phase-gain theorem requires that the phase lag be less than 180 degrees at unity gain. For the free-space system, this requires the introduction of phase lead (derivative gain).

When the system is in contact with a spring-like environment, the dynamics are quite

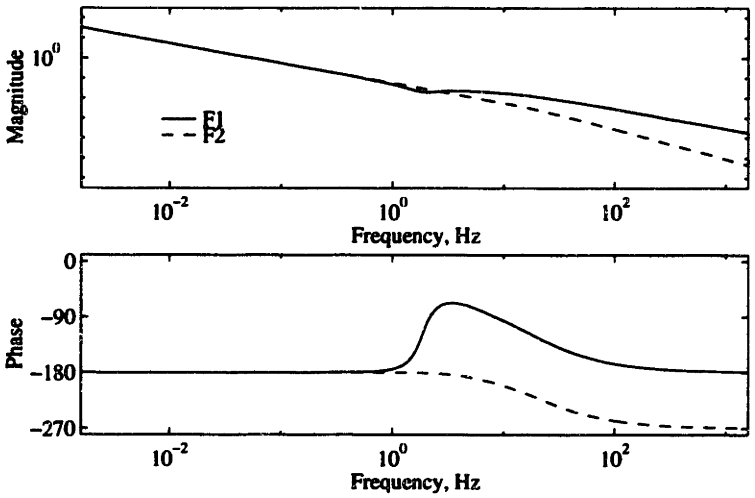

Figure 4-2: **Frequency Response in free space.** $\frac{X_1(s)}{F1(s)}, \frac{X_1(s)}{F2(s)}$ where X_1 is the displacement of the endpoint, F_1 is the force command to the micro-actuator and F_2 is the force command to the macro-actuator.

different. In this case, the system has a large amount of phase margin and the loop gain may be increased dramatically with the addition of pure integral gain. The 90 degree lag introduced by integral gain is relatively unimportant since the system shows zero lag up to its resonant frequency. Further, when the environment is stiff addition of phase lead from a position derivative is quite difficult since the position changes are small. The dynamics of the actuator will be discussed again when the control law for the actuator is described.

In the following sections, the performance of the actuator will be evaluated under several performance metrics.

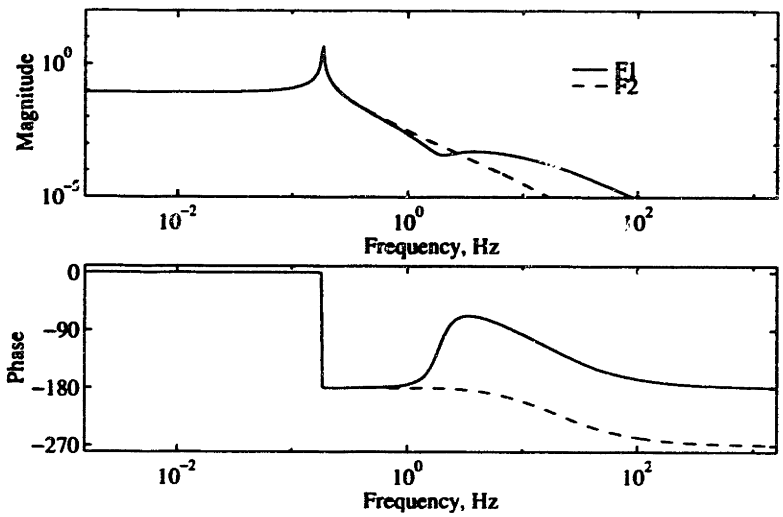

Figure 4-3: **Frequency Response with a soft environment.** $\frac{X_1(s)}{F1(s)}, \frac{X_1(s)}{F2(s)}$ where X_1 is the displacement of the endpoint, F_1 is the force command to the micro-actuator and F_2 is the force command to the macro-actuator.

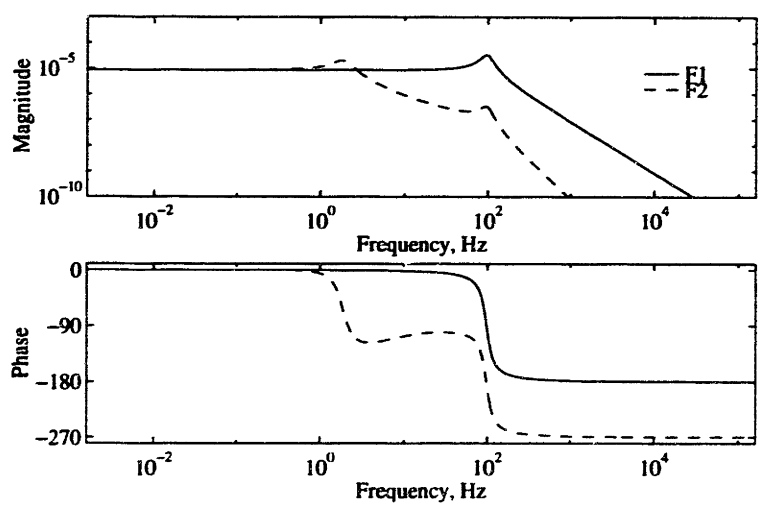

Figure 4-4: **Frequency Response with a stiff environment.** $\frac{X_1(s)}{F1(s)}, \frac{X_1(s)}{F2(s)}$ where X_1 is the displacement of the endpoint, F_1 is the force command to the micro-actuator and F_2 is the force command to the macro-actuator.

4.3 Position Control Performance

This section addresses the performance limits of the PaCMMA model while in free space. When the actuator is in free-space (i.e. $K_e = 0$), the system position may be commanded to follow a position trajectory. Force saturation of the actuator limits the maximum acceleration and therefore, the bandwidth of the system. If perfect knowledge of the past and future inputs is assumed an estimate of the best case performance of the actuator can be easily determined. (The following analysis may be used on any dynamic system with saturation limits.)

Consider the case where a sinusoidal trajectory is desired. The actuator may operate in two regions. The first region is where the desired output may be achieved without saturating the actuators. In the second region, the actuator can not achieve the desired output because the actuators have saturated. The boundary of these two regions is the operating point where both actuators have saturated, *and* the desired trajectory is being achieved. At this point, the two actuator inputs are:

$$F_1 = F_{1sat}\sin(\omega t)$$

and

$$F_2 = F_{2sat}\sin(\omega t + \phi)$$

Substituting into equation 4.7,

$$X_1(s) = \frac{(M_2 s^2 + B_t s + K)}{\Delta(s)} H_{1OL}(s)\,\mathcal{L}\{F_{1sat}\sin(\omega t)\} \tag{4.8}$$

$$+ \frac{(K_t + B_t s)}{\Delta(s)}\,\mathcal{L}\{F_{2sat}\sin(\omega t + \phi)\} \tag{4.9}$$

where

$\Delta(s) = s^2(M_1 M_2 s^2 + B_t(M_1 + M_2)s + K_t(M_1 + M_2))$

and

$\mathcal{L}$ is the Laplace Transform.

In order to maximize X_1, ϕ must be chosen with the appropriate phase such that the vector contributions from F_1 and F_2 are in the same direction:

$$\phi = \tan^{-1}\left(\frac{B_t\omega}{K_t - M_2\omega^2}\right) - \tan^{-1}\left(\frac{B_t\omega}{K_t}\right) \tag{4.10}$$

When this occurs, the magnitude of X_1 may be shown to be:

$$X_1(\omega) = \sqrt{\frac{(K_t - M_2\omega^2)^2 + (B_t\omega)^2)}{\Delta(\omega)}} F_{1sat} + \sqrt{\frac{(K_t{}^2 + (B_t\omega)^2)}{\Delta(\omega)}} F_{2sat} \tag{4.11}$$

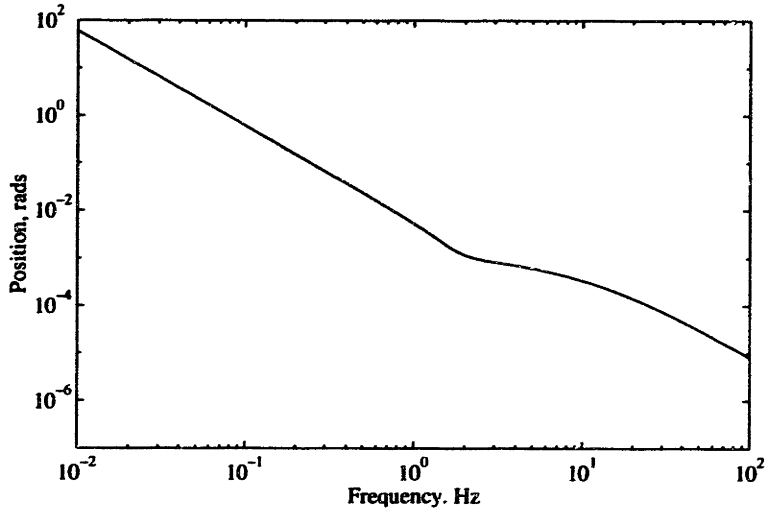

Figure 4-5: **Maximum Position Response.** This figure shows the position response if both actuators are saturated and their forces are summing constructively. It provides an upper bound on the achievable position bandwidth.

This equation represents the relationship between amplitude of displacement and frequency of excitation. It is a theoretical limit on the maximum achievable displacement at a given frequency. (Note that the magnitude axis has units of displacement, unlike a typical frequency response magnitude plot where units are dimensionless and expressed in decibels.) In practice, few systems ever operate at this limit due to unmodelled dynamics and control law implementation issues. A system operating in this region will not respond to corrective measures and is typically in danger of becoming uncontrollable. While actuators may saturate under various operating conditions, the actual system frequency response must lie on or below the line described by the equation above.

4.4 Force Control Performance

Force control response is a measure of the system response to both changes in the desired force and force disturbances. Chapter 3 introduced this definition, and it is repeated here:

$$H_{fc}(\omega) = \left. \frac{F_e(\omega)}{F_{des}(\omega)} \right|_{X_e=0} \tag{4.12}$$

where

F_{des} = the desired force

F_e = the force exerted on the environment

X_e = the position of the end effector

Using the argument of the previous section we can determine the maximum possible force control response. The operating point where the output force is maximized is:

$$F_1 = F_{1sat}\sin(\omega t)$$

and

$$F_2 = F_{2sat}\sin(\omega t + \phi)$$

The assumption of perfect control means that for a desired amplitude, we can select ϕ so that there is no phase difference in the contribution from each actuator and the applied force will be maximized. For this case, the force output in the frequency domain is:

$$F_e(s) = F_{1sat}H_{1OL}(s) + \frac{F_t(s)}{F_t(s) + M_2 s^2}F_{2sat}$$

Using a traditional spring/damper model for the transmission ($F_t(s)/\Delta X(s) = B_t s + K_t$), this function becomes:

$$F_{des}(s) = F_{1sat}H_{1OL}(s) + \frac{F_{2sat}}{\frac{M_2}{K_t}s^2 + \frac{B_t}{K_t}s + 1} \tag{4.13}$$

The second term in equation 4.13 is readily recognized as forced harmonic vibration where M_2 is being driven by F_2. Figure 4-6 shows how the two inputs are summed to determine the maximum amplitude of the system output. The function may be inverted to determine the maximum achievable amplitude at a given frequency, i.e. when the actuator is driven to saturation in order to meet the desired trajectory. As an example, if the desired torque is 1.0mNm, then the maximum frequency is easily determined through graphical means to be 3.92Hz. This equation represents a relationship between desired amplitude and maximum operating frequency and represents a fundamental hardware limit of the system.

4.5 Impedance Performance

Impedance performance of the PaCMMA will be one of its most important characteristics. The low mass of the micro-actuator and the compliant transmission will produce much lower impedance at the same bias forces than could be achieved with the macro-actuator alone. Impedance performance was defined in Chapter 3 and is repeated below.

$$Z(\omega) = \left.\frac{F_{error}(\omega)}{X_{in}(\omega)}\right|_{F_{des}=\text{constant}}$$

In the case of impedance response, perfect control is taken to be the control strategy which maximizes the apparent admittance and minimizes the impedance of the PaCMMA. This is equivalent to maximizing x_1. Using equations 4.1 and 4.2 we can derive an expression

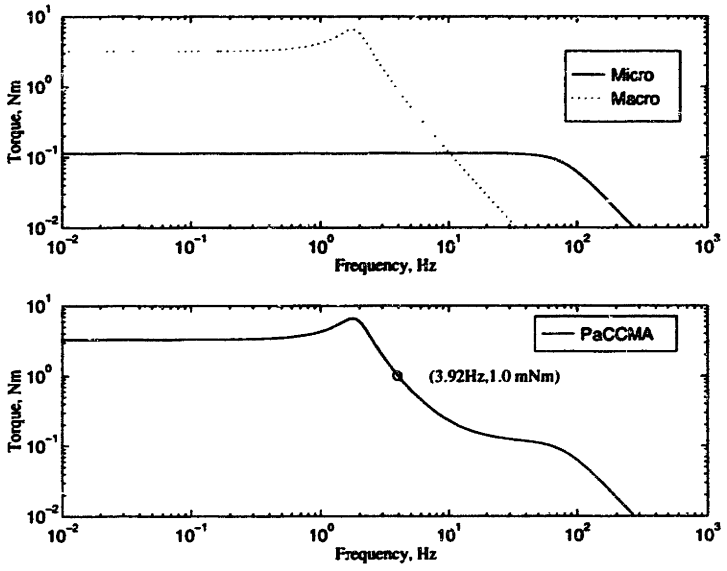

Figure 4-6: **Maximum Force vs. Frequency.** The top graph shows the micro and macro-actuator responses independently while the bottom graph shows the PaCMMA response. The PaCMMA response is the sum of the two responses due to the parallel arrangement.

for x_1 which contains three driving terms (F_1, F_2, F_e):

$$X_1(s) = \frac{(F_1(s)H_{1OL}(s) - F_e(s))(M_2s^2 + B_ts + K_t) + F_2(s)(B_ts + K_t)}{s^2(M_2M_1s^2 + B_t(M_1 + M_2)s + K_t(M_1 + M_2))} \tag{4.14}$$

For the purposes of a frequency response analysis, we can take $F_e(t)$=$A\sin(\omega t)$. In order to maximize the amplitude of $X_1(s)$, the contributions from F_1 and F_2 should be given the necessary phase to add to the response from $F_e(t)$. $X_1(s)$ is maximized when:

$$F_1(t) = -\frac{F_{1sat}}{H_{1OL}}\sin(\omega t) \tag{4.15}$$

and

$$F_2(t) = -F_{2sat}\sin(\omega t + \phi) \tag{4.16}$$

This case is similar to the case of pure position control, except that the environment force, F_e, appears in the equation. The admittance of the PaCMMA can now be written:

$$\begin{aligned}\frac{X_1(s)}{F_e} &= \frac{(\frac{F_{1sat}}{F_e}H_{1OL}(s) - 1)(M_2s^2 + B_ts + K_t)}{\Delta(s)} \\ &+ \frac{\frac{F_{2sat}}{F_e}(B_ts + K_t)(\cos(\phi) + \sin(\phi)s)}{\Delta(s)}\end{aligned} \tag{4.17}$$

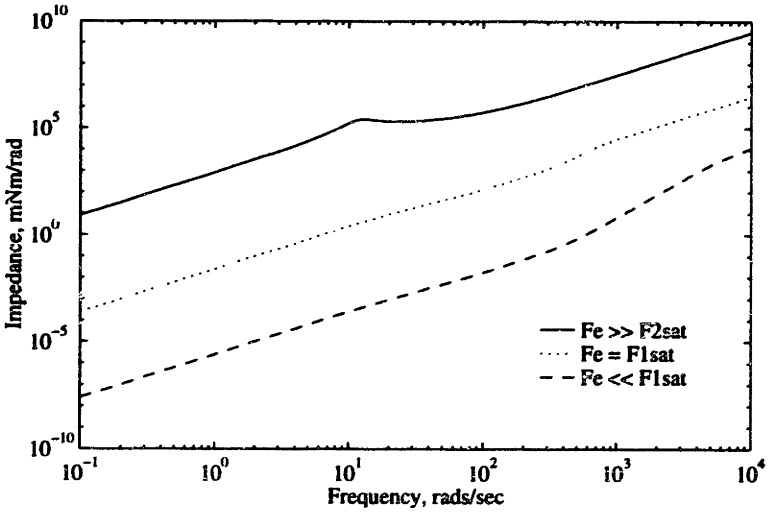

Figure 4-7: **Minimum Impedance vs. Frequency.** The impedance response, $F_e(s)/X_1(s)$, is dependent on the magnitude of the disturbance force, F_e.

Equation 4.17 is very similar to the system response in position control and the impedance response of the system is roughly the reciprocal of the position response. This is not surprising since the actuator must move its endpoint mass in both cases. Secondly, the minimum achievable impedance is dependent on the magnitude of F_e. Finally, it is important to remember that this expression represents the best possible performance, under perfect control. In general, we do not have full knowledge of the disturbance input, F_e and as a result, the minimum achievable impedance will be considerably higher. Figure 4-7 shows a typical plot for the actuator impedance, $F_e(s)/X_1(s)$.

Careful analysis of the transfer functions in the preceding section suggests that with perfect control, lower impedance and higher position control bandwidth may be achieved with a stiffer transmission. However, the control law has limited bandwidth and the dynamics of the undriven system will dominate the system at frequencies above that bandwidth. In manipulation, collisions are part of normal interaction and impacts typically contain high frequencies. In these cases, low impedance can only be achieved through passive methods such as a low inertia and a soft transmission. This issue will be discussed in greater detail in section 4.7

4.6 Force Step Response

Time domain performance is another important benchmark for the actuator system. In manipulation tasks time domain specifications are a useful way to evaluate the system's response to sudden changes in the desired force and position.

Force step response will be computed under the same conditions as force control response in the section above, i.e. a fixed endpoint. Further, it is assumed that the micro-actuator

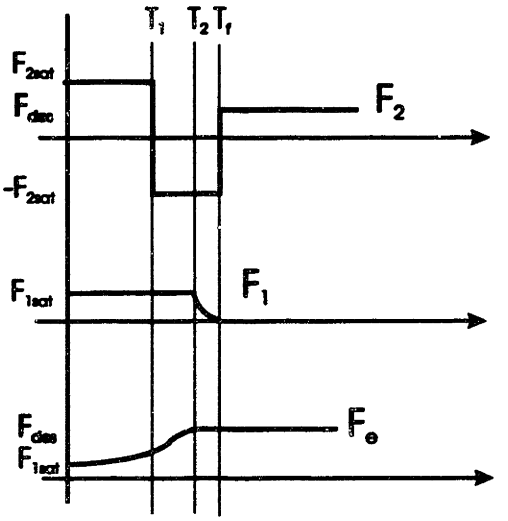

Figure 4-8: Control strategy for a step change in force

force, F_1, responds much more quickly than the force imposed by the macro-actuator, $K_t\Delta x + B_t\Delta\dot{x}$. For a step input in desired force, the fastest possible response is achieved by applying full saturation force to both actuators, then reversing F_2 at t_1 and finally stopping both masses at the desired force (position) at t_2. In the final resting position, F_1 should be zero to ensure that the response to random transients will be as fast as possible. Figure 4-8 presents these events graphically.

The minimum settling time for F_e is determined by t_2. Equation 4.5 may be solved directly for $x_2(t)$. On the interval $[0, t_1]$,

$$x_2(t) = \frac{F_{2sat}}{K_t}\left(1 - \frac{e^{-\zeta\omega_n t}}{\sqrt{1-\zeta^2}}\sin\left(\sqrt{1-\zeta^2}\omega_n t + \phi\right)\right)$$

where

$$\zeta = \frac{B_t}{2\sqrt{K_t M_2}}$$

$$\omega_n = \sqrt{K_t/M_2}$$

$$\phi = \tan^{-1}\left(\frac{\sqrt{1-\zeta^2}}{\zeta}\right)$$

On the interval $[t_1, t_f]$,

$$\begin{aligned} x_2(t) &= e^{-\zeta\omega_n(t-t_1)}\left(\left(x_2(t_1) + \frac{F_{2sat}}{K_t}\right)\cos\left(\sqrt{1-\zeta^2}\,\omega_n(t-t_1)\right)\right. \\ &+ \left.\frac{\dot{x}_2(t_1) + \left(\frac{F_{2sat}}{K_t} + x_2(t_1)\right)\zeta\omega_n}{\sqrt{1-\zeta^2}\,\omega_n}\sin\left(\sqrt{1-\zeta^2}\,\omega_n(t-t_1)\right)\right) \end{aligned}$$

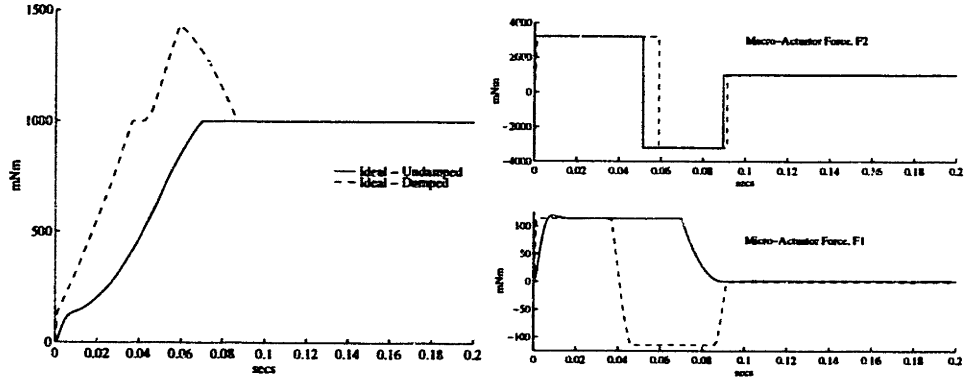

Figure 4-9: **System Step Response - Perfect Control.** $\zeta = 0.25$ for damped case

These two equations can be solved numerically for t_1 and t_f using the boundary conditions. Finally, the equation for t_2 may be solved:

$$F_{des} = F_{1sat} + K_t x_2(t_2) + B_t \dot{x}_2(t_2)$$

Figure 4-9 shows the response of the system to this strategy. It is important to remember that this solution gives the minimum settling time solution. The applied force, $K_t x_2 + B_t \dot{x}_2$, will exceed F_{des} if the transmission damping, B_t, is nonzero. Another interesting feature of this simulation are the discontinuities in the applied force. These small discontinuities reflect the response of the micro-actuator. Consider the case of the damped transmission, when the applied force is sufficiently close (within F_{1sat} of the desired force) the micro-actuator can cancel the error. With the use of optimal control techniques (dynamic programming), equation 4.5 may be solved with additional constraints such as a requirement that the applied force not exceed some fraction of the desired force: $(1 + \alpha)F_{des} > (K_t x_2 + B_t \dot{x}_2)$.

4.7 Impacts

In many applications, a manipulator moves from free space into contact with the environment and an impact results. Sometimes the collision occurs because there are unexpected errors in the position of the manipulator or the environment. Other times the collision is part of a deliberate manipulation movement. In both cases, it is useful to determine the effects of the impact on the environment and the actuator.

Consider the case of a manipulator moving in free space which suddenly detects a collision, as shown in figure 4-10. Perfect control in this case requires that both actuators are turned on to full saturation force in order to reverse the collision as soon as the collision is detected. A discussion of the dynamics follows.

The conditions are tabulated in table 4.1. At $t = 0$, the collision occurs and energy is transmitted to the environment. At $t = t_1$, the collision is detected and the actuator

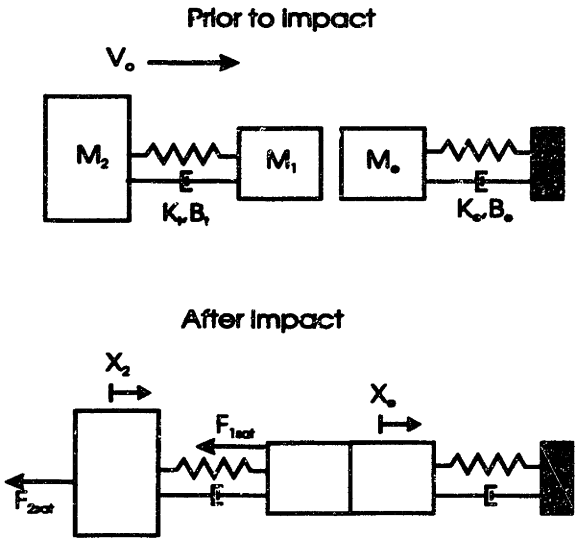

Figure 4-10: Impact - Perfect Control

torques, F_1, F_2 are set to full saturation. At $t = t_2$, the displacement of the transmission reaches its maximum and the contact force begins to decrease. After this point in time, higher level control determines whether the manipulator should maintain or break contact with the environment.

Two quantities are of interest during the collision. The first is the energy dissipated when M_1 hits the environment and the second is the maximum force transmitted by the transmission to the environment. In the case where the collision is inelastic the energy

	$t = 0^-$	$t = 0^+$	$t = t_1$	$t = t_2$
x_1	0			
$\dot{x_1}$	V_c	$\frac{M_1}{M_1+M_e}V_o$		0
x_2	0			
$\dot{x_2}$	V_o	V_o		
x_e	0	x_1	x_1	x_1
$\dot{x_e}$	0	$\dot{x_1}$	$\dot{x_1}$	$\dot{x_1}$
F_1	0	0	$-F_{1sat}$	$-F_{1sat}$
F_2	0	0	$-F_{2sat}$	$-F_{2sat}$
F_e	0		$K_e x_1 + B_e \dot{x_1}$	$F_{max}=K_e x_1$

Table 4.1: Impact Dynamics

transmitted to the environment is:

$$\Delta E = \frac{M_1 M_e}{M_1 + M_e} \frac{V_o^2}{2} \tag{4.18}$$

If the transmission damping B_t is large, then the transmission is effectively rigid during impact and nearly all the kinetic energy of the macro-actuator is transmitted to the environment. This is generally undesirable and therefore, the transmission should not be heavily damped if impacts are likely.

After the collision but before detection, the displacement of the macro-actuator is described by:

$$x_2(t) = e^{-\zeta\omega_n t} \frac{V_o}{\omega_n} \frac{1}{\sqrt{1-\zeta^2}} \sin\left(\sqrt{1-\zeta^2}\omega_n t\right) \tag{4.19}$$

$$\dot{x}_2(t) = e^{-\zeta\omega_n t} V_o \frac{-1}{\sqrt{1-\zeta^2}} \sin\left(\sqrt{1-\zeta^2}\omega_n t + \phi\right) \tag{4.20}$$

where

$\phi = \tan^{-1}\left(\frac{\sqrt{1-\zeta^2}}{-\zeta}\right)$

If B_t is assumed to be small the force exerted on the environment by the macro-actuator is given by:

$$F_{macro} = K_t x_2 = \sqrt{K_t M_2} V_o \sin\left(\sqrt{\frac{K_t}{M_2}} t\right) \tag{4.21}$$

Equation 4.21 highlights several issues. If the transmission stiffness, K_t, is large then two bad things happen. First, F_{macro} becomes large because the force changes rapidly as $x_2 - x_1$ changes. Secondly, the detection time, t_1 becomes large compared to the natural frequency of the system, $\sqrt{\frac{K_t}{M_2}}$, and the sine function reaches its maximum value (1.0) thereby increasing F_{macro}. Reducing the transmission stiffness decreases the rate of force application by the macro-actuator. Since all systems have finite response time, transmission compliance can be effective in reducing the force applied during impact.

In the general case, the maximum contact force may be determined by solving a series of equations. The general equations and solution method are presented below.

Computing the Laplace transforms on each state yields:

$$\begin{aligned} X_1(s) &= \frac{(K_t + B_t s)X_2(s) + U_1(s) + IC_1(s)}{\Delta_1(s)} \\ IC_1(s) &= (M_1 + M_e)\dot{x}_1(0^+) + ((M_1 + M_e)s + B_t + B_e)x_1(0^+) - B_t x_2(0^+) \\ \Delta_1(s) &= (M_1 + M_e)s^2 + (B_t + B_e)s + K_t + K_e \end{aligned} \tag{4.22}$$

$$X_2(s) = \frac{(K_t + B_t s)X_1(s) + U_2(s) + IC_2(s)}{\Delta_2(s)}$$

$$\begin{aligned} IC_2(s) &= M_2\dot{x}_2(0^+) + (M_2 s + B_t)x_2(0^+) - B_t x_1(0^+) \\ \Delta_2(s) &= M_2 s^2 + B_t s + K_t \end{aligned} \tag{4.23}$$

Solving for each state gives:

$$\begin{aligned} X_1(s) &= \frac{(K_t + B_t s)(U_2(s) + IC_2(s)) + \Delta_2(s)(U_1(s) + IC_1(s))}{\Delta_1(s)\Delta_2(s) - (K_t + B_t s)^2} \\ X_2(s) &= \frac{(K_t + B_t s)(U_1(s) + IC_1(s)) + \Delta_1(s)(U_2(s) + IC_2(s))}{\Delta_1(s)\Delta_2(s) - (K_t + B_t s)^2} \end{aligned} \tag{4.24}$$

On the interval t=$[0^+, t_1]$ the initial conditions and inputs in table 4.1 may be substituted to get:

$$X_1(s) = \frac{(M_e + M_1)\dot{x}_1(0^+)\Delta_2(s) + (K_t + B_t s)M_2 V_o}{\Delta_1(s)\Delta_2(s) - (K_t + B_t s)^2} \tag{4.25}$$

$$X_2(s) = \frac{M_2 V_o \Delta_1(s) + (K_t + B_t s)(M_1 + M_e)\dot{x}_1(0^+)}{\Delta_1(s)\Delta_2(s) - (K_t + B_t s)^2} \tag{4.26}$$

Inversion of the two equations using the inverse Laplace Transform will yield a time-domain solution to the system dynamics and the values of $x_1(t_1)$, $\dot{x}_1(t_1)$, $x_2(t_1)$, and $\dot{x}_2(t_1)$ may be determined on the interval t=$[0^+, t_1]$. At $t = t_1$, the system equations must be solved using $x_1(t_1)$, $\dot{x}_1(t_1)$, $x_2(t_1)$, and $\dot{x}_2(t_1)$ as initial conditions and non-zero inputs.

$$\begin{aligned} X_1'(s) &= \frac{(K_t + B_t s)(-F_{2sat} + M_2\dot{x}_2(t_1) + (M_2 s + B_t)x_2(t_1) - B_t x_1(t_1))}{\Delta_1(s)\Delta_2(s) - (K_t + B_t s)^2} \\ &+ \frac{\Delta_2(s)(-F_{1sat} + (M_1 + M_e)\dot{x}_1(t_1) + ((M_1 + M_e)s + B_t + B_e)x_1(t_1) - B_t x_2(t_1))}{\Delta_1(s)\Delta_2(s) - (K_t + B_t s)^2} \end{aligned}$$

The expression for $sX_1'(s)$ may be inverted to determine the velocity as a function of time. Setting the velocity equal to zero and solving for time will give the value of $t_2 - t_1$. The value of $t_2 - t_1$ may then be used to determine the force on the environment by direct substitution into the expression $F_{max} = K_e x_1'(t_2 - t_1) + B_e \dot{x}_1'(t_2 - t_1)$.

Several conclusions may be drawn from this model. First, it is clear from equation 4.18 that reduction of the endpoint mass of the actuator, M_1, and the approach velocity, V_o, will minimize the energy delivered to the environment when contact occurs. This result is independent of any control strategy or actuator limit and represents very real physical limit on performance. Second, equation 4.21 shows that reducing K_t, the transmission stiffness, M_2, the macro-actuator mass, and t_1, the time it takes to detect a collision, will reduce the impact energy and contact force resulting from the macro-actuator. In effect, the transmission shields the environment from the mass of the macro-actuator by using the spring to store energy rather than dissipating the energy in a collision and by using

a soft transmission to decrease the rate of force increase once contact occurs. Decreasing the rate of force rise allows more time for the controller and actuator force to decelerate M_2. It should be noted that this analysis may be applied to any manipulator impact, not just the PaCMMA. This analysis shows that a traditional stiff manipulator will transmit more energy to the environment on contact and will generate greater contact forces than a compliant manipulator.

4.8 Causal Control

The control relations derived in the previous section assume an unrealistic amount of information - they assume that the desired force and any disturbances are known for both the past and future. A more reasonable approach assumes that one has some amount of knowledge about the current state and perhaps some past state history upon which to base the current control efforts. Under these assumptions, the system bandwidth will be lower. Nonetheless, the metrics provided above may be used to determine upper bounds on system performance. When the control law is developed in Chapter 5, these metrics will prove useful for evaluating the control system performance.

4.9 Consideration of Nonlinearities

In addition to force saturation, the PaCMMA system contains several other nonlinearities. Some of these nonlinearities may be avoided using different system configurations while others are present in all configurations. The analyses above do not specifically address these nonlinearities but some comments are presented below.

4.9.1 Stiction

With a brushed motor, stiction from motor brushes and bearings at the endpoint can produce a limit cycle at some minimal force level (Townsend, 1988). Even the best control law for F_1 will produce some small force error. Townsend quantified this error and showed that it is best to minimize any system friction between the actuator and the endpoint.

Stiction which occurs in the macro-actuator is filtered out by the transmission because small changes in position (limit cycles) are passed through the transmission as extremely small changes in force. As long as the damping in the transmission is minimal, then the stiction limit cycle will not have a significant effect on the endpoint force. This is one outstanding benefit of using a compliant transmission.

4.9.2 Velocity Saturation

Velocity saturation may occur independently of force saturation, especially in systems which employ large reductions on the macro-actuator or low voltage power supplies. Velocity saturation in the micro actuator is unlikely since manipulation speeds are typically low. In most cases velocity saturation may be avoided in the macro actuator by using a more forceful actuator with a smaller reduction (lower torque density)

4.9.3 Position Saturation

The model presented above assumes that neither actuator has limits on position displacement. This is generally a valid assumption for electric motors and other rotary actuators. Some actuators have limited displacement capability (voice coils, hydraulic cylinders) and this limitation may present a significant constraint on the performance of the system. Since the actuators act in parallel, both actuators must be capable of traveling the full displacement range. This is distinctly different from the serial micro-macro configuration in which the micro-actuator needn't have the full position range of the system.

4.9.4 Backlash

Because backlash can introduce harmonic frequencies above the driving frequency, a macro-actuator with backlash can introduce force disturbances above the controllable frequencies of both the macro and micro-actuators. This can happen any time the gearhead is unloaded which occurs when the transmission deflection is small or when the position changes in the macro-actuator position are very fast. Precise force generation is the main purpose of this design and backlash can defeat this purpose.

4.9.5 Transmission Dynamics

The transmission model used in this analysis is massless (i.e. K_t and B_t). A real transmission has mass and dynamics which may or may not affect the performance of the system. For example, a transmission which has high frequency resonances may produce disturbances above the controllable frequency of the micro-actuator. In this situation several actions may be taken. First, the transmission may be redesigned to have lower frequency dynamics via the addition of mass or damping. Second, the control algorithm may be modified to avoid exciting the transmission resonance.

4.10 Summary

The performance limits derived in this chapter provide guidance for the designer as well as highlighting the design advantages of the PaCMMA concept. The reduced mass of the micro-actuator, M_1, and the intentional use of compliance in the transmission result in lower impact forces than could be achieved with the macro-actuator alone using a stiff transmission. The micro-actuator can produce high force control bandwidth up to it's saturation torque. The position bandwidth of the device is limited by the acceleration values of the actuators, F_1/M_1 and F_2/M_2.

Chapter 5

Control System

In manipulation, a wide range of dynamic events may occur. Users of robotic manipulators or other dynamic machines would generally like the devices to be able to follow positions accurately in free space, to make contact with objects in the environment in a non-destructive manner, and to be able to maintain contact with a wide variety of environments. During these operations, particularly contact, the user typically wants motions to be smooth, stable and predictable. The PaCMMA concept performs these tasks well while using a single control system. This chapter addresses some of the control issues of the parallel coupled micro-macro actuator system.

5.1 Control Issues

As mentioned in Chapter 1, control of manipulation forces against stiff environments is very difficult when the actuator and sensor are not collocated. The achievable control bandwidth is limited by the structural bandwidth of the transmission (Eppinger, 1988). For this reason, transmissions are typically made quite stiff. However, most transmissions are insufficiently damped and adding damping to the transmission is hard to accomplish computationally since derivatives are difficult to calculate with very small displacements. Typical position encoders impose significant limits on velocity computation in this case.

A second issue is the control of the transition from free space to contact with the environment. The robot may be damaged as a result of the energy dissipated during the collision. As shown in section 4.7, reducing the mass and the approach velocity help prevent this. Second, the control law may become unstable when the actuator contacts the environment due to the change in dynamics. As mentioned in section 1.2.2, control of impacts and contact transitions has typically involved switching control algorithms.

The ability to continuously modify the system impedance is the primary benefit that force control actuators offer over a position controlled actuator with passive elements on the endpoint. An ideal actuator would allow the user to continuously adjust the impedance of the system so that the system could be stiff when contacts were unlikely, softer when an impact is expected and perhaps stiffer again when contact has been established. The ideal system would remain stable in all environments despite these changes. Colgate introduces the requirement of "passivity" and proposes several techniques for designing a control system

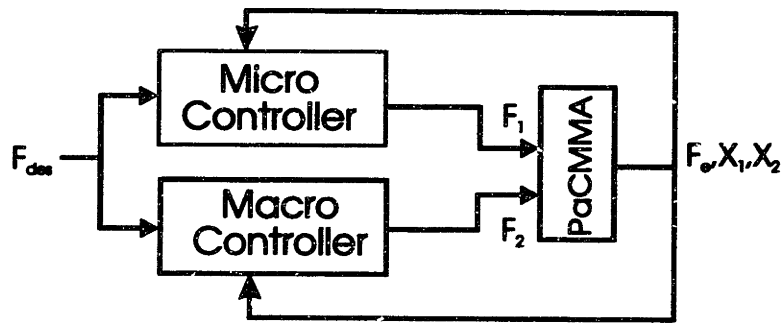

Figure 5-1: Control Strategy

which is guaranteed to be passive (Colgate and Hogan, 1989).

A number of best-case operating conditions were discussed in chapter 4. In those cases it was assumed that the actuators produced the commanded force and that all model parameters were well known. In reality there are modeling errors, parameter uncertainties and unmeasured quantities which require feedback of errors in addition to the feedforward control described in chapter 4.

The primary quantity of interest in this control system is force. Hogan argues that manipulators should present an *impedance* which implies that the system should accept position inputs and output force (Hogan, 1985). Thus a system which can accurately produce the desired force over a large range of frequencies, can be programmed to produce the appropriate impedance for a given task. In addition to accurate force generation the system must be stable in a wide range of configurations. The goal of the control algorithm is to modulate the applied force in the presence of disturbance forces and endpoint motion. Since there are two control inputs (F_1 and F_2) and one output (F_e), the question arises: What is the appropriate strategy for dividing the control efforts in order to best control the output? Figure 5-1 shows the basic control structure.

One approach is to formulate the problem as a Linear Quadratic Control problem. In this technique a cost function is created which weights the control efforts and states to obtain an optimal gain strategy. A cost function for the PaCMMA might apply some penalty to the control efforts of the two actuators, a penalty on the force error and perhaps some penalty on the energy dissipated or stored by the transmission in order to make sure the actuators are not working against each other.

There are several drawbacks to this approach. First, saturation is only accounted for by modifying the control costs to prevent saturation from occuring. Ultimately, the designer avoids saturation by tuning the coefficients in the cost function. The LQ representation is particularly useful when the measurements, states, and cost functions are related to each other in a nonintuitive way. When the quantities of interest and the effects of the inputs are both easily observed, the LQ representation offers increased complexity without greater insight. Another limitation is that the gain matrix produced by LQ control may not yield insight into how to modify the system to obtain better performance nor will LQ control generate a control law which adds an integrator or uses a nonlinear strategy. Finally, a

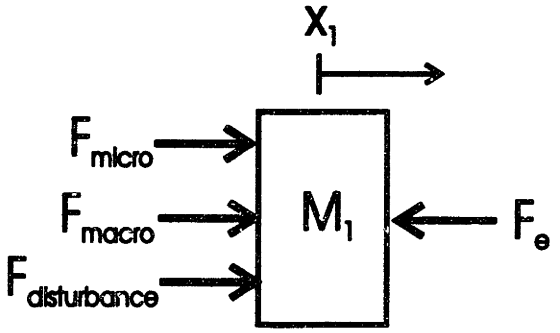

Figure 5-2: Forces Acting on the Endpoint

fourth order system requires solving ten simultaneous quadratic equations. This approach will be used once numerical values have been assigned to the various parameters, but this approach will not produce a symbolic solution for systems greater than second or third order.

5.2 PaCMMA Control Strategy

The PaCMMA dynamics are relatively simple; the states and measurements involve very simple transformations and the goals of the control law are clear. The system matrix is not strongly coupled. Further, many optimization problems find solutions along the boundary of the search space. For this reason it may be possible to find an adequate strategy by maximizing or minimizing the performance of each actuator seperately.

Consider the forces acting on the endpoint mass, M_1, in figure 5-2. These two forces F_{macro} and F_{micro} have distinctly different frequency characteristics. When the endpoint is stationary against a stiff environment:

$$\begin{aligned} F_{micro} &= F_1 H_{1OL}(s) \\ F_{macro} &= F_2 H_{2OL}(s) = F_2 \frac{1 + \frac{B_t}{K_t} s}{\frac{M_2}{K_t} s^2 + \frac{B_t}{K_t} s + 1} \\ F_e &= F_{micro} + F_{macro} + F_{disturbance} - M_1 \ddot{x}_1 \end{aligned}$$

By design, F_{micro} is much faster than F_{macro}. There are two primary operating conditions to consider. The first is constant force regulation in the presence of disturbance forces and the second is force tracking of a desired force input. In the case of constant force regulation and transient disturbance rejection, it is clear that the ideal control law would attempt to keep $F_{micro} = 0$. In this case, the system's ability to respond to a future unknown force transient is maximized. Further, we would like the contribution from the macro-actuator, F_{macro}, to reach F_{des} as quickly as possible.

In the case of force tracking, we would like the control effort from the macro actuator to be as fast as possible so that the micro-actuator has the maximum range available to reject disturbances. We would also like the micro-actuator to use its full range if necessary.

In the case where the endpoint is moving with some trajectory $x_1 = A\sin(\omega t)$, the control for disturbance rejection is similar. The macro-actuator should modulate the force as best it can while the micro-actuator effort should be used to correct for errors. In steady state, the micro-actuator should be kept as close to zero as possible. Using these heuristics, the control problem becomes one of maximizing the performance of the macro-actuator for the various operating conditions and then applying the micro-actuator as a high frequency corrector. In the context of rejecting transients, these heuristics will maximize the performance of the PaCMMA.

The previous arguments assume the micro-actuator can be made faster than the force applied by the macro-actuator in all contexts. In this case, it is always safe to assume that the macro-actuator represents the performance bottleneck. These heuristics are not as easily applied if the frequency characteristics of the two force terms, F_{micro} and F_{macro}, are close in range.

5.3 Macro-actuator Control

The goal of the macro-actuator control law is to make F_{macro} as close to F_{des} as possible. Since the transmission and actuator dynamics can be measured, a feedforward controller should work well. In addition, the system will need some active damping to prevent excitation of any unmodelled dynamics and to avoid velocity saturation of the gearhead. Finally, the macro-actuator should try to reduce the micro-actuator force to zero. To do this, it can use integral gain on the force error.

$$\begin{aligned} F_2 &= G_{ff}H_{ff}(s)F_{des} \\ &+ G_{d1}\left(sX_1(s) - sX_2(s)\right) \\ &- G_{d2}sX_2(s) \\ &+ \frac{G_{integral}}{s}(F_{des} - F_e) \end{aligned}$$

Several aspects of this control law are important. First, the compliance in the transmission allows the use of active damping. The damping terms are very important for stabilizing the system. Second, the feedforward model is easily obtained by measuring the system response from F_2 to F_e and inverting the transfer function. Finally, the integral term will be used to make sure that the errors in the feedforward model are reduced when the system settles to a constant force. This controller works well and is analyzed in greater detail in section 5.5.

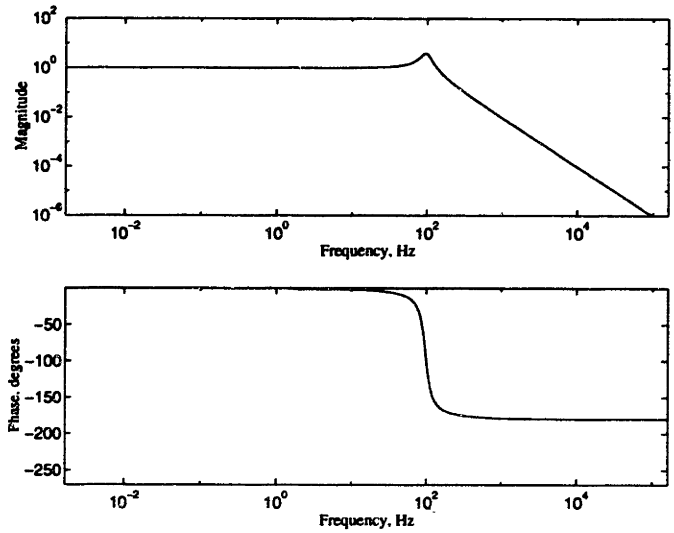

Figure 5-3: **Frequency Response of an electric motor and a force sensor.** The frequency response function has the form $H(s) = \frac{\omega^2}{s^2+2\zeta\omega s+\omega^2}$.

5.4 Micro-Actuator Control

The micro-actuator can transmit forces to the endpoint at high bandwidth due to the direct-drive connection to the torque sensor. Unfortunately, the velocity of the torque sensor deflection is not easily measured and active damping is hard to obtain.

Integral force control has been shown to be stable against a wide range of environments and to be stable when making contact with the environment (Youcef-Toumi and Gutz, 1989). In fact, integral control provides the best performance for linear closed loop force feedback against all environments (Volpe and Khosla, 1993). The form of this control is:

$$F_1 = \frac{G_i}{s}(F_{des} - F_e)$$

Consider a typical open loop transfer function for a force actuator such as an electric motor connected to a force sensor (figure 5-3). This figure shows constant gain out to some nominal frequency. At this frequency, the resonance of the dynamics between the actuator and sensor are excited and a resonance occurs. The actuator force rolls off above this frequency.

Good controller design for a closed loop control law consists of increasing the gain as much as possible when phase lag is less than 180 degrees or alternately, by maximizing the phase lead at unity gain. It is clear that use of proportional control must decrease the gain in order to reduce the magnitude of the transmission resonance. It should also be clear that a pure integral control law will increase the gain at low frequency, while decreasing

the gain at high frequency. Since the fundamental dynamics have *no* phase lag up to the transmission resonance, the lag from integral gain has relatively little effect on the stability at frequencies lower than the first resonance.

This result is not profound, but should be considered carefully nonetheless. A quasi-static motor in free space has radically different dynamics ($1/Ms^2$). This transfer function has 180 degrees of phase lag and PD control provides the required phase lead to stabilize this plant. Although commonly used for motor position control, PD control laws are not indicated for force control and it should come as no surprise that PD control is not as effective for controlling force given the difference in the plant dynamics. Force feedback with pure integral feedback results in a stable, fast response (Colgate and Hogan, 1989; Paljug et al., 1992; Volpe and Khosla, 1992; Youcef-Toumi and Gutz, 1989).

5.5 PaCMMA Force Control Law

The control laws of the previous sections can be combined into one control law for the PaCMMA. This control law is shown in block diagram format in figure 5-4 and in the equations below:

$$F_1 = \frac{G_1}{s}(F_{des} - F_e) \tag{5.1}$$

$$\begin{aligned} F_2 &= G_{ff} H_{ff}(s) F_{des} \\ &+ G_p F_1 H_{1OL}(s) \\ &+ G_{d1}\left(sX_1(s) - sX_2(s)\right) \\ &- G_{d2} s X_2(s) \end{aligned} \tag{5.2}$$

where

$$H_{1OL}(s) = \frac{\omega_{co1}^2}{s^2 + 2\zeta_1\omega_{co1} + \omega_{co1}^2}$$

$$H_{ff}(s) = \frac{\hat{M}_2}{\hat{K}_t}s^2 + \frac{\hat{B}_t}{\hat{K}_t}s + 1$$

The control law has several components which are used to maximize performance.

Feed-forward of the desired force ($G_{ff} < 1$) is used to account for plant dynamics with estimates of mass, stiffness, and damping. However, backlash, friction and other unmodelled dynamics produce errors which require feedback terms.

Gain G_p causes the macro-actuator to reduce the control effort of the micro-actuator (which represents the integrated force error).

Gain G_{d1} provides damping between M_1 and M_2 to prevent excessive excitation of the transmission.

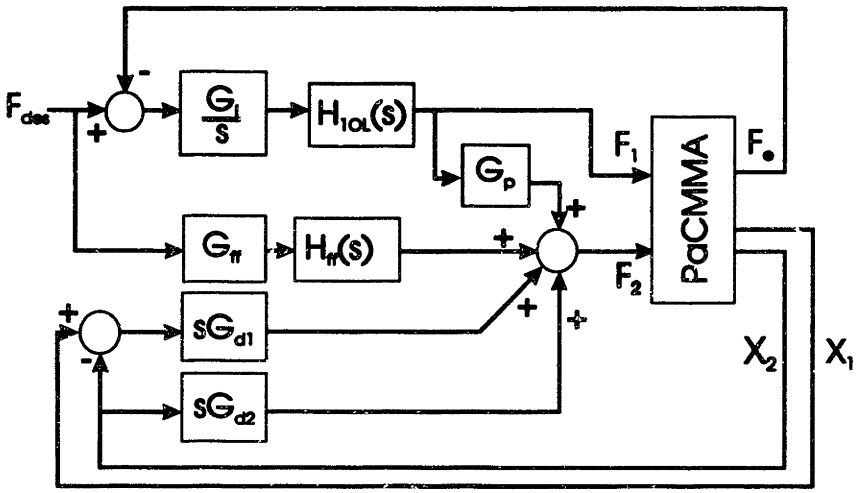

Figure 5-4: Control Law

Gain G_{d2} provides damping from M_2 to ground. This is necessary to prevent the macro-actuator from exceeding its velocity limits.

The model developed in chapter 4 is repeated below in figure 5-5. Using the control law described above the equations of motion become:

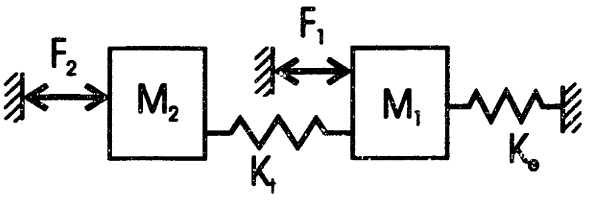

Figure 5-5: Lumped Element Model of PaCMMA

$$\begin{aligned} M_1 s^2 X_1(s) &= \frac{G_1}{s} H_{1OL}(s)\left(F_{des} - K_e X_1(s)\right) \\ &\quad -\left(K_t + B_t s\right)\left(X_1(s) - X_2(s)\right) - K_e X_1(s) \end{aligned} \tag{5.3}$$

$$\begin{aligned} M_2 s^2 X_2(s) &= \frac{G_p G_1}{s} \frac{\omega_{co1}^2}{s^2 + 2\zeta_1 \omega_{co1} + \omega_{co1}^2}\left(F_{des} - K_e X_1(s)\right) \\ &\quad +G_{d1} s\left(X_1(s) - X_2(s)\right) \\ &\quad +G_{d2} s X_2(s) \end{aligned}$$

$$+G_{ff}\left(\frac{\hat{M}_2}{\hat{K}_t}s^2+\frac{\hat{B}_t}{\hat{K}_t}s+1\right)F_{des}$$
$$+(K_t+B_ts)(X_1(s)-X_2(s)) \tag{5.4}$$

These equations may be rearranged to separate the input, F_{des}:

$$X_1(s) = \left(\frac{\frac{G_1K_eH_{1OL}(s)}{s}}{\Delta_1(s)}\right)F_{des} + \left(\frac{B_ts+K_t}{\Delta_1(s)}\right)X_2(s) \tag{5.5}$$

$$X_2(s) = \left(\frac{\frac{G_pG_1H_{1OL}(s)}{s}+G_{ff}\left(\frac{\hat{M}_2}{\hat{K}_t}s^2+\frac{\hat{B}_t}{\hat{K}_t}s+1\right)}{\Delta_2(s)}\right)F_{des} + \left(\frac{(B_t+G_{d1})s+K_t-\frac{G_pG_1H_{1OL}(s)K_e}{s}}{\Delta_2(s)}\right)X_1(s) \tag{5.6}$$

where

$$\Delta_1(s) = M_1s^2+B_ts+K_e+K_t+\frac{K_eG_1H_{1OL}(s)}{s}$$
$$\Delta_2(s) = M_2s^2+(B_t+G_{d1}+G_{d2})s+K_t$$

The characteristic polynomial for this 7th order system is:

$$\Delta(s)=\Delta_1(s)\Delta_2(s)-(K_t+B_ts)\left((B_t+G_{d1})s+K_t-\frac{G_pG_1H_{1OL}(s)K_e}{s}\right) \tag{5.7}$$

General stability analysis for various gains may be performed using equations 5.5 & 5.6 and the characteristic polynomial. In section 5.7, a procedure for tuning the gains of the control system will be presented.

5.6 Control of the PaCMMA Impedance

The impedance of the PaCMMA may be controlled using the control law of the previous section and a simple impedance model. Figure 5-6 depicts this concept. Position is commanded and the impedance controller determines what force should be applied. This force is then used as an input command to the force control system. For first order impedances, this may be represented as follows:

$$Z_{des}(s)=B_{des}s+K_{des} \tag{5.8}$$

Given a desired position, X_{des}, and the desired impedance about that position, $Z_{des}(s)$, the desired force, F_{des}, can be calculated:

$$\begin{aligned} F_{des}(s) &= Z_{des}(s)(X(s) - X_{des}(s)) \\ &= Z_{des}(s)\Delta X(s) \end{aligned}$$

or

$$F_{des}(t) = B_{des}\Delta\dot{x}(t) + K_{des}\Delta x(t)$$

In general, it is hard to accurately measure $\ddot{x}$ so simulation of arbitrary masses is not trivial. However, estimates or measurements of $\dot{x}$ are generally achievable.

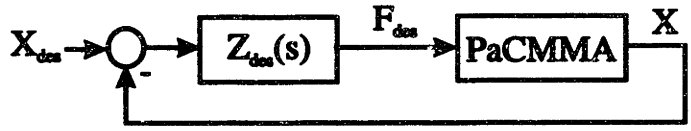

Figure 5-6: Impedance Control Architecture

5.7 Gain Tuning

Tuning the gains on the control is more straightforward than it might appear initially. The strategy is to first tune the fastest parts of the system so that they are stable and can reject all disturbances in a stable manner. Then, the slower parts of the system may be adjusted. The following procedure demonstrates this.

Measure the force control bandwidth from F_1 to F_e, and determine the appropriate lowpass filter to avoid resonance (H_{1OL}).

Set G_i so that the integral control of the micro-actuator is as fast as possible. The amount of overshoot may be tuned by increasing or decreasing G_i.

Estimate M_2, K_t, and B_t. With G_i=0, set G_{ff} to so that feedforward response is as close as possible to the desired large signal response. Depending on the nature of the macro-actuator, the errors may be due to backlash, friction or nonlinearities in the transmission.

With G_i=0, set G_{d1} to get good force control bandwidth (fixed endpoint) from the macro-actuator. The amount of damping required from G_{d1} will depend on the amount of natural damping in the transmission.

With the micro-actuator operating, set G_{d2} to get good position control/impedance performance from the macro-actuator. If G_{d2} is too low then the system will be unstable

under position/impedance control. The instability can occur because the feedforward model is imperfect and the macro-actuator needs a small amount of phase lead to be stable with the feedforward controller.

Set G_p to reduce the steady-state control effort of the micro-actuator. This term of the macro-actuator control law should be a small fraction of the total control effort. The system will become unstable if it is too large.

The effect of this procedure is to treat the macro-actuator as a passive stable disturbance force which by design is lower bandwidth than the micro-actuator bandwidth. Since integral force control on the micro-actuator is stable for all conditions, the overall system is stable.

5.8 Simulated Control Law Performance

In order to evaluate the effectiveness of the control law, several simulations were run under a variety of scenarios. The performance of the control law is compared to the best possible response which could be achieved with perfect knowledge and control. The simulation results are described below, while the details of the simulation are discussed in Appendix B.

5.8.1 Simulated Force Step Response

Ideal step response performance can be defined a number of ways. In some cases, it is the fastest possible rise time. It may also be defined as the fastest rise time with no overshoot or the smallest settling time. For the fixed endpoint model of section 4.6, perfect control was taken to be the minimum settling time and it was shown that a perfectly timed bang-bang strategy is the fastest way to accomplish this.

The response of the controller to several step changes in the desired force was simulated and is compared to the cases for perfect control in figures 5-7 and 5-8. The controller gains were selected by observing the step response and using the gain tuning algorithm presented in section 5.7. Some judgment comes into play when selecting the amount of overshoot and these simulations do not represent an optimal solution. They are intended to show the reader that the proposed control law gets close to the optimal solution.

"Perfect control" for the damped case results in very large force overshoot due to the large force contribution from the transmission damping, B_t. The plots show that the PaCMMA controller proposed in the previous section is slightly slower than the bang-bang controller, but force overshoot is smaller. This is probably advantageous in most applications. Clearly, a transmission with zero damping and a bang-bang controller produces the best response - fast and no overshoot.

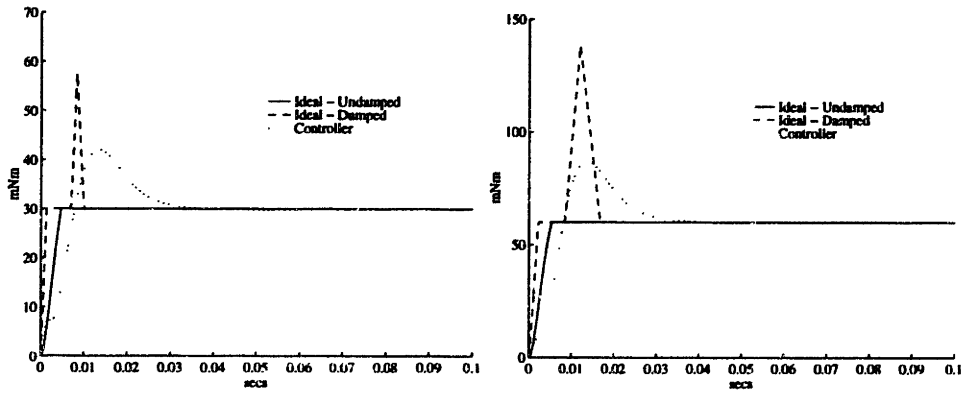

Figure 5-7: **Simulated Force Step Response.** F_{des} = 30 mNm and F_{des} = 60 mNm. This figure shows a comparison of three systems: Bang-bang control on an undamped transmission, bang-bang control on a damped system and the PaCMMA force controller. For the damped case, $\zeta = 0.25$.

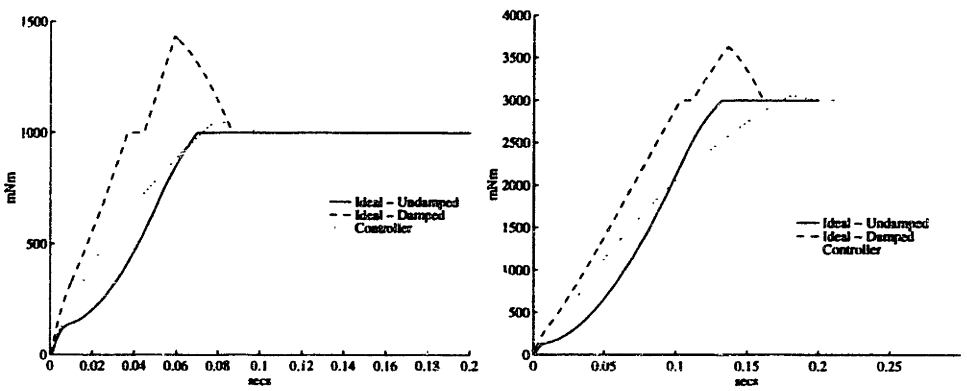

Figure 5-8: **Simulated Force Step Response.** F_{des} = 1000 mNm and F_{des} = 3000 mNm. This figure shows a comparison of three systems: Bang-bang control on an undamped transmission, bang-bang control on a damped system and the PaCMMA force controller. For damped case, $\zeta = 0.25$

5.8.2 Simulated Position Step Response

In many applications the PaCMMA system may be used as a manipulator which follows motion trajectories in free space. This section presents a comparison of position controlled performance for three simulations:

Bang-Bang control - The switching times were calculated and the system was simulated with saturation as the only performance limit.

Proportional-Derivative control - A PD controller was designed such that the velocity saturation limit on the macro-actuator was violated only for large steps.

PaCMMA under impedance control - A stiff, but stable impedance was specified for the PaCMMA (section 5.6) and step changes in the desired position were specified as inputs. A velocity saturation limit was imposed on the control system.

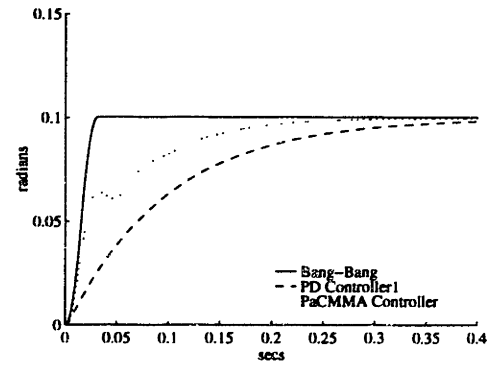

Figure 5-9: **Simulated Position Step Response.** $x_{des} = 0.1$rad

The switching times are easily derived for a Bang-Bang control strategy and a *single* mass:

$$t_1 = \sqrt{\frac{x_{des} M}{F_{sat}}}$$

and

$$t_2 = 2\sqrt{\frac{x_{des} M}{F_{sat}}}$$

For bang-bang control with *two* masses connected by a transmission the best case may be assumed to be the case where no energy is dissipated in the transmission, i.e. the transmission is rigid and all input power is used to move the masses. In this case, the

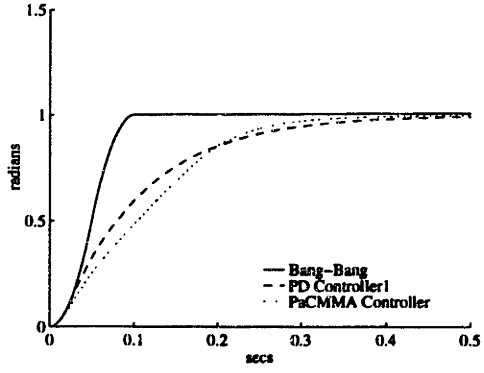

Figure 5-10: **Simulated Position Step Response.** $x_{des} = 1.0$rad

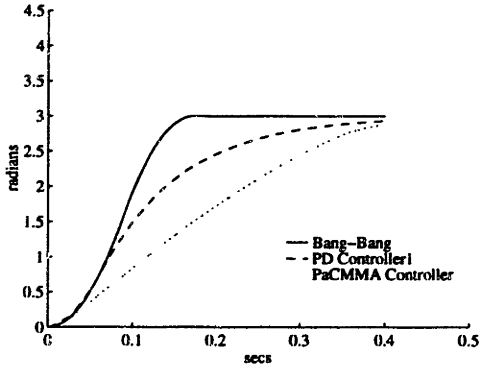

Figure 5-11: **Simulated Position Step Response.** $x_{des} = 3.0$rad

switching times may be calculated by substituting: $F_{sat} = F_{1sat} + F_{2sat}$ and $M = M_1 + M_2$. This approximation will produce time estimates that represent the fastest possible time. If the transmission is non-rigid then the actuator with the lower acceleration will determine the response time.

The PD controller is also simulated assuming a rigid transmission. This will yield performance that is unrealistically fast since a stiff, but non-rigid transmission will present high frequency dynamics that may be uncontrollable. For this case, it will be assumed that a transmission of adequate bandwidth may be used and that the performance is limited *only* by the saturation torque and velocity limits of the two actuators. As with most PD controllers, some degree of gain tuning is required to determine what kinds of performance are acceptable. Large gains may improve performance for small displacements but result in unacceptable overshoot and velocity saturation for large displacements. In most cases, the transmission stiffness is not infinite and the small displacement bandwidth is limited by the structural bandwidth of the transmission, while the large displacement bandwidth is limited by the saturation torques and velocity limit.

For small signals, it is clear that the PaCMMA is almost as fast as the bang-bang controller and *faster* than the PD controller. This is because the gains that must be used by the PD controller are too low for small inputs. Turning up the gains to improve small signal performance may cause the velocity limit to be violated. The large signal performance shows that the PaCMMA controller is slower than the PD controller. This shows the effect of active damping on the velocity of the macro-actuator; The PD controller was not restricted to the same velocity limit in this simulation. While the rise time for large steps is longer for the PaCMMA controller, the 2% settling time is not drastically different.

Examination of the control signals reveals that the PaCMMA uses signals that are bang-bang initially and then stabilize on the error. Obviously a more clever use of PD control, with some non-linear switching, could improve the performance of a position control loop. The point of these simulations is to emphasize that the proposed control law for the PaCMMA does about as well as can be expected from a system with saturation and velocity limitations. (These limitations were ignored for the simulation of optimal bang-bang control.)

5.9 Implementation Issues

5.9.1 Feedforward Model

The creation of a feedforward model required a lowpass filter in order to make the system realizable. This does not present a significant problem because the control system bandwidth is significantly higher than the mechanical bandwidth of the macro-actuator/transmission system. For this system the feedforward model was:

$$\frac{(M_2 s^2 + B_t s + K_t)\omega_n^2}{s^2 + 1.414\omega_n s + \omega_n^2} \tag{5.9}$$

The roll-off frequency, ω_n, was 320 Hz. The macro-actuator/transmission had a resonant frequency of approximately 2 Hz.

5.9.2 Force Sensing

The transmission compliance may be used as a low frequency force sensor provided there are no disturbances applied to the endpoint. This may or may not be a valid assumption, depending on the application. Figure 5-2 shows the forces which act on the endpoint. A balance of forces may be written:

$$F_e = F_{micro} + F_{macro} + F_{disturbance} - M_1 \ddot{x}_1 \tag{5.10}$$

If the disturbance force, $F_{disturbance}$, is taken to be zero, then the force applied to the environment may be derived from measurements of $\ddot{x}_1$, $x_1 - x_2$ and knowledge of F_{micro}. However, if there is any uncertainty in these measurements, or the model parameters of the transmission, then a direct measurement of F_e is required. The repeatability and accuracy of these measurements is dependent on the transmission implementation and micro-actuator model accuracy.

5.9.3 Peak Force

Clever use of the control efforts can produce exceptional small signal performance. Most motors have a thermal time constant and can exert peak torque significantly larger than the steady state torque. This means that both actuators' control efforts for transient signals could be significantly larger than for the steady state case. Performance for impacts and step changes in position and force could be made much faster with temporary use of peak torque capacity.

Chapter 6

Design Guidelines

The PaCMMA concept is a general one and as a result, a wide range of possible configurations exists. This section will identify the relevent design parameters and generate some performance relationships. A design procedure will be presented.

The designer is typically faced with a number of performance specifications which may or may not be achievable. Often times the design specifications are not hard constraints and are subject to revision as the problem becomes better understood. With that in mind, this section will provide some general guidelines for successively pruning the range of configurations until the designer has a reasonable estimate of achievable system performance.

6.1 Component Considerations

Individual component selections will determine the overall response of the system. Some of the elements in the design only affect one or two performance dimensions, while other components impact every aspect of performance. Each component will be identified and its effect on performance will be explained.

6.1.1 Sensors

All control systems impose implicit or explicit demands on sensor accuracy. The control system proposed in chapter 5 relies explicitly on force measurement. The torque sensor should be accurate enough to measure the desired resolution. Since the control algorthim relies on integral control, the system will generally attempt to control the system down to 1 bit error.

The control system also relies on position measurements. The position sensors on the micro and macro-actuators are used for measuring the actual robot position and for creating computational damping in the transmission. These two uses may not require the same accuracy. In the case of determining robot position, this requirement is dependent on the task and the impedance requirements. A stiff impedance requires more precise position measurement since force must change over a small displacement.

Active damping is the second use of position information. In order to get good resolution for damping, position resolution needs to be scaled inversely with the transmission stiffness. A stiff transmission requires fine position resolution in order to measure the deflection of

the transmission. This requirement is generally not a hard one to satisfy in the PaCMMA since the transmission is usually explicitly compliant and high accuracy position sensors are a well developed technology.

6.1.2 Micro-actuator Selection

The endpoint inertia, M_1, is the sum of the link inertia and the rotor inertia of the micro-actuator and has the greatest effect on the system's performance during endpoint motion. The impedance and impact relationships derived in chapter 4 show that this quantity should be minimized. Often, the link inertia is significantly larger than the rotor inertia so that the rotor inertia is not a dominant constraint on the design.

The maximum acceleration is another important quantity in determining the impedance of the endpoint. The actuator torque is finite and the acceleration is limited. When the quantity, $X_1 M_1 \omega^2 / F_{1sat}$, is less than one, the micro-actuator torque (with perfect control) can eliminate the inertia of the link mass[1]. When this number exceeds one then the micro-actuator can reduce, but not eliminate the impedance due to the endpoint inertia. As such, the ratio M_1/F_{1sat} (maximum acceleration) must be chosen to provide the desired small signal impedance performance.

Friction between the source of effort, F_1, and the point of contact, F_e (i.e. brush and bearing friction) will result in a measurable error or limit cycle (depending on the use of proportional or integral control). The magnitude of the error or limit cycle is directly related to the magnitude of the friction, therefore friction should be minimized (Townsend, 1988).

In the distributed configuration (figure 2-1), the micro-actuator may be mounted some distance from the macro actuator and its housing inertia may affect the dynamics of another joint. In general, one should seek to reduce the inertia of the micro-actuator housing if it is mounted on a moving link. The effect of the micro-actuator housing inertia will be on the previous link, not the link being controlled by the micro-actuator.

The micro-actuator is connected to ground in all configurations of the PaCMMA system. This is a fundamental requirement of the design. However, it is worth noting that this connection need not be "rigid". In fact, the only requirement is that the connection be dynamically stable and have dynamics that are lower bandwidth than the micro-actuator force response, H_{1CL}. The movement of the housing in a non-rigid connection is seen as another disturbance and that disturbance may be rejected by the controller if the disturbance is slower than the micro-actuator. Mounting the micro-actuator housing in a well-damped support should not present a difficult design task.

6.1.3 Transmission Selection

The transmission stiffness is an extremely important characteristic. Varying the transmission stiffness allows the designer to trade off low impedance against high force control bandwidth. To illustrate this point, consider figure 6-1 which shows the force control bandwidth of the PaCMMA for increasing transmission stiffness, K_t. As expected, the force

[1] A manipulator may idealized as a mass with a force source. When a position trajectory, $A\sin(\omega t)$, is desired, the force required is $F = M_1 \omega^2 A\sin(\omega t)$. Thus, when the actuator saturates at $F = F_{1sat}$, the ratio, $X_1 M_1 \omega^2 / F_{1sat}$ is greater than one.

control bandwidth increases as the transmission stiffness increases.

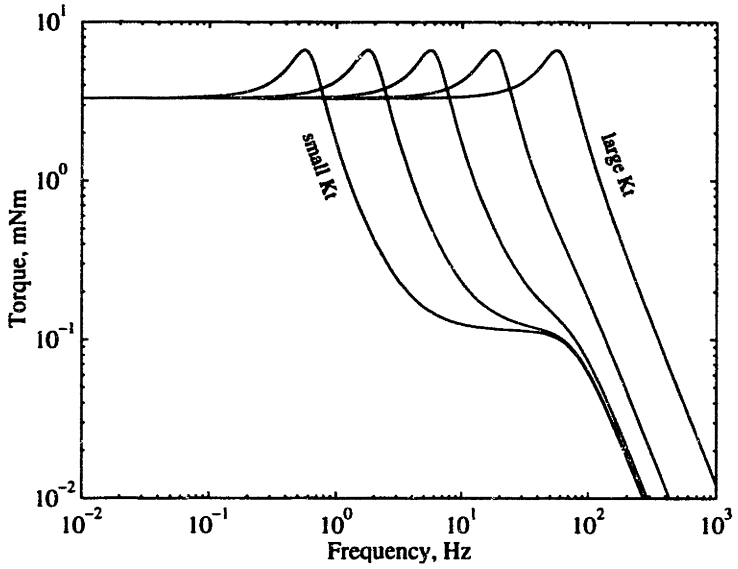

Figure 6-1: **Force Control Bandwidth for Varied Transmission Stiffness.** The force control bandwidth was calculated using equation 4.13 and the simulation parameters can be found in Appendix A. The transmission stiffness, K_t, was given the following values: 114,1.14×10^3,1.14×10^4,1.14×10^5,1.14×10^6 mNm/rad.

It should be noted that this figure assumes constant damping ratio. In reality, damping gets harder to implement as the transmission stiffness increases and a low pass filter below the resonant frequency is generally required. As a result, the gains in bandwidth are not as great as shown in this figure. Nonetheless, high transmission stiffness generally results in high force control bandwidth.

Unfortunately, a stiff transmission creates a larger passive impedance. When the actuators saturate or the dynamics are faster than the control law, the system performance reverts back to the passive dynamics of the system. Figure 6-2 shows the passive (undriven) impedance of the PaCMMA for varying transmission stiffnesses. There are two asymptotes, $(M_1 + M_2)s^2$ and $M_1 s^2$ and the transmission stiffness is varied to modify the impedance at a given frequency. A very soft transmission results in the impedance approaching the $1/M_1 s^2$ asymptote at a low frequency, while a stiff transmission causes this to occur at a higher frequency. In other words, the soft transmission reduces the effect of mass M_2 at a lower frequency. The designer must chose between force control bandwidth and low passive impedance based on the application.

The transmission impedance (stiffness and damping) also impose some stability limits. Typically, transmissions are made of aluminum or steel both of which are poorly damped. Undesired resonances in the system may be controlled three ways:

- Passive mechanical damping may be introduced to the transmission

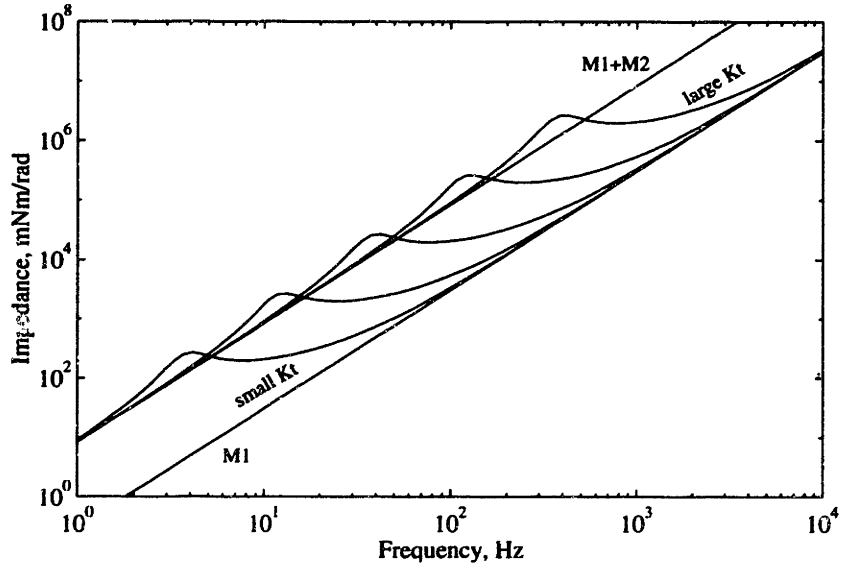

Figure 6-2: **Passive Impedance for Varied Transmission Stiffness.** The passive impedance of the system was calculated using equation 4.17 and the parameters in Appendix A. Inputs F_1 and F_2 were set to zero. Two asymptotes, $M_1 s^2$ and $(M_1 + M_2)s^2$ are also shown. The transmission stiffness, K_t, was given the following values: 114,1.14×10^3,1.14×10^4,1.14×10^5,1.14×10^6 mNm/rad.

- Active damping may be added using velocity measurements
- The control signal can be lowpass filtered to avoid the system resonance altogether

Typically, mechanical damping alone is insufficient. Computational damping is less effective as the stiffness increases since position measurements (and therefore velocity measurements) become smaller and harder to measure. A low pass filter is easily implemented, but is overly conservative in bandwidth. The PaCMMA concept requires active damping of the transmission in the control of the macro-actuator and as a result, an extremely stiff transmission will have the effect of destabilizing the macro-actuator. The micro-actuator also uses a lowpass filter to avoid resonance since neither velocity measurements nor passive means are sufficient.

6.1.4 Macro-actuator Selection

The macro-actuator is generally the easiest component to select since it is not subject to the same low friction and low mass requirements as the micro-actuator.

Saturation torque of the macro-actuator determines the maximum torque for the system. This is typically an easy requirement to meet since the macro-actuator may be located some distance from the robot endpoint.

Maximum acceleration, F_{2sat}/M_2, proves to be an important specification for the macro-actuator. Maximum acceleration combined with the transmission stiffness determines the large signal bandwidth of the PaCMMA system. If the macro-actuator is slow then the rate of change of force due to the macro-actuator will be small. Conversely, if the macro-actuator is fast, then the rate of change of force will be large. The macro-actuator clearly benefits from high power density. If large signal bandwidth is not an important specification, then a reduction may be used to obtain greater torque density from a low power actuator. Impedance is also affected by acceleration performance. If the maximum acceleration is small, then the macro-actuator will saturate at a lower frequency and the passive dynamics of the system will dominate at a lower frequency.

For many of the reasons mentioned above, velocity saturation also imposes similar limits on the force bandwidth and impedance of the system. The macro-actuator reduction will determine whether velocity saturation or acceleration limits dominate the performance of the macro-actuator.

Reductions (gear, cable, or friction drives) may be used to great advantage on the macro-actuator but a few caveats are in order. A large reduction allows the designer to generate large torque density from a low power actuator. For many applications where size, weight, or cost present limitations and large signal bandwidth is not required (e.g. slow manipulation), the use of a reduction is desirable. However, a transmission reduction (e.g. a gearhead) generally introduces nonlinear dynamics such as friction and backlash. In the experiments which will be reported in chapter 7, backlash proved to be a very undesirable characteristic. In short, backlash is a complex nonlinearity which introduces error signals at frequencies above the frequency of excitation. This harmonic distortion can not be eliminated by the micro-actuator when it occurs above the bandwidth of the micro-actuator control system. For this reason backlash should be avoided.

When the system is heavily loaded (i.e. a large mean force) and power required from the macro-actuator is relatively low (slow changes in position/force), the backlash effects may be reduced or eliminated since the gearhead is always loaded with a bias force. However, the gearhead can still become unloaded during very fast changes in the position of the macro-actuator. Even though the force applied to the output shaft of the gearhead stays positive, the force applied to the input shaft can become negative and an impact will occur as the gear teeth unload, move in free space and then load in the opposite direction. This introduces another undesirable high frequency disturbance force.

Conversely, friction and/or stiction in the reduction does not pose a large problem. Friction acts as an additional form of velocity damping and the only negative effect is the excess power that is consumed. Except for power efficiency concerns, nominal amounts of friction should not be detrimental to the system performance.

6.2 Design Procedure

Given the heuristics described above and the performance relationships derived in chapter 4, the designer can now develop some kind of quantitative performance relationships for a PaCMMA system. The calculations of the previous chapters incorporate a large number of parameters. A complete search of the design space for simultaneous solutions to all performance criteria might yield a solution, but an iterative less exhaustive approach is more

likely to yield an acceptable solution in a reasonable amount of time. The following section breaks the actuator into its component parts and presents an iterative design procedure.

The process is as follows:

- Select a force sensor - The resolution and performance of the system is entirely dependent on the force sensor. Be sure that quantization noise from A/D conversion is acceptable.
- Determine the small signal force bandwidth requirement - The small signal force bandwidth is limited by the mechanical coupling between the force sensor and the micro-actuator. The first system resonance will need to occur at a frequency above the desired force bandwidth in order to maintain stability of the control law. The exact requirements will be determined by the passive damping of the connection. For example, aluminum is poorly damped and could require a transmission bandwidth 4-6 times higher than the desired force bandwidth.
- Determine the maximum acceleration required - The maximum required acceleration is driven by both the small signal position bandwidth and the minimum impedance performance. When $F_{1sat} < M_1 X_{des}\omega^2$, the small signal impedance and position performance must deteriorate.
- Select a micro actuator with acceptable F_{1sat} - Based on the manipulator inertia, M_1, and the desired small signal performance, a micro-actuator can be selected. The brush friction of the micro-actuator should be smaller than the desired resolution.
- Select servo rate - The servo rate should be 8-10 times faster than the first resonance between the force sensor and the micro-actuator. This will ensure adequate control of the resonance under integral force control.
- Close the control loop on the micro-actuator and evaluate small signal force bandwidth and impedance - At this point the micro-actuator gain, G_i, and the lowpass filter, $H_{1OL}(s)$, should be tuned to provide the desired small signal force bandwidth, impedance and position control response. Inadequate performance should be corrected at this time by reducing mass, increasing torque and increasing the stiffness of the torque sensor coupling.

The system with only the micro-actuator represents the best case performance for small signals. With these limits established, the designer must now select the macro-actuator and the transmission. The dominant parameters are K_t, F_{2sat}, and M_2:

- Determine large signal force bandwidth requirements - Large signal force bandwidth will be limited by $\sqrt{K_t/M_2}$.
- Determine the maximum acceleration from large signal impedance and position control requirements. As stated above, when $F_{2sat} < M_2 X_{des}\omega^2$, the system performance will degrade.
- Check for velocity saturation - velocity saturation will degrade large signal performance.

- Select transmission and macro-actuator as a coupled pair

Appendix A contains detailed response data for the the prototype system.

6.3 Force Control Performance Space

Nearly all actuator systems have amplitude and frequency limitations and the PaCMMA is no different. The performance relationship between the micro-actuator and the macro-actuator was illustrated in Chapter 3 and is repeated in figure 6-3. The region defined in this plot is the similar to the region defined by the force control performance plot in figure 4-6 .

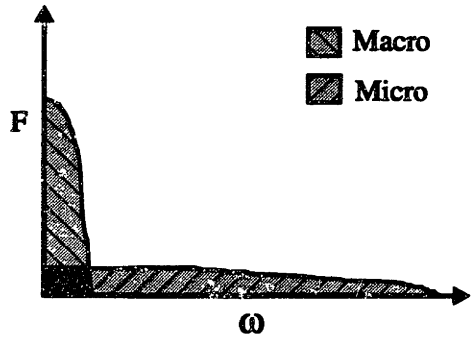

Figure 6-3: **Performance Space for the Micro and Macro-actuators.** The regions are bounded by curves of constant error.

The performance advantages of the PaCMMA are clear when visualized in performance space. Examining figure 6-3, it can be seen that the macro-actuator has a large force amplitude but relatively low frequency while the micro-actuator can produce small amplitude but at high frequency. Figure 6-4 shows the performance of the PaCMMA system. It is clear that the force control performance of the PaCMMA is the union of the micro and macro-actuators. This will be experimentally verified in Chapter 7.

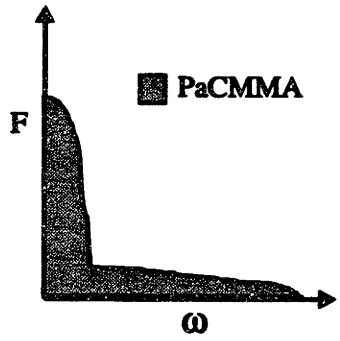

Figure 6-4: Force Control Performance Space for PaCMMA System

6.4 Extension to N-Actuators

The ability to form the union of two different operation spaces raises the obvious question: If two actuators are better than one, are three actuators better than two? Figure 6-5 depicts this concept.

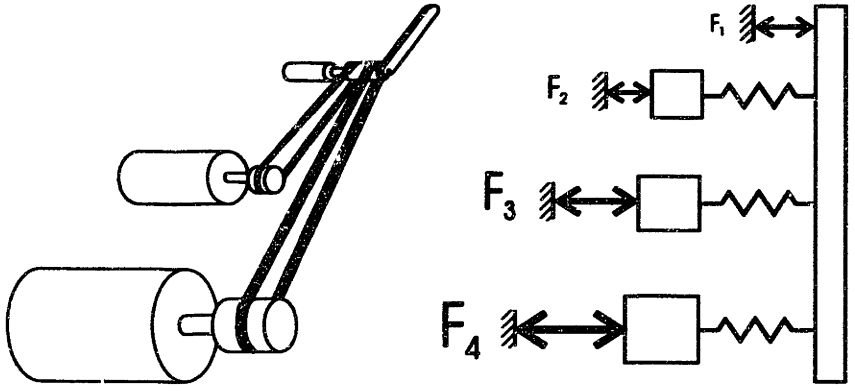

Figure 6-5: N-Actuator Concept

Extension of the concept to more than two actuators is clearly possible. With regard to force control performance, the operation space concept makes it clear that actuators with different operating spaces may be coupled to increase the operating region. Of course, additional actuators will create additional impedance which may be a detriment, depending on the application. Finally, additional actuators bring additional mechanical complexity. A more thorough analysis of the multi-actuator concept is worth pursuing.

6.5 Integration into Existing Systems

The PaCMMA concept is clearly capable of providing better performance than a single actuator system. The reader may be wondering how to take advantage of this concept on an existing manipulator. There are two conceptual possibilities when converting an existing system to a PaCMMA configuration: addition of a micro-actuator or addition of a macro-actuator.

Adding a macro-actuator to an existing system is a relatively simple prospect. All that is required is a point to attach the compliant transmission. For example, suppose we have a system with good force and position bandwidth, but the system is not powerful enough. One simply adds a pulley onto the existing drive axis and connects the PaCMMA transmission to the pulley. The macro-actuator may be located some distance away from the joint if necessary. The addition of the macro-actuator provides a substantial increase in force range without reducing the original system performance! There would be a small increase in impedance due to the additional actuator, but examination of the results in chapter 7 should provide a convincing argument for the PaCMMA configuration.

Addition of a micro-actuator is likely to be more difficult. The goal in this case is to

find a way to attach a micro-actuator to the endpoint using a high bandwidth coupling. This may be accomplished one of two ways. The first method is simply to attach the micro-actuator to the joint axis where the single actuator was attached. This may yield an improvement in force resolution but will not improve bandwidth. The second method is to find a way to connect the micro-actuator to the endpoint with a coupling that is higher bandwidth than the existing actuator coupling. This might entail mounting the micro-actuator closer to the force sensor and the point of force application. The reduced size of the micro-actuator will make this possible in some configurations, while other systems will be too tightly constrained to allow this modification.

6.6 Nonlinear Transmissions

Examination of contact tasks in manipulation suggests that low stiffness and low impedance are most important when a manipulator has a collision or deliberately makes contact with the environment. In both of these cases the transmission deflection is typically small prior to contact because the endpoint is light. If the contact force becomes large during a manipulation, low transmission stiffness may not be as important. For this reason, a nonlinear, stiffening transmission is worth considering. A stiffening transmission offers the benefit of low stiffness and impact energy when making contact with the environment while reducing the transmission volume and increasing the maximum force range. In fact, a stiffer transmission may result in better large signal performance.

Two other aspects of transmission design are the range of forces that the transmission will withstand without deforming and the volume required for the transmission to deflect under full load. A soft transmission offers low impedance but can not typically withstand a large applied force. A soft transmission also requires a large volume in which to compress and expand. Conversely, a stiff transmission can withstand high loads but will not produce the desired reduction in impact energy and impedance.

Chapter 7

Experimental Results

This chapter reports on the experimental results obtained with a prototype testbed. In order to better understand the advantages and disadvantages of the PaCMMA system, an experimental comparison was performed between the PaCMMA and several other component configurations.

7.1 Prototype

A prototype actuator system was assembled to test the parallel actuator concept (figure 7-1) and specifications for the system components are contained in Appendix A. A third motor was used to provide environment dynamics, i.e. to simulate a moving environment.

In addition to the PaCMMA testbed, the performance of the macro-actuator (a permanent magnet, DC brushed, gearhead motor) connected to a traditional transmission and controller was measured in order to provide an accurate comparison between the PaCMMA concept and traditional actuator implementations. The performance of the micro-actuator also yields insight into the performance enhancements of the PaCMMA concept.

In the following sections, results will be reported for several actuator configurations. The configurations are listed in table 7.1.

Test Configuration	Actuator	Transmission	Controller
1	Micro Only	Direct Drive (300 Hz)	Impedance
2	Macro Only	Stiff Cable	Impedance
3	Macro Only	Stiff Cable	PD position
4	PaCMMA1	Compliant	Impedance
5	PaCMMA2	Compliant	Impedance

Table 7.1: Experimental Configurations

The first configuration is a traditional design though it is direct-drive. The micro-actuator is attached to the joint with a solid aluminum shaft and the direct drive connection puts the force bandwidth of this system up near 60 Hz. Appendix A contains a frequency response plot of the open loop dynamics of the micro-actuator and torque sensor.

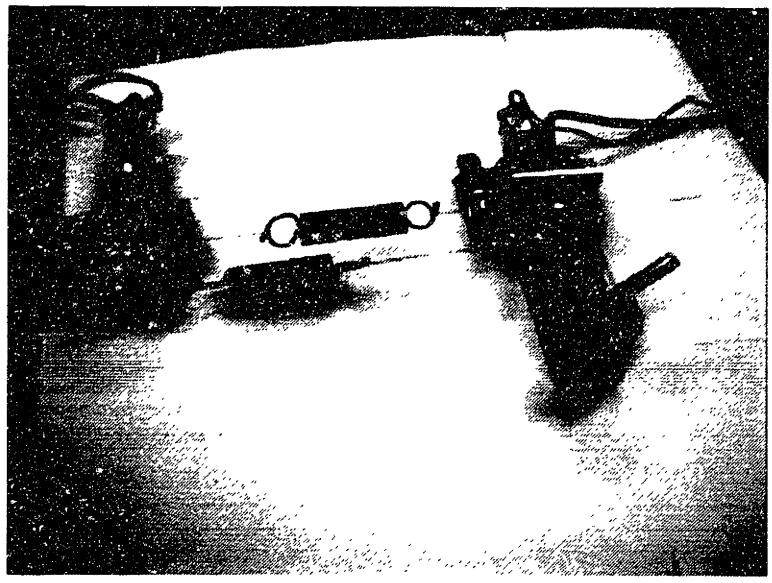

Figure 7-1: PaCMMA Prototype

The second configuration is a traditional,"stiffer is better" design. The macro-actuator is located remotely and a cable drive transmission transmits power to the joint. Using this configuration, the first resonance in the force response occurs at 12 Hz. The macro-actuator uses a 36:1 planetary gearhead.

The third configuration uses the same hardware as configuration 2, but the control system uses a PD position control architecture. In this configuration the system is run under position control, which is sometimes called open-loop impedance control. In this case, the force is not measured and it is assumed that the torque commanded to the actuator is transmitted to the endpoint with minimal losses.

Configurations 4 & 5 represent the PaCMMA with two different transmissions. The first configuration, PaCMMA1, uses a transmission stiffness, K_t of 1140 mNm/rad. The second configuration, PaCMMA2, uses K_t=3000 mNm/rad. The majority of the tests are performed with PaCMMA1 except for impedance, which is measured for both systems.

7.2 Performance Data

In order to evaluate the performance of the actuator system, a number of performance metrics must be defined. It is common to evaluate actuators on performance specifications such as power/mass and force/mass. These specifications are useful but neglect several important dynamic characteristics which affect performance in robot haptics and manipulation. To quantify robot characteristics in force controlled tasks, I will present several measures of performance.

- Force Control Frequency Response

- Force Control Step Response
- Force Fidelity (Distortion)
- Force Control Performance Space
- Impedance Frequency Response
- Position Control Frequency Response
- Position Control Step Response
- Impact Response
- Control of the PaCMMA Impedance
- Dynamic Range and Precision

The results of the experiments using these measure are presented in table 7.2.

Before presenting the data, a few remarks are in order. Frequency response measurements do a good job of presenting a large amount of information, but may not reflect true response if the output signal is not a pure sinusoid. Nonetheless, they provide a useful way to compare the performance of various systems. For the results presented in the following sections, the frequency response was calculated by determining the Fourier coefficients of the input and output signal at the excitation frequency. From these values, phase and amplitude of the transfer function were determined. The system is amplitude dependent due to saturation of the micro-actuator. Further, friction and backlash contribute to the response in a nonlinear manner which depends on both frequency and amplitude. As a result, the response of the system to small disturbances is not the same as the system response to large disturbances. Response data for both large and small disturbances will be presented in order to illustrate this point.

Time domain measurements such as rise time and settling time are also useful since many applications will rely on step inputs and many disturbances are fast enough to approximate a step function. It is important to remember that step response inputs are the least "smooth" and therefore are most likely to saturate the inputs. Avoiding these kinds of discontinuities at the control inputs will reduce high frequency transients.

	Micro	Macro	PaCMMA1	PaCMMA2
Force Control Bandwidth				
Small - F_{des}=0.08 sin(ωt) Nm	56 Hz	12 Hz	56 Hz	56 Hz
Large - F_{des}=0.32 sin(ωt) Nm	NA	12 Hz	4.5 Hz	8 Hz
Force Distortion less than 20%				
Small - F_{des}= 30 sin(ωt) mNm	60 Hz	3 Hz	60 Hz	
Large - F_{des}= 400 sin(ωt) mNm	NA	20 Hz	8 Hz	
Position Bandwidth				
Small - X_{des}=0.014 sin(ωt) rad	10 Hz	0[a],1.6[b] Hz	10 Hz	
Large - X_{des}=1.1 sin(ωt) rad	6 Hz	4[c],1.6[b] Hz	3 Hz	
Impedance Bandwidth (F_{des}=0)				
Small - X_{in}=0.23 sin(ωt) rad	10 Hz	0.16 Hz	2.9 Hz	2.9 Hz
Large - X_{in}=0.92 sin(ωt) rad	5 Hz	0.08 Hz	1.6 Hz	1.6 Hz
Maximum Impact Force				
V_o= 1.9 rad/sec	83 mNm	495 mNm	66 mNm	
V_o= 7.5 rad/sec	252 mNm	1400 mNm	240 mNm	
Force Dynamic Range	58:1	52:1	800:1	
Force Precision	1.7%	1.9%	0.12%	

NA – test could not be performed

[a]Performance was insufficient for test

[b]Using impedance controller

[c]Using PD controller

Table 7.2: Performance Summary

7.2.1 Force Control Response

The force control response of the PaCMMA approaches the theoretical predictions of Chapter 4. The small signal bandwidth of the micro-actuator is maintained, while the bias force is determined by the macro-actuator. Recall the definition of force control response from Chapter 4:

$$H_s(\omega) = \frac{F_e(\omega)}{F_d(\omega)} \Bigg|_{X_e=0}$$

Force control bandwidth was measured by clamping the endpoint to a rigid environment and setting the desired force to be a number of sinusoids of different amplitudes and frequencies. Since saturation is an important characteristic of this research, frequency response measurements were taken with a variety of desired amplitudes as well as at a variety of mean force values. Step responses were measured by simply applying various step changes in desired force from various bias forces.The data for these experiments is presented below.

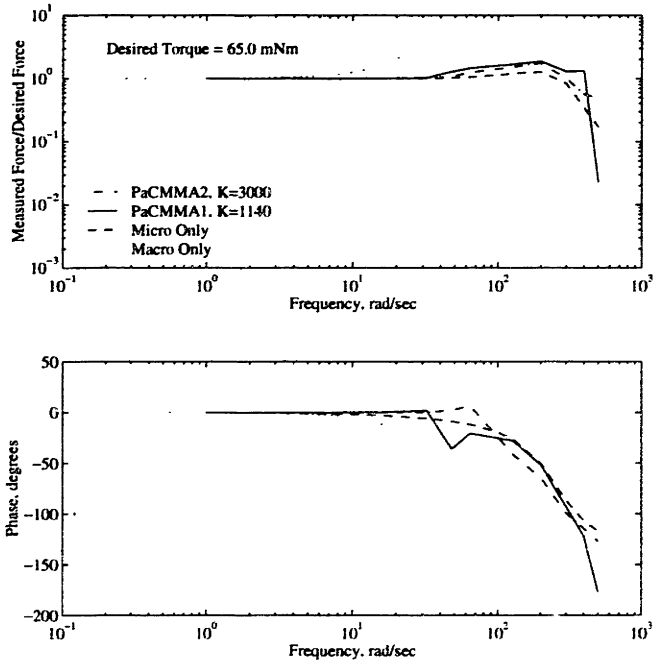

Figure 7-2: **Small Signal Force Control Bandwidth.** $F_{des} = 0.08$, $F_{2sat} = 0.57F_{1sat}$. Performance was measured using explicit force control

As expected, the force control bandwidth of the PaCMMA for small signals (figure 7-2) is nearly as good as the response of the micro-actuator alone (56 Hz). However, the large signal performance (figure 7-3) of the PaCMMA (4-6Hz) is lower than the macro-actuator can achieve with a stiff transmission (12Hz). This is expected - the ability of the macro-

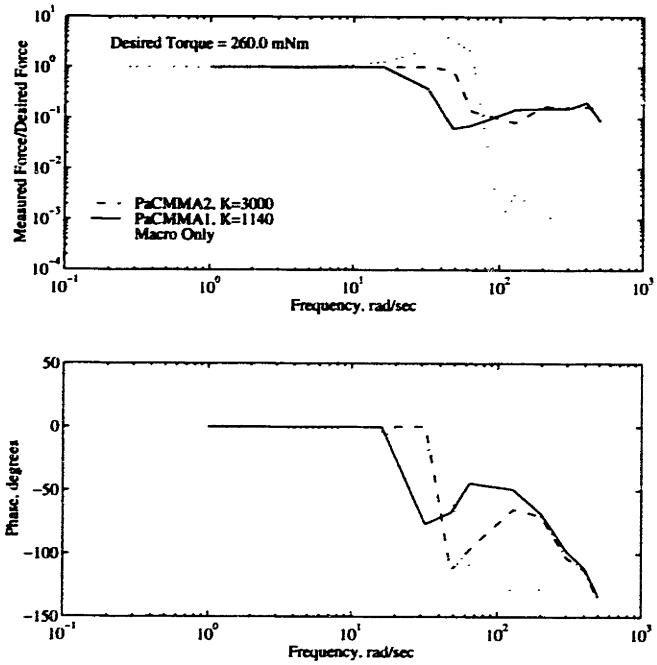

Figure 7-3: **Large Signal Force Control Bandwidth.** $F_{des} = 0.32$, $F_{2sat} = 2.3F_{1sat}$. Performance was measured using explicit force control.

actuator to transmit force is directly affected by the transmission bandwidth. Since the PaCMMA transmission is softer than the stiff cable transmission, it can not use the large signal capacity of the macro-actuator as effectively. Figure 7-4 shows how the theoretical performance curve from section 4.4 compares to the actual bandwidth measurements. The data from all of the force control experiments is plotted in this figure. The difference in the experiment and theory reflects the non-perfect performance of the control law.

The step response of the PaCMMA is also as expected. Small changes in force are very fast (15msecs), while large changes in force require the macro-actuator to displace the transmission a significant distance. The slower response reflects the velocity and acceleration limits of the macro-actuator. This performance can be improved by choosing a macro-actuator with faster acceleration, or by choosing a stiffer transmission.

Figure 7-5 shows a small oscillation after the step value has stabilized. This oscillation is caused by the transmission springs vibrating after the sudden change in displacement of the macro-actuator. As mentioned in section 4.9.5, the transmission was modeled as a mass-less spring and damper. Since the unmodelled resonance (100 Hz) occurs above the frequency of the micro-actuator control system, there is no way to actively suppress it. A solution to this problem is to reduce the resonance of the transmission by a) increasing the transmission mass to reduce the frequency of oscillation or b) to add enough damping to eliminate the resonance all together.

It is clear that large signal force control performance is not maximized with the PaCMMA

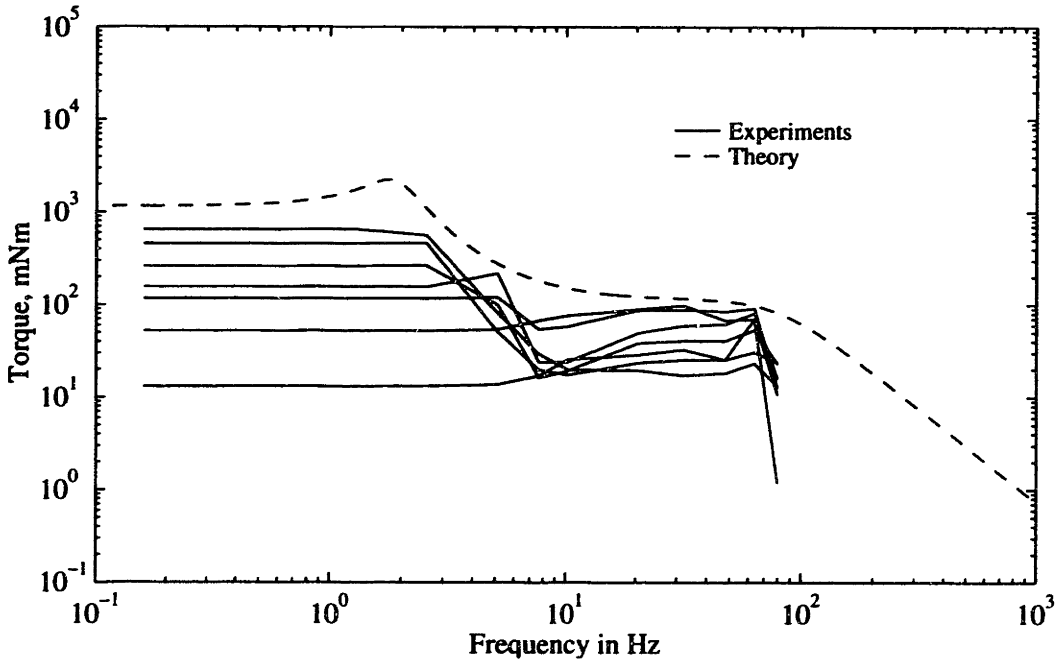

Figure 7-4: **Force Control Response – Theory vs. Experimental.** Solid lines represent swept sinusoidal inputs at various force amplitudes.

concept. Nonetheless, the performance gains in some of the experiments that follow will more than justify the concept for many applications.

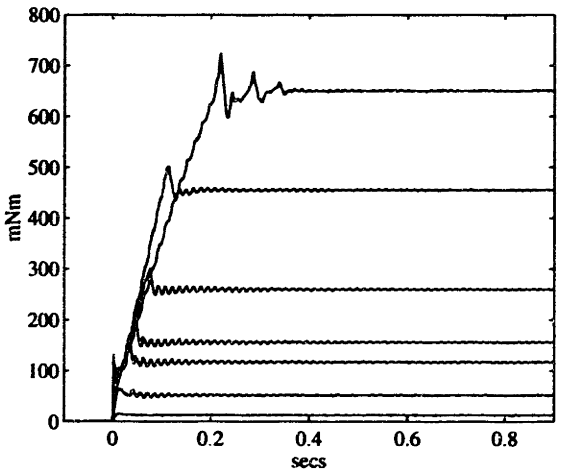

Figure 7-5: **Large Step Response for PaCMMA1.** The small oscillations in the force which persist after reaching the desired force represent the unmodelled dynamics in the transmission. The steel extension springs are vibrating at 100 Hz due to the sudden change in force. Since this disturbance is greater than the micro-actuator bandwidth, they can not be suppressed.

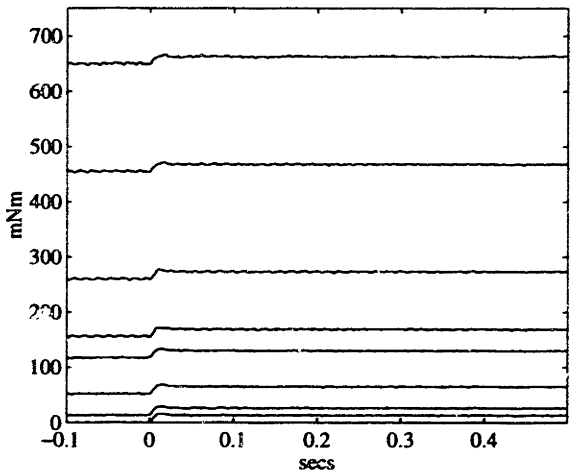

Figure 7-6: **Small Step Response for PaCMMA1.** This graph shows the fast response to small steps, regardless of force bias. The rise time is approximately 15 milliseconds.

7.2.2 Force Fidelity

The force fidelity of the PaCMMA was very good. The micro-actuator was able to reduce distortion up to 60Hz. A metric for least squares distortion was described in Chapter 3. Figures 7-7 and 7-8 show the force fidelity versus frequency for small and large amplitudes.

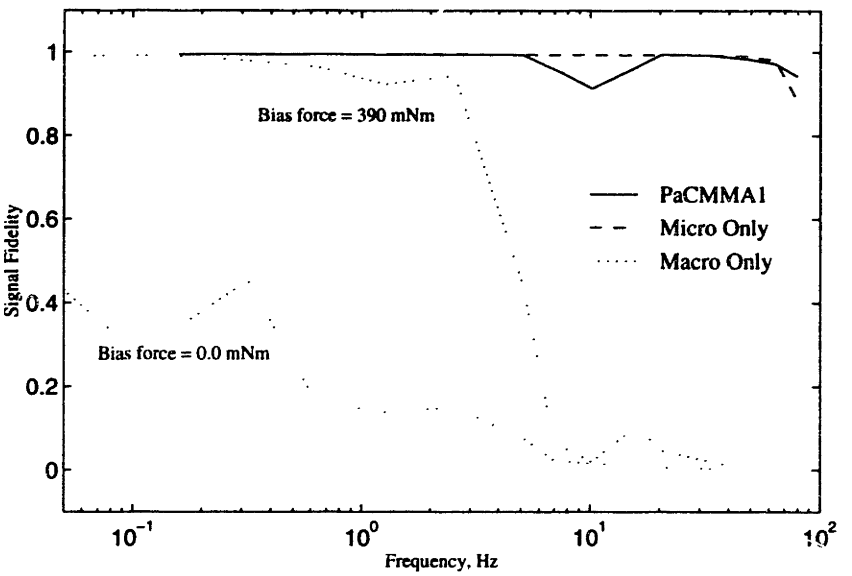

Figure 7-7: **Small Signal Distortion.** *Fdes* = 13 mNm. The figure shows that the PaCMMA and the micro-actuator perform much better than the macro-actuator for small amplitude force commands. While a force bias improves the performance of the macro-actuator somewhat, it is still not as accurate as the PaCMMA or the micro-actuator.

Figure 7-7 shows the response of the system to a small force command (13mNm = 10% F_{1sat}). The macro-actuator alone is very distorted. This is due to the friction and backlash that are introduced by the gearhead. A second trial with the macro-actuator was performed with a large bias (390mNm). The distortion was improved but still falls short of the performance that can be obtained with the micro-actuator and the PaCMMA.

Figure 7-8 shows the large signal force fidelity. In this case, the PaCMMA signal deteriorates first, but this is largely due to attenuation (remember the force bandwidth of the PaCMMA is lower than the macro-actuator for large forces). As the frequency increases the PaCMMA maintains a higher level of fidelity.

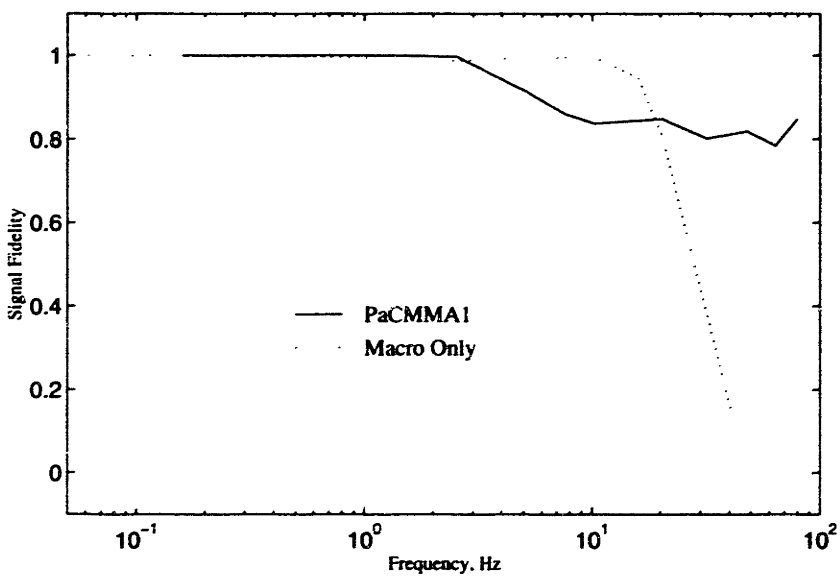

Figure 7-8: **Large Signal Distortion.** F_{des} = 520 mNm. The macro-actuator performs more accurately than the PaCMMA for some frequencies, but the PaCMMA fidelity is better overall.

7.2.3 Force Performance Space

The force performance space data of the experiments does a good job of simultaneously displaying the bandwidth data and the distortion data of the previous sections. Figures 7-9 and 7-10 show the performance space for the individual actuators and the PaCMMA respectively.

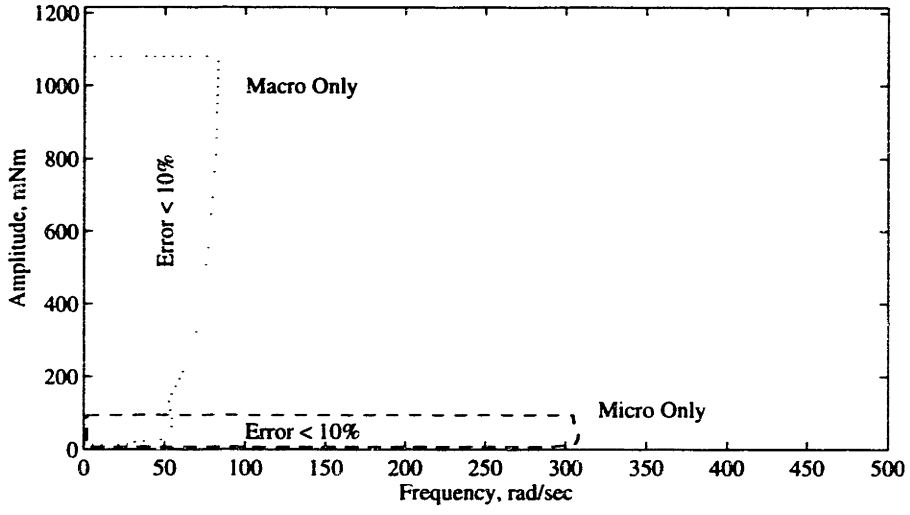

Figure 7-9: **Force Performance Space for Macro and Micro Actuators.** The force control response data of section 7.2.1(explicit force control) was analyzed to determine the amplitudes and frequencies at which the RMS error was less than 10%.

On figure 7-9, the macro and micro-actuator performance boundaries delimit different regions of the space. Notice that the error boundary for the macro-actuator shows the degradation of signal accuracy at small amplitudes.

Figure 7-10 shows the performance space for the PaCMMA. The performance of the micro-actuator is preserved and the overall performance is augmented by the macro-actuator. The contribution from the macro-actuator is smaller than in figure 7-9 but this was expected. The PaCMMA transmission is softer than the transmission used for the macro-only tests and thus, will not be able to transmit force at the same bandwidth.

The ability to augment the performance of the high-performance micro-actuator with large bias forces is an important result. In the next sections, the benefits for using a compliant transmission will be shown. The reduction in large signal force bandwidth is the price that is paid.

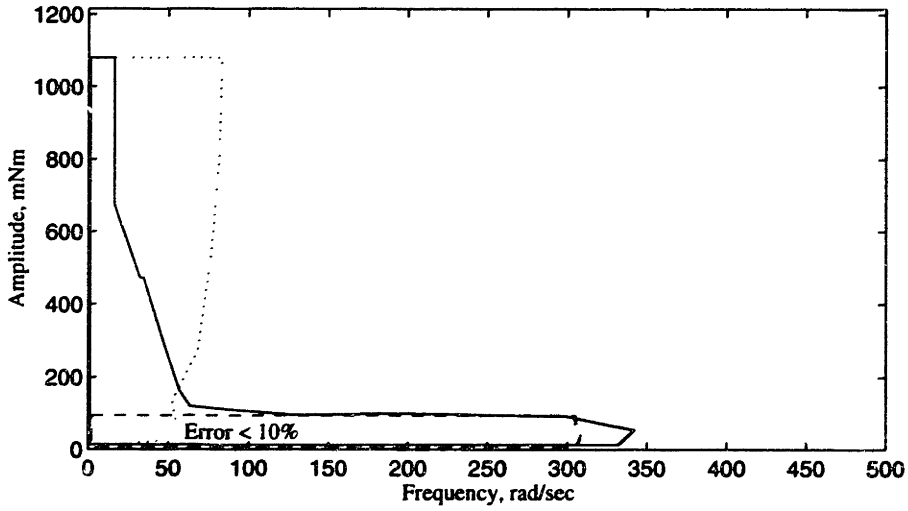

Figure 7-10: **Force Performance Space for PaCMMA1.** The performance space of the micro and macro-actuators is included. This shows how the PaCMMA's parallel coupling of the micro and macro-actuators can be used to get better performance than either actuator operating alone.

7.2.4 Impedance Response Bandwidth

The compliant transmission of the PaCMMA was shown to reduce the impedance dramatically. Impedance response was also measured using the definition from chapter 3:

$$Z(\omega) = \left. \frac{F_{error}(\omega)}{X_{in}(\omega)} \right|_{F_{des}=\text{constant}}$$

For these measurements a high torque, position controlled motor was attached to the end effector and used to create position disturbances. Position disturbances of varying magnitude and frequency were applied to the PaCMMA with F_{des}=0. The results here show the minimum achievable impedance for the PaCMMA system. The results of the impedance response measurements are given below.

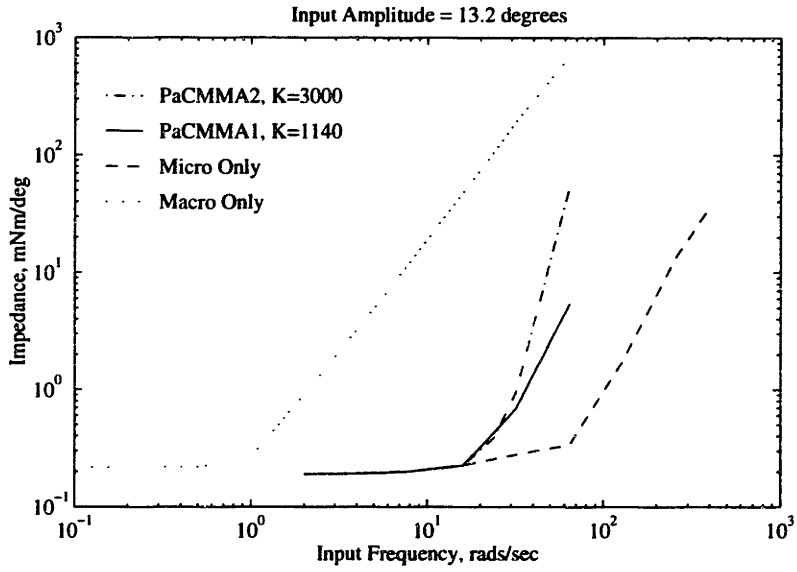

Figure 7-11: **Small Amplitude Impedance Response.** Impedance response data is shown for F_{des}=0. All systems used explicit force control algorithms.

Several aspects of the data are noteworthy. First, there is a minimum impedance value which represents the force noise level divided by the displacement amplitude. This lower limit is created by the force measurement resolution. As the frequency of the disturbance increases, the impedance begins to increase. Several effects are responsible for this increase. When the micro-actuator saturates, it can no longer cancel the inertial force of the end-point mass. When the macro-actuator saturates, it can no longer keep the transmission from deflecting. The relative magnitude of each term (F_{macro} and F_{micro}) depends on the amplitude of displacement and the component specifications.

A comparison of the three cases shows that the macro-actuator with a stiff transmission presents the largest impedance while the micro-actuator presents the smallest impedance.

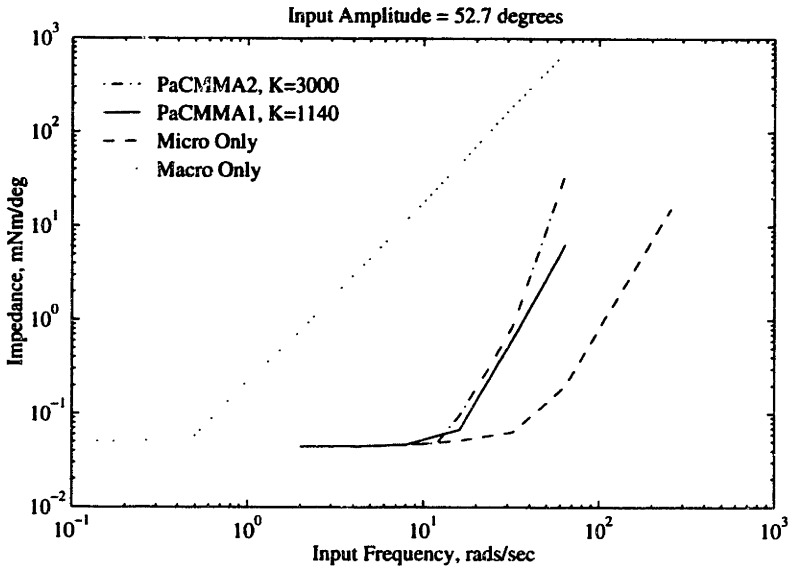

Figure 7-12: **Large Amplitude Impedance Response.** Impedance response data is shown for F_{des}=0. All systems used explicit force control algorithms.

The PaCMMA generates an impedance in between these two values. It should be clear that the stiff transmission creates a large impedance while the compliant transmission creates a smaller impedance. The data for the micro-actuator and macro-actuator alone provide bounds on the maximum and minimum impedance.

7.2.5 Position Control Experiments

The PaCMMA was run using the impedance controller of Chapter 5 and commanded to follow both step and sinusoidal position trajectories. The desired impedance was set to the stiffest impedance possible in order to maximize the position bandwidth. The results of these tests are shown below.

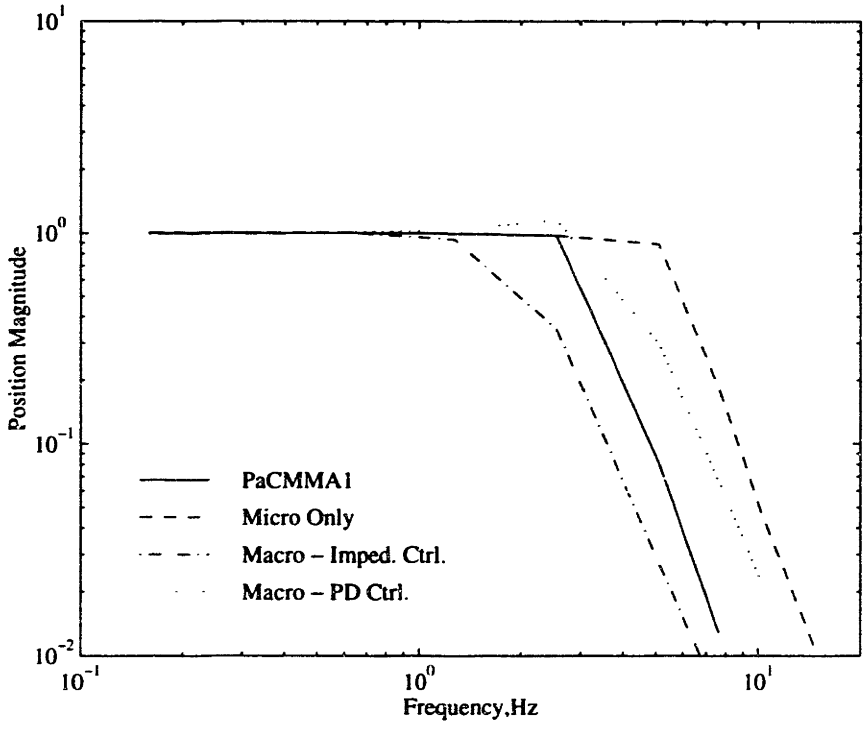

Figure 7-13: **Large Signal Position Bandwidth.** X_{des}= 62.0 degrees

Figure 7-13 shows the position bandwidth of four systems. The micro-actuator, macro-actuator and PaCMMA were run with the impedance control method described in Chapter 5, and the macro-actuator was also run with a standard PD position control law. Clearly, the micro-actuator offers the highest bandwidth, and the macro-actuator under impedance control is the slowest. The PaCMMA position performance is almost as good as the macro-actuator under PD position control. This is a particularly useful though initially unexpected result.

For force control bandwidth, the PaCMMA's transmission compliance limited the large signal bandwidth. For position bandwidth the large signal performance actually *exceeds* the performance that could be achieved with only the macro-actuator and the compliant transmission. The micro-actuator stabilizes the vibrations that arise from the step input and the transmission compliance. As a result, the control effort to the macro-actuator can be very large and discontinuous (i.e. Bang-bang) without the penalty of transient vibration.

For small position commands it is clear that PaCMMA performance is as good as the

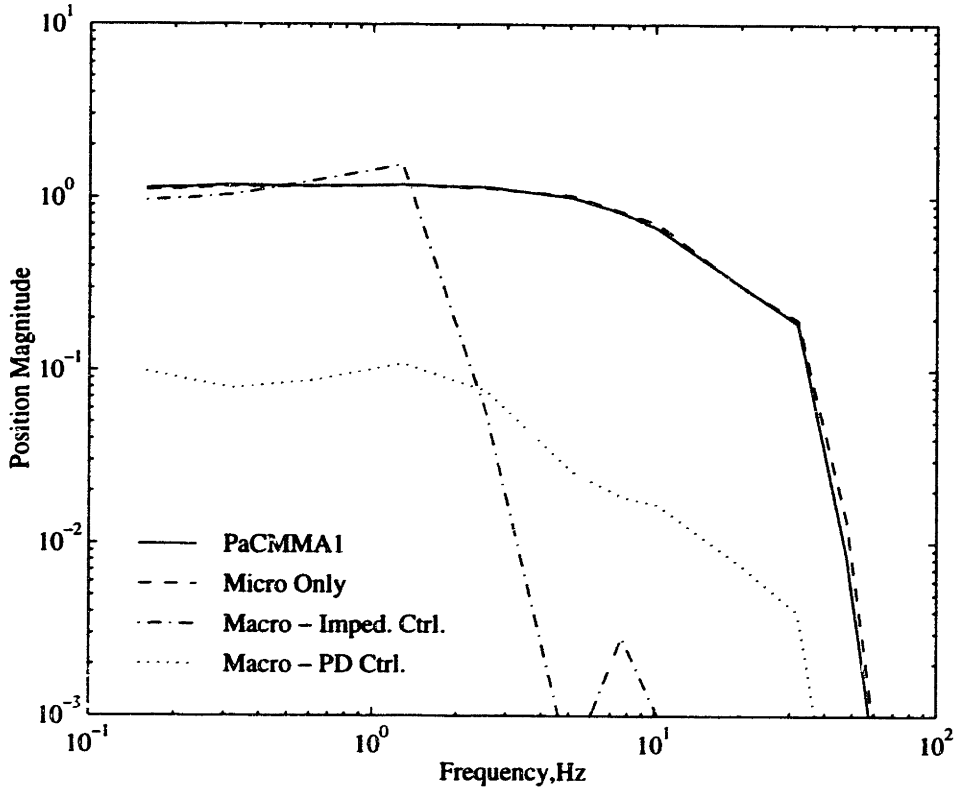

Figure 7-14: **Small Signal Position Bandwidth.** X_{des}=0.8 degrees, Backlash = 0.7 degrees

micro-actuator alone while backlash limits the performance of the macro-actuator.

The step performance in figure 7-15 shows that the PaCMMA can perform step moves with faster rise time and less overshoot than the macro-actuator under conventional PD position control.

Overall, the PaCMMA system is able to recover the full position performance of the macro-actuator while reducing the endpoint impedance through the use of a complaint transmission.

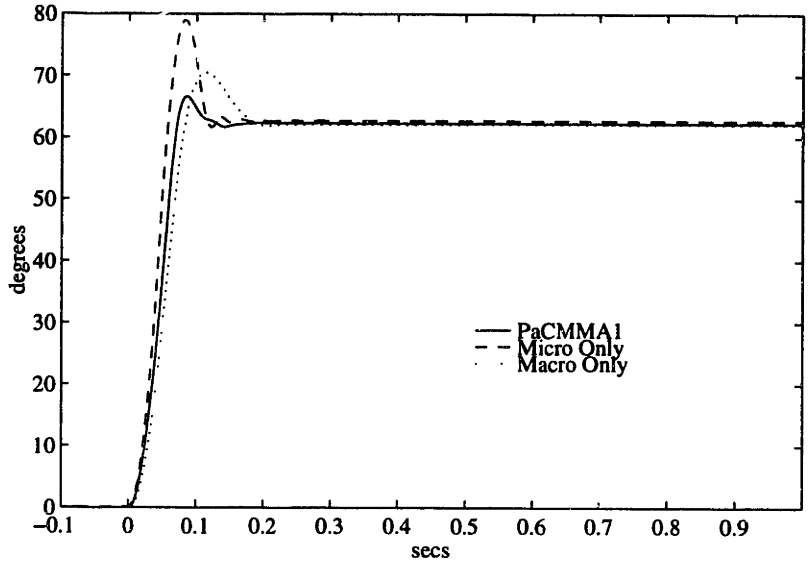

Figure 7-15: **Large Step Response.** F_{des} = 62.5 degrees

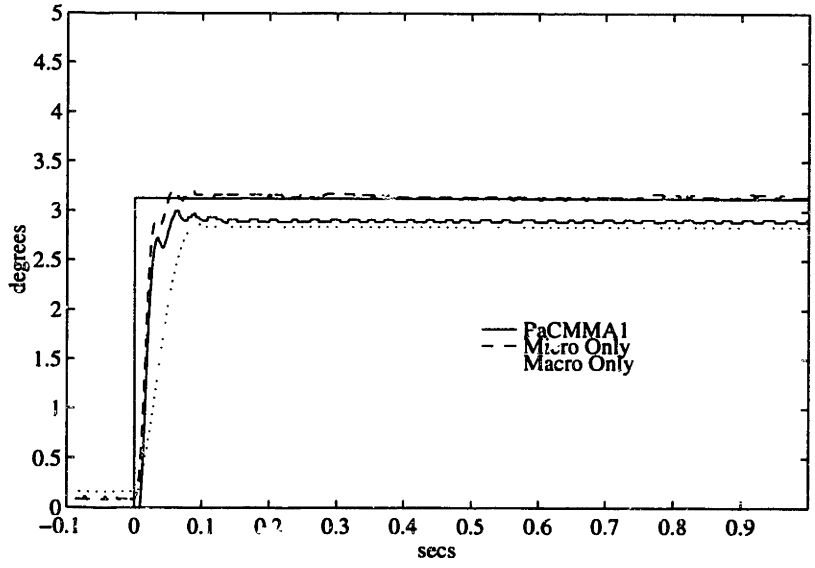

Figure 7-16: **Small Step Response.** F_{des} = 3.125 degrees

7.2.6 Impact Experiments

Impacts highlight the effectiveness of the PaCMMA's low impedance. The PaCMMA was given a velocity input command (V_o) and programmed to stop when impact was detected based on a force threshold of 20mNm. Thresholds smaller than 20mNm could not be used because the inertial force of the accelerating link caused the threshold to trigger. The results of these tests are shown in figures 7-17& 7-18.

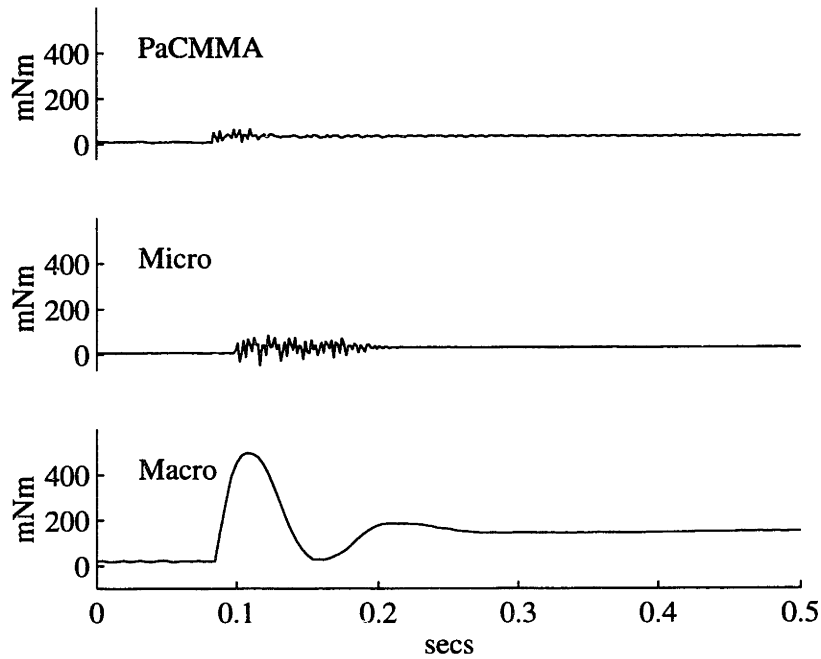

Figure 7-17: **Impact Response.** V_o = 1.9 rad/sec. This graph shows the drastic reduction in impact force when a compliant transmission is attached to the macro-actuator in the PaCMMA system. Notice that the PaCMMA transients settle more quickly than even the micro-actuator by itself.

The reduction in impact force is substantial. In fact, it is clear that the PaCMMA has the fastest settling response. One nice feature in these results is the minimal bounce of the end effector. While the impact forces are certainly a function of velocity, the position response of the system is stable and monotonic.

Several other issues are demonstrated by these experiments. First, the control law is a single impedance control law which does not rely on any switching behavior upon impact. Position commands are easily followed, and force is accurately controlled. Second, impacts typically occur in under a servo cycle. The energy transmitted to the environment from the endpoint is unavoidable. The intentional use of compliance in the transmission prevents the kinetic energy of the macro-actuator from being dissipated during the collision.

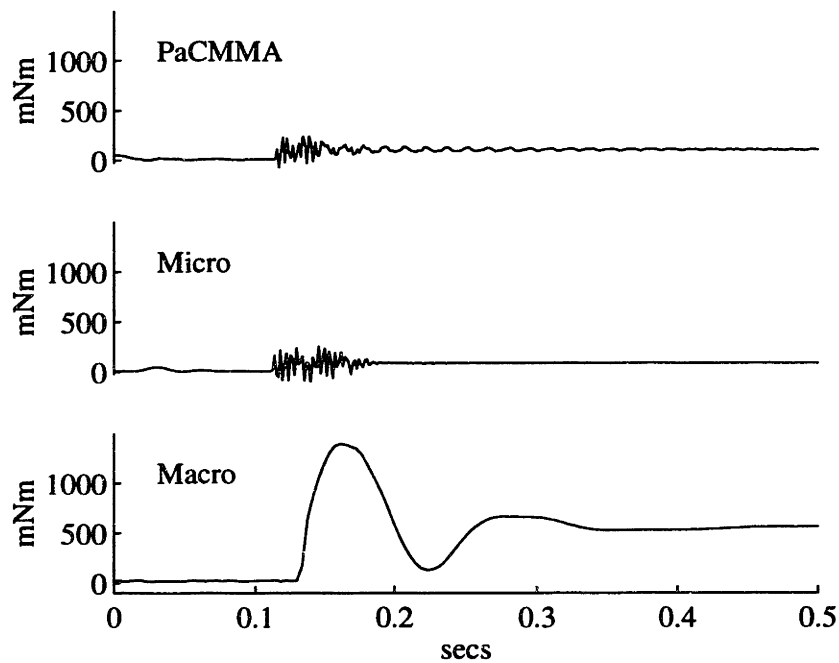

Figure 7-18: **Impact Response.** V_o = 7.5 rad/sec.

7.2.7 Control of PaCMMA Impedance

The PaCMMA was programmed to exhibit different impedances using the impedance control architecture described in section 5.6. Figures 7-19 through 7-24 show the performance of the PaCMMA, micro and macro-actuators for three impedances.

A comparison of the data shows the added range of the PaCMMA in each of these tests. For large displacements, it is clear that the micro-actuator has limited capability for simulating impedances despite the direct-drive bandwidth. The PaCMMA does a much better job of emulating the same impedance at larger amplitudes.

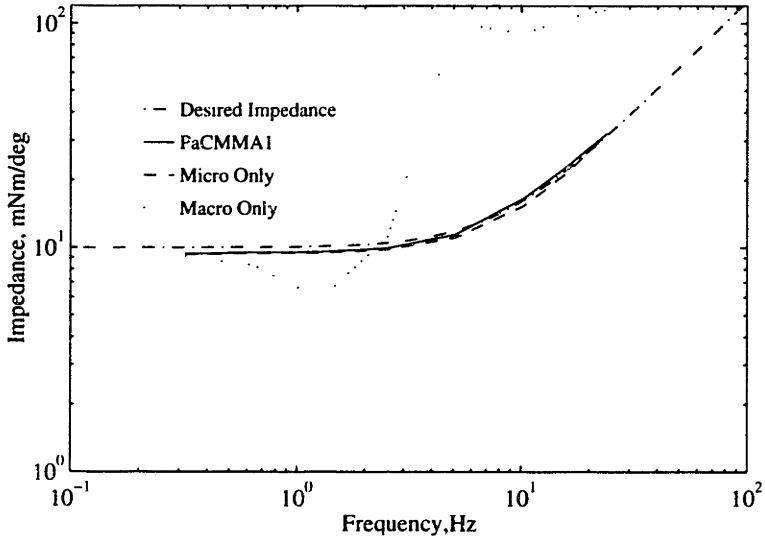

Figure 7-19: **Programmed Impedance.** $Z(s) = 10 + 0.66s$ (Small Displacement). This shows that the micro-actuator and PaCMMA can effectively produce the desired impedance. The macro-actuator can not emulate the impedance as accurately.

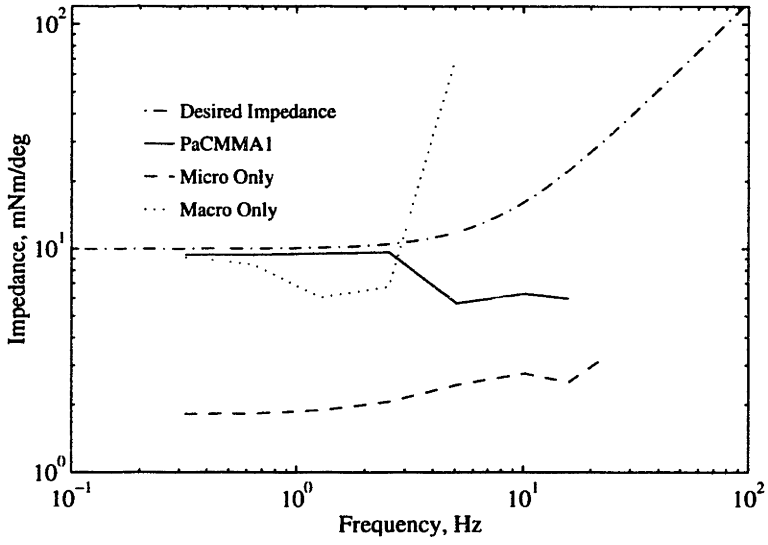

Figure 7-20: **Programmed Impedance.** $Z(s) = 10 + 0.66s$ (Large Displacement). For large disturbances, the PaCMMA outperforms both the micro and macro-actuators. The micro-actuator saturates and can not produce enough force. An additional benefit of the PaCMMA is that its high frequency impedance is much lower than the macro-actuator.

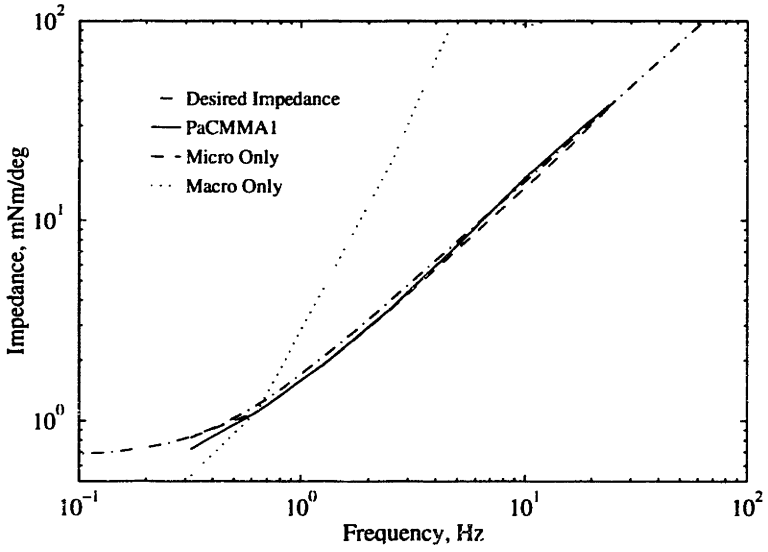

Figure 7-21: **Programmed Impedance.** $Z(s) = 0.67 + 0.25s$ (Small Displacement)

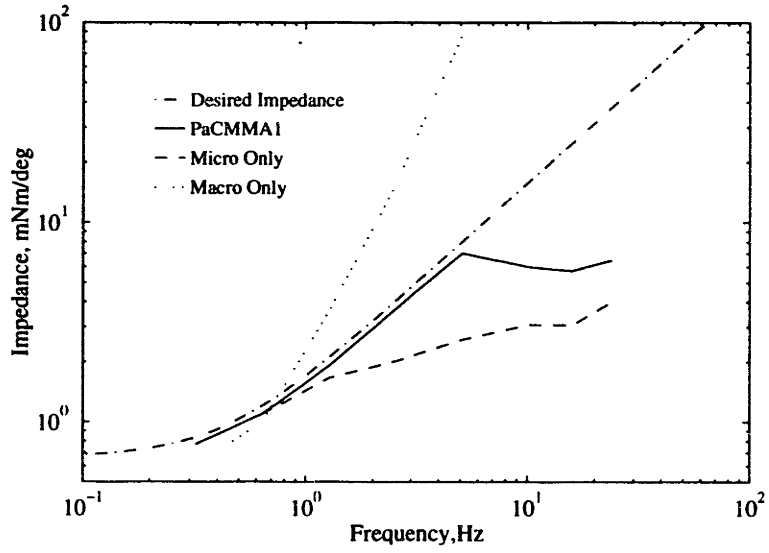

Figure 7-22: **Programmed Impedance.** $Z(s) = 0.67 + 0.25s$ (Large Displacement)

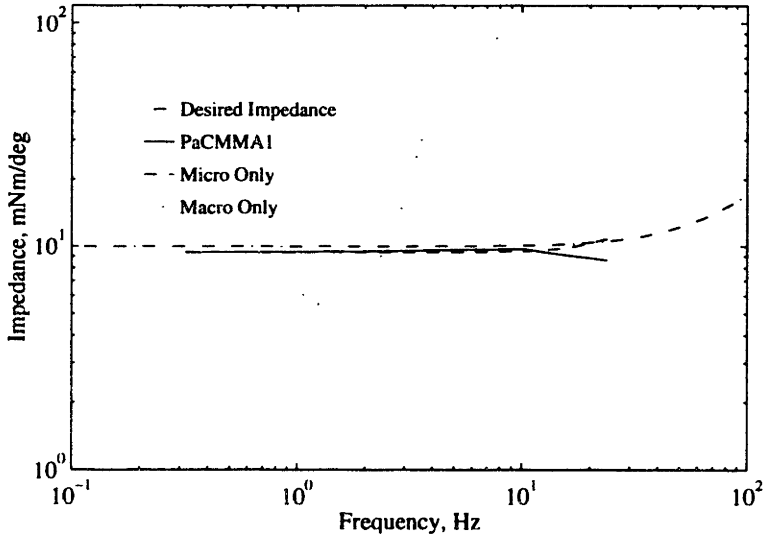

Figure 7-23: **Programmed Impedance.** $Z(s) = 10 + 0.02s$ (Small Displacement)

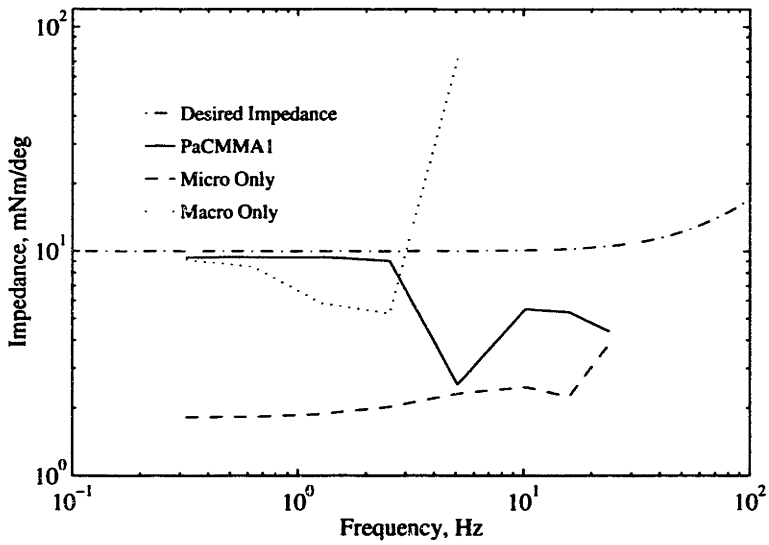

Figure 7-24: **Programmed Impedance.** $Z(s) = 10 + 0.02s$ (Large Displacement)

7.2.8 Dynamic Range and Force Precision

The force precision and dynamic range of the various systems are as follows:

	Force Precision (%)	Force Precision (absolute)	Dynamic Range
Micro Only	1.7%	1.3mNm	58:1
Macro Only	1.9%	15 mNm	52:1
PaCMMA	0.12%	1.3mNm	800:1

Clearly the PaCMMA offers a dramatic improvement in precision and dynamic range.

Chapter 8

Conclusions

8.1 Contributions

This thesis makes several contributions to the area of actuator research. The parallel coupled micro-macro actuator system (PaCMMA) described in this thesis was shown to exhibit superior characteristics when compared to typical single actuator systems. The benefits of this system are:

- Improved Small Signal Force Control Bandwidth
- Reduced Impedance (more backdrivable)
- Reduced Distortion
- Reduced Impact Forces
- Improved Small Signal Position Bandwidth
- Improved Force Resolution and Dynamic Range

In addition to the actuator system, this thesis also formalizes several performance metrics so that designers will have a more complete set of tools when choosing actuator systems.

8.2 Thesis Summary

This thesis presents an actuator concept which combines two actuators to obtain improved performance and compares the performance to two typical actuator configurations. Chapter 1 presents the motivation and background for understanding the thesis and chapter 2 introduces the Parallel Coupled Micro-Macro Actuator concept.

Chapter 3 proposed several actuator performance metrics. Some of these metrics are well established while others are new to the area of actuator design.

Chapter 4 provided a model of the PaCMMA system and derived a number of performance limits. It was shown that micro and macro-actuators in the PaCMMA system have limits on both frequency and amplitude. Analytic expressions for force control bandwidth,

position control bandwidth and impedance were derived for the PaCMMA system. A brief discussion of nonlinear effects is presented.

Chapter 5 presented a control law for the system. The control law performance was compared to an optimal control law and was shown to be nearly optimal in some conditions and adequate in other operating conditions.

Chapter 6 discussed the design parameters for the system and presented a design procedure. As with all design procedures, the process is likely to be iterative when resolving the large number of simultaneous constraints.

Chapter 7 presents the results from a large number of experiments. The data shows conclusively that the PaCMMA concept is both physically realizable and effective in achieving the desired performance goals.

8.3 Further Work

The work presented here provides the starting point for understanding how two scaled actuators may be used in parallel to achieve better performance than a single actuator. As with most theses, there are a number of research directions to explore in greater detail.

Nonlinear Transmission: The elasticity in the transmission is a fundamental characteristic of the PaCMMA concept. Consideration of various manipulation tasks suggests that the low stiffness is most important when the actuator is in the process of making contact with the environment. In this case, the transmission deflection is small. Conversely, when the contact forces are large and the transmission is under considerable load, the low stiffness is not as important. This leads to the conclusion that the transmission should probably be soft when the forces are small and stiffer when the forces are high. The use of a nonlinear transmission will be an important extension of this concept.

Compact Design: The current implementation places the micro-actuator at the endpoint and the macro-actuator is located some distance from the endpoint. The configuration shown in figure 2-2 represents a PaCMMA in a compact package. This configuration is obviously of interest since it can be readily connected to existing hardware.

Control Law: The control law presented here was chosen for its simplicity and generally good performance across a wide range of operating conditions. There are obviously applications where the dynamics are less likely to change and a more specialized controller might yield improved performance.

Other Actuator Technologies: Electric motors were used because of their broad popularity and ease of use. However, other actuators may influence the design and performance. Actuators with limited position range (like voice coils and hydraulic cylinders) may produce slightly different performance relationships. Extension of the concept to other actuators remains an interesting implementation project.

8.4 Applications

The PaCMMA concept may be useful in a number of applications. Haptic interfaces are placing very large demands on actuator technology and creation of a high fidelity interface is a current research topic (Massie and Salisbury, 1994; Hayward, 1995; Salcudean and Wong, 1993; Maclean, 1996). Much of this work focuses on maximizing the fidelity to human perception because success in this field is determined by a "Haptic Turing Test" (Maclean, 1996).

Unstructured environments constantly test the robustness of control laws and mechanical hardware. Impact resistance and error tolerance are of prime importance and performance is often defined as not breaking, rather than high speed or dexterity.

Active tactile sensing is another area of application. The ability to sense features dynamically is dependent on the ability to move smoothly, with precision in force and position. Effective algorithms for dynamic sensing rely on high quality actuation (Eberman, 1995). The quality of the information is directly related to the quality of movement. Humans benefit from very smooth, well damped actuation.

Appendix A

Prototype Specifications

The prototype actuator has the following specifications:

Micro-actuator	Maxon RE035
Rotor inertia	67.6gmcm^2 (0.0068 mNm sec^2)
Maximum Torque	114 mNm
Position Resolution	4.36×10^{-4} rad/count (14400 counts/rev)

Macro-actuator	Maxon RE035 w/gearhead
Reduction	36 : 1
Inertia (includes gearhead) (M_2)	8mNms^2
Maximum Output Torque	3.2 Nm
Maximum Output Velocity	14.5 rad/sec (140 RPM)
Position Resolution	8.72×10^{-5} rad/count (72000 counts/rev)
Backlash	0.7 degrees

Link Properties	
Inertia	0.3 mNm

Transmission 1	Steel Extension Spring
Stiffness (K_t)	1140 mNm/rad
Damping (B_t)	48 mNm/rad/sec

Transmission 2	Steel Extension Spring
Stiffness (K_t)	3000 mNm/rad

Force Sensing	Transducer Techniques TRT-50
Maximum Torque	50 in lbs (5650 mNm)
A/D Resolution	1.3 mNm/count

Micro Actuator Amplifier	Copley 211A
PWM Switching Frequency	80 KHz
D/A Resolution	6.1×10^{-4} volts/count

Macro Actuator Amplifier	Copley 306A
PWM Switching Frequency	20 KHz
Amplifier Gain	1.2 amps/volt
D/A Resolution	6.1×10^{-4} volts/count

A.1 Design example

The transfer function from micro-actuator torque to the torque sensor must be measured first. The connection between these two elements will become the upper limit on force bandwidth. Figure A-1 shows the experimentally measured bandwidth for the micro-actuator to the clamped endpoint.

This transfer function has a large resonant peak at 300 Hz. The next step of the design process is to apply a lowpass filter (H_{1OL}) and integral gain to this transfer function so that the resonant peak is below unity gain when the phase crosses 180 degrees. Figure A-2 shows the combined open loop response of the controller and the micro-actuator.

The spring deflection can be measured and K_t can be determined. For this system,

K_t= 1140mNm/rad.

Using a series of known input torques, the inertia, M_2 can also be determined. A series of step forces was input, the resulting accelerations measured and the best estimate for the macro-actuator inertia was:

M_2= 8mNm s^2.

The feedforward model for the macro-controller is obtained by measuring the macro-actuator transfer function, $G(s) = F_e(s)/F_2(s)$, and inverting the system response. The function is:

$H_{ff} = \frac{1}{G(s)} = \frac{2.782s^2+25.92s+100}{s^2+20s+100}$

The remaining gains to tune are G_{d1}, G_{d2}, and G_p. These may be tuned by performing step response tests and adjusting the gains based on the response.

Start by setting G_{d2} to a large value to inhibit motion of the macro-actuator. Set G_{d1} to a large value. Set F_{des}=0. Move the endpoint around very quickly. Reducing G_{d2} will reduce the impedance by increasing the velocity limit of the macro-actuator. When the velocity limit has been increased to an acceptable level, gain G_{d1} can be gradually reduced. Reducing G_{d1} too much will make the system unstable. The lower limit on G_{d1} is more likely to be determined by the transmission's structural resonances and the designer's tolerance for noise and vibration.

Gain G_p may be gradually increased until the control effort on F_1 is reduced to a value

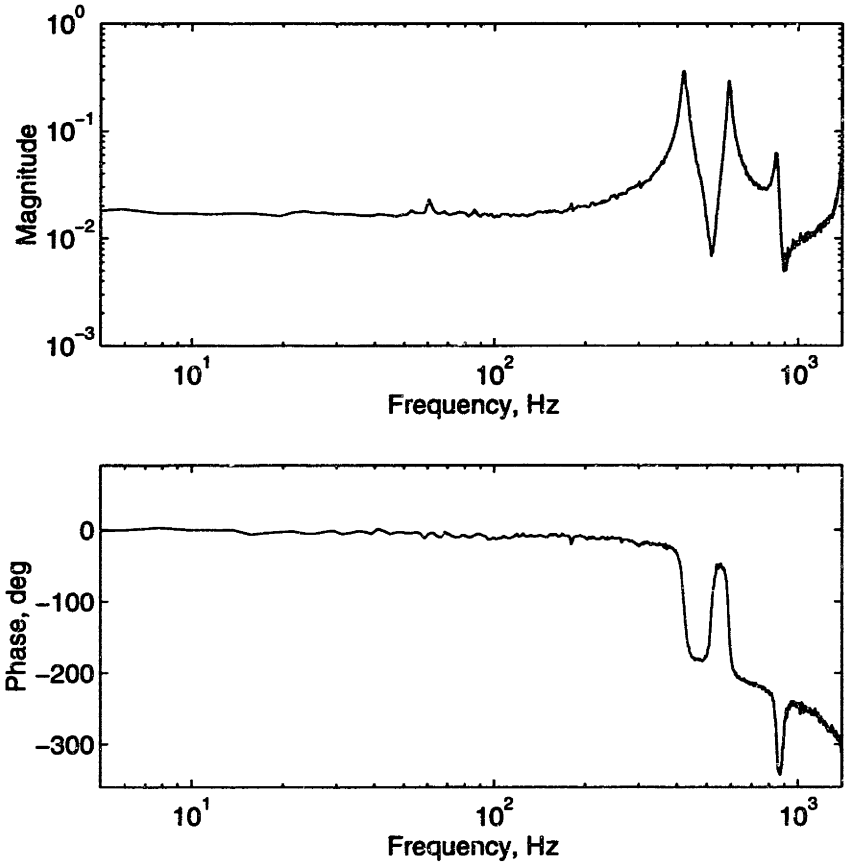

Figure A-1: **Micro Actuator Transfer Function.** $\frac{F_e(s)}{F_1(s)}$ - Experimentally measured by clamping the output shaft and doing a frequency sweep, $F_1 = A\sin(\omega t)$

close to zero. G_p should not be increased arbitrarily - it will destabilize the system if it is too large.

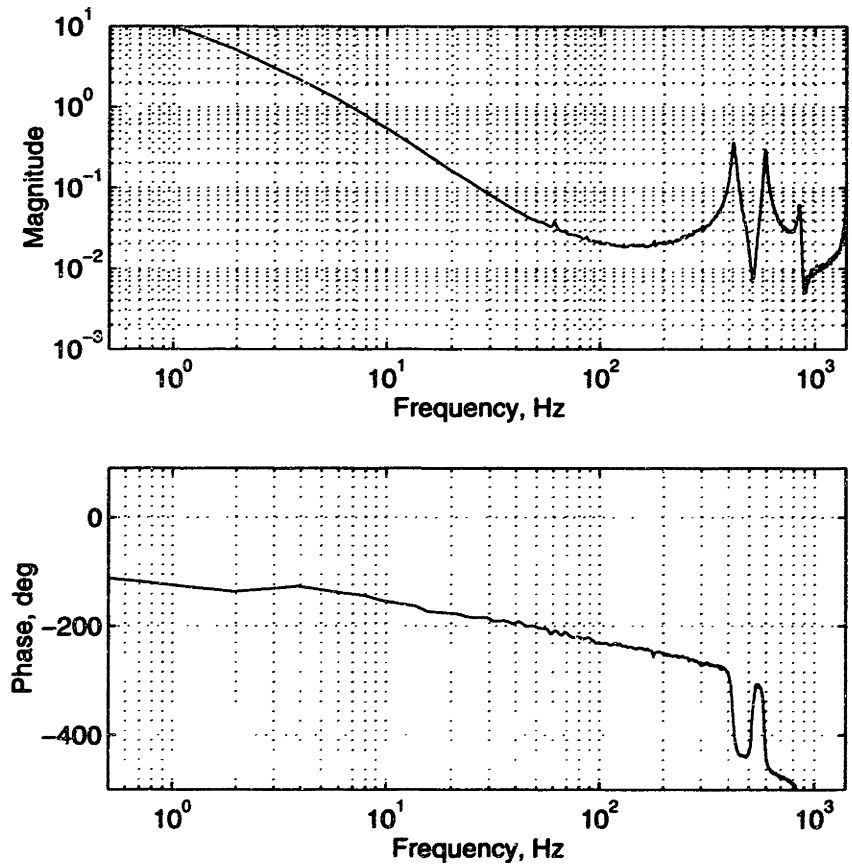

Figure A-2: **Micro Actuator and Controller.** This figure shows the open loop response of the micro-actuator controller and the micro-actuator together.

Appendix B

Simulation Parameters

Simulation of the PaCMMA system proved useful in several parts of this thesis. The equations derived in Chapter 4 were used with the parameters below to predict system performance.

Model Parameters for Simulations and Performance Predictions

Parameter	Value
M_1	0.306 mNm secs^2
M_2	8.1 mNm secs^2
K_t	1140 mNm/rad
B_t	48.35 mNm/rad/sec
$H_{1OL}(s)$	$\frac{\omega_{co1}^2}{s^2+1.414\omega_{co1}+\omega_{co1}^2}$
ω_{co1}	80 Hz (502 rad/sec)
F_{1sat}	114 mNm
F_{2sat}	1.0 Nm

Control Law Gains for Simulations

The control law in Chapter 5 was simulated with the following gains:

Gain	Value
G_{ff}	1.0
H_{ff}	$\frac{2.782s^2+25.92s+100}{s^2+20s+100}$
G_{d1}	70
G_{d2}	50
G_p	4
G_i	100

Augmented Model

In order to properly simulate the inertial effects of the micro-actuator and the torque sensor, a third model element was added. Figure B shows the augmented model.

For this model, the torque sensor properties were estimated from the open loop transfer function in figure A-1.

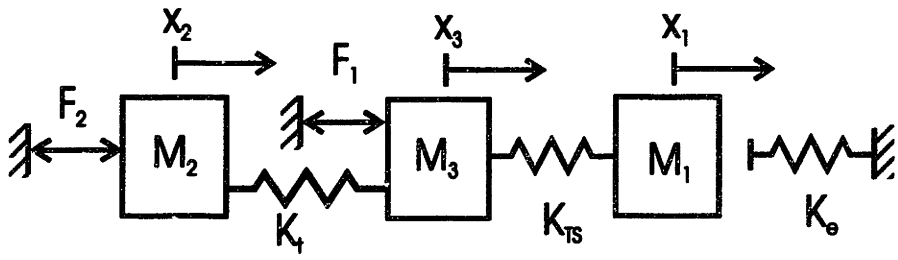

Figure B-1: Augmented Model for Simulation

Parameter	Value
M_1	0.30 mNm secs^2
M_3	0.0068 mNm secs^2
K_{ts}	100000 mNm/rad
B_{ts}	20.8 mNm/rad/sec

A state-space model of the various parts of the system follows.

PaCMMA dynamics:
State Vector and Inputs:

$$x = \begin{bmatrix} x_1 \\ \dot{x}_1 \\ x_2 \\ \dot{x}_2 \\ x_3 \\ \dot{x}_3 \end{bmatrix} \quad \text{and} \quad F = \begin{bmatrix} F_1 H_{1OL}(s) \\ F_2 \end{bmatrix}$$

System Matrices:

$$A = \begin{bmatrix} 0 & 1 & 0 & 0 & 0 & 0 \\ -(K_{ts}+K_e)/M_1 & -(B_{ts}+B_e)/M_1 & 0 & 0 & K_{ts}/M_1 & B_{ts}/M_1 \\ 0 & 0 & 0 & 1 & 0 & 0 \\ 0 & 0 & -K_t/M_2 & -B_t/M_2 & K_t/M_2 & B_t/M_2 \\ 0 & 0 & 0 & 0 & 0 & 1 \\ K_t/M_3 & B_t/M_3 & K_t/M_3 & B_t/M_3 & -(K_{ts}+K_t)/M_3 & -(B_{ts}+B_t)/M_3 \end{bmatrix}$$

$$B = \begin{bmatrix} 0 & 0 \\ 0 & 0 \\ 0 & 0 \\ 0 & 1/M_2 \\ 0 & 0 \\ 0 & 1/M_3 \end{bmatrix}$$

$$C = \begin{bmatrix} -K_{ts} & -B_{ts} & 0 & 0 & K_{ts} & B_{ts} \\ 0 & 0 & 1 & 0 & 0 & 0 \\ 0 & 0 & 0 & 0 & 10 & \\ 0 & 0 & 0 & -G_{d2}-G_{d1} & 0 & G_{d1} \end{bmatrix}$$

$$D = \begin{bmatrix} 0 & 0 \\ 0 & 0 \\ 0 & 0 \\ 0 & 0 \end{bmatrix}$$

Micro-Actuator Controller

$$A = \begin{bmatrix} 0 & 1 & 0 \\ 0 & 0 & 1 \\ 0 & -252000 & -710 \end{bmatrix} B = \begin{bmatrix} 0 \\ 0 \\ 1 \end{bmatrix}$$

$$C = \begin{bmatrix} 10096234 & 0 & 0 \end{bmatrix} D = \begin{bmatrix} 0 \\ 0 \end{bmatrix}$$

Feedforward Macro-Actuator, $G_{ff}H_{ff}$

$$A = \begin{bmatrix} -20 & -100 \\ 1 & 0 \end{bmatrix} B = \begin{bmatrix} 1 \\ 0 \end{bmatrix}$$

$$C = \begin{bmatrix} -29.71 & -178.2 \end{bmatrix} D = \begin{bmatrix} 2.782 \end{bmatrix}$$

Impedance Function Z(s) for position control experiments

$$Z(s) = \frac{28000s+400000}{s+400}$$

Bibliography

An, C. H. (1986). *Trajectory and Force Control of A Direct Drive Arm.* PhD thesis, MIT, Department of Electrical Engineering and Computer Science.

An, C. H. and Hollerbach, J. M. (1987). Dynamic stability issues in force control of manipulators. In *Proc. IEEE International Conference on Robotics and Automation.*

Boulet, B. and Hayward, V. (1993). Characterization, modeling and identification of a high performance hydraulic actuator for robotics. Technical Report TR-CIM-93-9, McGill Centre for Intelligent Machines.

Cannon, R. H. and Rosenthal, D. E. (1984). Experiments in control of flexible structures with noncolocated sensors and actuators. *AIAA Journal of Guidance and Control*, 7(5).

Chiang, W.-W., Kraft, R., and Cannon, R. H. (1991). Design and experimental demonstration of a rapid precise end-point control of a wrist carried by a very flexible manipulator. *International Journal of Robotics Research*, 10(1).

Colgate, J. E. and Brown, J. M. (1994). Factors affecting the z-width of a haptic display. In *Proc. IEEE International Conference on Robotics and Automation*, pages 3205–3210.

Colgate, J. E. and Hogan, N. (1989). An analysis of contact instability in terms of passive physical equivalents. In *Proc. IEEE International Conference on Robotics and Automation*, pages 404–409.

Drake, S. (1975). *Using Compliance in Lieu of Sensory Feedback for Automatic Assembly.* PhD thesis, MITME.

Eberman, B. (1995). Contact sensing: A sequential decision approach to sensing manipulation contact features. Technical Report 1543, MIT Artificial Intelligence Laboratory.

Eppinger, S. (1988). *Modeling Robot Performance For Endpoint Force Control.* PhD thesis, MIT, Department of Mechanical Engineering.

Eppinger, S. D. and Seering, W. P. (1987). Understanding bandwidth limitations in robot force control. In *Proc. IEEE International Conference on Robotics and Automation.*

Gescheider, G. (1985). *Psychophysics: Method, Theory and Application.* Lawrence Erlbaum and Associates, Hillsdale,New Jersey, second edition.

Glosser, G. D. and Newman, W. S. (1994). The implementation of a natural admittance controller on an industrial manipulator. In *Proc. IEEE International Conference on Robotics and Automation*, pages 1209–1215.

Goldenberg, A. A. (1992). Analysis of force control based on linear models. In *Proc. IEEE International Conference on Robotics and Automation.*

Grant, D. and Hayward, V. (1995). Design of shape memory alloy actuator with high strain and variable structure control. In *Proc. IEEE International Conference on Robotics and Automation.*

H. Asada, K. K. and Takeyama, I. (1983). Control of a direct-drive arm. *Transactions of the ASME*, 105:136–142.

Hayward, V. (1995). Toward a seven axis haptic device. In *IROS.*

Hayward, V. and Astley, O. R. (1995). Performance measures for haptic interfaces. In *Proceedings of the 7th International Symposium on Robotics Research*, Munich, Germany. Springer-Verlag.

Henri, P. D. and Hollerbach, J. M. (1994). An analytical and experimental investigation of a jet pipe controlled electropneumatic actautor. In *Proc. IEEE International Conference on Robotics and Automation*, pages 300–306.

Hogan, N. (1983). Impedance control of industrial robots. *Robotics and Computer Integrated Manufacturing*, 1(1):97–113.

Hogan, N. (1985). Impedance control: An approach to manipulation: Part i - theory. *ASME Journal of Dynamic Systems Measurement and Control*, 107(1).

Hyde, J. M. and Cutkosky, M. R. (1993). Contact transition control: An experimental study. In *Proc. IEEE International Conference on Robotics and Automation.*

Jacobsen, S. C., Smith, C. C., Biggers, K. B., and Iverson, E. K. (1989). Behavior based design of robot effectors. In Brady, M., editor, *Robotics Science.* MIT Press.

Johansson, R. and Spong, M. W. (1994). Quadratic optimization of impedance control. In *Proc. IEEE International Conference on Robotics and Automation*, pages 616–621.

John M. Hollerbach, I. W. H. and Ballantyne, J. (1991). A comparative analysis of actuator technologies for robotics. In Khatib, O., Craig, J., and Lozano-Pérez, T., editors, *Robotics Review 2.* MIT Press.

Kazerooni, H. (1985). *A Robust Design Method For Impedence Control Of Constrained Dynamic Systems.* PhD thesis, MIT, Department of Mechanical Engineering.

Khatib, O. (1990). Reduced effective inertia in macro-/mini-manipulator systems. In Miura, H. and Arimoto, S., editors, *Robotics Research 5*, pages 279–284. MIT Press.

Laurin-Kovitz, K. F., Colgate, J. E., and Carnes, S. D. (1991). Design of components for programmable passive impedance. In *Proc. IEEE International Conference on Robotics and Automation.*

Levin, M. D. (1990). Design and control of a closed-loop brushless torque actuator. Technical report, MIT Artificial Intelligence Laboratory, AI-TR 1244.

Liu, G. and Goldenberg, A. A. (1991). Robust hybrid impedance control of robot manipulators. In *Proc. IEEE International Conference on Robotics and Automation*, pages 287–292.

Liu, G. and Goldenberg, A. A. (1994). Robust hybrid impedance control of robot manipulators via a tracking control method. In *International Conference on Intelligent Robots and Systems*, pages 1594–1601.

Maclean, K. E. (1996). *Emulation of Haptic Feedback for Manual Interfaces.* PhD thesis, MIT, Department of Mechanical Engineering.

Massie, T. and Salisbury, J. K. (1994). The phantom interface: A device for probing virtual environments. In *Winter Meeting of the ASME.*

Morita, T. and Sugano, S. (1995). Development of one-d.o.f. robot arm equiped with mechanical impedance adjuster. In *International Conference on Intelligent Robots and Systems*, pages 407–412.

Nagai, K. and Yoshikawa, T. (1994). Impedance control of redundant macro-micro manipulators. In *Intl. Conf. on Intelligent Robots and Systems*, pages 1438–1445.

Narikiyo, T., Nakane, H., Akuta, T., Mohri, N., and Saito, N. (1994). Control system design for macro/micro manipulator with application to electrodischarge maching. In *Intl. Conf. on Intelligent Robots and Systems*, pages 1454–1460.

Paljug, E., Sugar, T., Kumar, V., and Yun, X. (1992). Some important considerations in force control implementation. In *Proc. IEEE International Conference on Robotics and Automation*, pages 1270–1275.

Park, J.-H. (1992). *Integrated Structure/Control Design of Nonrigid Robot Arms for High Speed Manipulation.* PhD thesis, MIT, Department of Mechanical Engineering.

Pratt, G. A. (1994). personal communication.

Pratt, G. A. and Williamson, M. M. (1995). Series elastic actuators. In *International Conference on Intelligent Robots and Systems.*

Qian, H. and DeSchutter, J. (1992a). Introducing active linear and nonlinear damping to enable stable high gain force control in the case of stiff contact. In *Proc. IEEE International Conference on Robotics and Automation*, pages 1374–1379.

Qian, H. and DeSchutter, J. (1992b). The role of damping and low pass filtering in the stability of discrete time implemented robot force control. In *Proc. IEEE International Conference on Robotics and Automation*, pages 1368–1373.

Raibert, M. H., Jr., H. B. B., Chepponis, M., Koechling, J., Hodgins, J. K., Dustman, D., Brennan, W. K., Barrett, D. S., Thompson, C. M., Hebert, J. D., Lee, W., and Borvansky, L. (1989). Dynamically stable legged locomotion. Technical report, MIT Artificial Intelligence Laboratory, AI-TR 1179.

Richter, K. and Pfeiffer, F. (1991). A flexible link manipulator as a force measuring and controlling unit. In *Proc. IEEE International Conference on Robotics and Automation.*

Rosenberg, L. B. and Adelstein, B. D. (1993). Perceptual decomposition of virtual haptic surfaces. In *Proceedings IEEE Symposium on Research Frontiers in Virtual Reality.*

Salcudean, S. and An, C. (1989). On the control of redundant coarse-fine manipulators. In *Proc. IEEE International Conference on Robotics and Automation*, pages 1834–1840.

Salcudean, S. and Wong, N. (1993). Course-fine motion coordination and control of a teleoperation system with magnetically levitated master and wrist. In *Experimental Robotics III, Third International Symposium.*

Salisbury, J. K. (1980). Active stiffness control of a manipulator in cartesian coordinates. In *19th IEEE Conference on Decision and Control*, Albuquerque, NM.

Salisbury, J. K. and Craig, J. J. (1982). Articulated hands: Force control and kinematic issues. *International Journal of Robotics Research*, 1(1).

Salisbury, J. K., Eberman, B., Levin, M., and Townsend, W. (1989). The design and control of an experimental whole-arm manipulator. In *Robotics Research: The Fourth International Symposium.*

Seraji, H. (1994). Adaptive admittance control: An approach to explicit force control in compliant motion. In *Proc. IEEE International Conference on Robotics and Automation*, pages 2705–2712.

Sharon, A. and Hardt, D. E. (1984). Enhancement of robot accuracy using endpoint feedback and a macro-micro manipulator system. In *Proceedings of the American Control Conference.*

Sharon, A., Hogan, N., and Hardt, D. E. (1988). High bandwidth force regulation and inertia reduction using a macro/micro manipulator system. In *Proc. IEEE International Conference on Robotics and Automation.*

Sharon, A., Hogan, N., and Hardt, D. E. (1989). Controller design in the physical domain (application to robot impedence control). In *Proc. IEEE International Conference on Robotics and Automation.*

Sharon, A., Hogan, N., and Hardt, D. E. (1993). The macro/micro manipulator: An improved architecture for robot control. *International Journal of Robotics and Computer Integrated Manufacturing*, 10(3):209–222.

Townsend, W. T. (1988). *The Effect of Transmission Design on the Performance of Force-Controlled Manipulators.* PhD thesis, Dept. Mechanical Eng., MIT.

Trevelyan, J. (1993). Robot force control without stability problems. In *Experimental Robotics III, Third International Symposium.*

Volpe, R. and Khosla, P. (1992). An experimental evaluation and comparison of explicit force control strategies for robotic manipulators. In *Proc. IEEE International Conference on Robotics and Automation*, pages 1387–1393.

Volpe, R. and Khosla, P. (1993). A theoritical and experimental investigation of impact control for manipulators. *International Journal of Robotics Research*, 12(4):361–365.

Wada, H., Kosuge, K., Fukada, T., and Watanabe, K. (1994). Design of force controller based on frequency characteristics. In *Proc. IEEE International Conference on Robotics and Automation*, pages 610–615.

Whitney, D. E. (1982). Quasi-static assembly of compliantly supported rigid parts. *ASME Journal of Dynamic Systems Measurement and Control*, pages 65–104.

Wilfinger, L. S., Wen, J., and Murphy, S. (1993). Integral force control with robustness enhancement. In *Proc. IEEE International Conference on Robotics and Automation*, pages 100–106.

Williamson, M. (1995). Series elastic actuators. Master's thesis, MIT, Department of Electrical Engineering and Computer Science.

Xu, Y., Hollerbach, J. M., and Ma, D. (1994). Force and contact transient control using nonlinear pd control. In *Proc. IEEE International Conference on Robotics and Automation*, pages 924–930.

Xu, Y., Ma, D., and Hollerbach, J. M. (1993). Nonlinear proportional and derivative control for high disturbance rejection and high gain force control. In *Proc. IEEE International Conference on Robotics and Automation*, pages 752–759.

Yoshikawa, T., Hosoda, K., Doi, T., and Murakami, H. (1994a). Quasi-static trajectory tracking control of flexible manipulator by macro-micro manipulator system. In *Proc. IEEE International Conference on Robotics and Automation*, pages 210–215.

Yoshikawa, T., Hosoda, K., Harada, K., Matsumoto, A., and Murakami, H. (1994b). Hybrid positon/force control of flexible manipulators by macro-micro manipulator system. In *Proc. IEEE International Conference on Robotics and Automation*, pages 2125–2130.

Youcef-Toumi, K. and Gutz, D. A. (1989). Impact and force control. In *Proc. IEEE International Conference on Robotics and Automation*, pages 410–416.

Youcef-Toumi, K. and Li, D. (1987). Force control of direct drive manipulators for surface following. In *Proc. IEEE International Conference on Robotics and Automation*, pages 2055–2060.

Zhen, R. R. and Goldenberg, A. A. (1994). Robust position and force control of robots using sliding mode control. In *Proc. IEEE International Conference on Robotics and Automation*, pages 623–628.

THESIS PROCESSING SLIP

FIXED FIELD: ill _____ name _____

index _____ biblio _____

▶ COPIES: (Archives) Aero Dewey (Eng) Hum

Lindgren Music Rotch Science

TITLE VARIES: ▶☐ _____

_____

_____

NAME VARIES: ▶☐ _____

_____

IMPRINT: (COPYRIGHT) _____

▶ COLLATION: 121 p _____

_____

▶ ADD. DEGREE: _____ ▶ DEPT.: _____

SUPERVISORS: _____

_____

_____ _____

_____ _____

_____ _____

_____ _____

_____ _____

_____ _____

_____ _____

NOTES:

cat'r: date:

page: F54

▶ DEPT: M.E.

▶ YEAR: 1996 ▶ DEGREE: Ph.D.

▶ NAME MORRELL, John Bryant

_____